

Alma Mater Studiorum – Università di Bologna

DOTTORATO DI RICERCA

SCIENZE FARMACEUTICHE

Ciclo XXI

Settore/i scientifico disciplinari di afferenza: CHIM 08

TITOLO TESI

**Design and Synthesis of Multi Target Compounds for the
Treatment of Alzheimer's Disease**

Presentata da: Rizzo Stefano

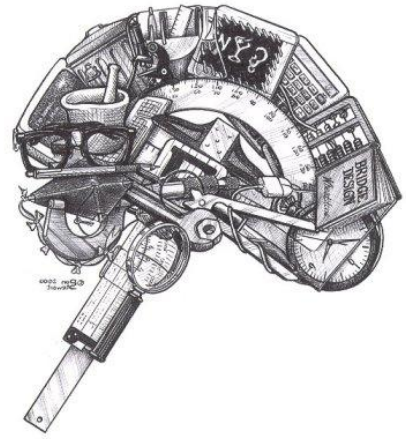
Coordinatore Dottorato

Relatore

Prof. Maurizio Recanatini

Prof.ssa Alessandra Bisi

Esame finale anno 2009



“Dulce est desipere in loco”.....Orazio

Table of contents:

1. Introduction

1.1. Alzheimer's disease

<i>1.1.1. Predementia</i>	<i>p. 4</i>
<i>1.1.2. Early dementia</i>	<i>p. 4</i>
<i>1.1.3. Moderate dementia</i>	<i>p. 5</i>
<i>1.1.4. Advanced dementia</i>	<i>p. 5</i>
<i>1.1.5. Pathological hallmarks</i>	<i>p. 5</i>
<i>1.1.6. Epidemiology and social costs</i>	<i>p. 6</i>

1.2. Etiopathology

<i>1.2.1. Cholinergic hypothesis</i>	<i>p. 7</i>
<i>1.2.2. Acetylcholinesterase</i>	<i>p. 8</i>
<i>1.2.3. Localization and function</i>	<i>p. 8</i>
<i>1.2.4. Structure</i>	<i>p. 9</i>
<i>1.2.5. Mechanism of action</i>	<i>p. 11</i>
<i>1.2.6. Amyloid-β peptide hypothesis</i>	<i>p. 12</i>
<i>1.2.7. Amyloid-β peptide formation</i>	<i>p. 13</i>
<i>1.2.8. BACE (beta amyloid cleaving enzyme)</i>	<i>p. 14</i>
<i>1.2.9. BACE inhibitors</i>	<i>p. 14</i>
<i>1.2.10. Tau protein theory</i>	<i>p. 16</i>

1.3. Acetylcholinesterase inhibitors	<i>p. 17-24</i>
---	-----------------

1.4. Therapeutic Approaches	<i>p. 24</i>
------------------------------------	--------------

1.5. New research's directions	<i>p. 25</i>
---------------------------------------	--------------

1.6. The Designed Multiple Ligands (DML) paradigm	<i>p. 25</i>
--	--------------

<i>1.6.1. Strategies for designing multiple ligands</i>	<i>p. 27</i>
<i>1.6.2. Classification of designed multiple ligands</i>	<i>p. 29</i>

2. Aim of the thesis	<i>p. 30-33</i>
-----------------------------	-----------------

3. Chemistry	<i>p. 34-41</i>
---------------------	-----------------

4. Results and discussion	<i>p. 42-48</i>
----------------------------------	-----------------

5. Conclusions	<i>p. 48</i>
-----------------------	--------------

6. Experimental section	<i>p. 49-75</i>
--------------------------------	-----------------

7. References	<i>p. 76-81</i>
----------------------	-----------------

1. Introduction

1.1. Alzheimer's disease



Fig. 1. Alois Alzheimer

Alzheimer's disease (AD), also called **Senile Dementia of the Alzheimer Type (SDAT)**, is the most common form of dementia. This neurodegenerative disease is named after the German psychiatrist Alois Alzheimer, who first described it in 1906. Generally it is diagnosed in people over 65 years of age⁽¹⁾, but the less-prevalent early-onset Alzheimer's can occur much earlier. The disease course can be divided into four stages⁽²⁾ and although each sufferer experiences Alzheimer's in a unique way, there are many common symptoms with a progressive pattern of cognitive and functional impairment from pre-dementia, to early, moderate and advanced dementia.

1.1.1. Predementia

The first symptoms are often mistaken as related to ageing or stress and they can affect the most complex daily living activities. The most noticeable deficit is memory loss, which shows up as difficulty in remembering recently learned facts and inability to acquire new informations. Subtle problems with the executive functions of attentiveness, planning, flexibility, and abstract thinking, or impairments in semantic memory (memory of meanings, and concept relationships), can also be symptomatic of the early stages of AD. Apathy can be observed at this stage, and remains the most persistent neuropsychiatric symptom throughout the course of the disease.

1.1.2. Early dementia

In people with AD the increasing impairment of learning and memory eventually leads to a definitive diagnosis. In a small proportion of them, difficulties with language, executive functions, perception (agnosia), or execution of movements (apraxia) are more prominent than memory problems. AD does not affect all memory capacities equally. Older memories of the person's life (episodic memory), facts learned (semantic memory), and implicit memory (the memory of the body on how to do things) are affected to a lesser degree than new facts or memories. Language problems are mainly characterized by a shrinking vocabulary and decreased word fluency, which lead to a general impoverishment of oral and written language. In this stage, the person with

Alzheimer's is usually capable of adequately communicating basic ideas. While performing fine motor tasks such as writing, drawing or dressing, certain movement coordination and planning difficulties may be present, making sufferers appear clumsy. As the disease progresses, people with AD can often continue to perform many tasks independently, but may need assistance or supervision with the most cognitively demanding activities.

1.1.3. Moderate dementia

Progressive deterioration eventually hinders independence. Speech difficulties become evident due to an inability to recall vocabulary, which leads to frequent incorrect word substitutions (paraphasias). Reading and writing skills are also progressively lost. Complex motor sequences become less coordinated as time passes, reducing the ability to perform most normal daily living activities. During this phase, memory problems worsen, and the person may fail to recognise close relatives. Long-term memory, which was previously intact, becomes impaired, and behavioral changes become more prevalent. Common neuropsychiatric manifestations are wandering, irritability and labile affect, leading to crying, outbursts of unpremeditated aggression, or resistance to caregiving. Approximately 30% of patients also develop illusionary misidentifications and other delusional symptoms. Urinary incontinence can develop.

1.1.4. Advanced dementia

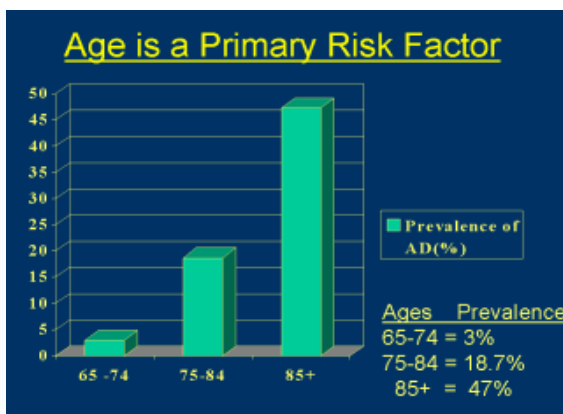
During this last stage of AD, the patient is completely dependent upon caregivers. Language is reduced to simple phrases or even single words, eventually leading to complete loss of speech. Despite the loss of verbal language abilities, patients can often understand and return emotional signals. Although aggressiveness can still be present, extreme apathy and exhaustion are much more common results. Patients will ultimately not be able to perform even the most simple tasks without assistance. Muscle mass and mobility deteriorate to the point where they are bedridden, and they lose the ability to feed themselves. Finally comes death, usually caused directly by some external factor such as pressure ulcers or pneumonia, not by the disease itself. The mean life expectancy following diagnosis is approximately seven years. Fewer than three percent of individuals live more than fourteen years after diagnosis.

1.1.5. Pathological hallmarks

Although the origin of AD is still unknown, three pathological hallmarks have been identified: amyloid- β plaques, neurofibrillary tangles (NFTs) and synaptic loss. At autopsy, the AD brain is

characterized by a number of important pathological changes, including a marked loss of neurons and synapses in many areas of the CNS, especially in regions involving higher order cognitive functions such as hippocampus and the association cortices. In addition, there is a global and dramatic reduction of neurotransmitters level, noradrenaline, dopamine, serotonin, glutamate, substance P and acetylcholine (ACh). Such depletion of neurotransmitters among which ACh is the most important one, is almost certainly the cause of the previously described clinical manifestations of AD.

1.1.6. Epidemiology and social costs



Two main measures are used in epidemiological studies: incidence and prevalence. Incidence is the number of new cases per thousand person-years; while prevalence is the total number of cases of the disease in the population at a given time. Regarding incidence, studies provide rates between 10–15 thousand person-years for all dementias and 5–8 for AD, which means that half of new dementia cases

each year are AD. Advancing age is a primary risk factor for the disease and incidence rates are not equal for all ages: every five years after the age of 65, the risk of acquiring the disease approximately doubles, increasing from 3 to as much as 69 per thousand person years. There are also sex differences in the incidence rates, women having a higher risk of developing AD particularly in the population older than 85. The World Health Organization estimated that in 2005 0.379% of people worldwide (26 millions) had dementia, and that the prevalence would increase to 0.441% in 2015 and to 0.556% in 2030, likely tripling by the year 2050. Dementia, and specifically Alzheimer's disease, may be among the most costly diseases for society in developed states and despite numbers vary between studies, dementia costs worldwide have been calculated around \$160 billion, of which about \$100 billion each year only in the United States. In addition to the impact on healthcare budget, there is also the emotional as well as the physical stress brought to the family of the sufferers.

1.2. Etiopathology

There are two main hypotheses trying to explain the onset of the disease: the first and oldest one, on which most currently available drug therapies are based, is the *cholinergic hypothesis*⁽³⁾, which

proposes that AD is caused by a severe impairment of the cholinergic system; the second one presented in 1991 is the *amyloid hypothesis*⁽⁴⁾, and postulates that amyloid beta (A β) deposits are the fundamental cause of the disease. Other processes seem to be involved, such as inflammatory injury, oxidative stress⁽⁵⁾ and intracellular deposition of neurofibrillary tangles⁽⁶⁾ made of hyperphosphorylated tau protein, pointing out the multi-factorial nature of AD and the urge for understanding how these processes are related in the cascade-events leading to its onset.

1.2.1. Cholinergic hypothesis

The cholinergic hypothesis⁽⁷⁾ was initially presented about 30 years ago and has become well established in the past decade almost to the point of dogma. In fact, starting from the mid-1970s, several groups, involved in the study of AD brains, reported loss of the main markers of the cholinergic activity such as significantly reduced choline acetyltransferase (CAT) activity in the cortex and hippocampus being CAT the enzyme responsible for the synthesis of acetylcholine from its precursors (acetyl coenzyme A and choline). Several other parameters of cholinergic function have been shown to be deranged in AD. High-affinity choline uptake, acetylcholine release and synthesis, together with cortical acetylcholine levels are in fact all reduced. The cholinergic hypothesis provided the first rational approach in the treatment of AD: six classes of compounds might be developed to contrast cholinergic deficit in AD patients.

- 1) Cholinesterase inhibitors (ChEIs), which block the enzyme acetylcholinesterase and thereby increase the synaptic availability of ACh by reducing its degradation.
- 2) Choline precursors, such as phosphatidylcholine, aimed at increasing the bioavailability of choline.
- 3) ACh releaser, which should facilitate the release of ACh from presynaptic end terminals.
- 4) M₁ and M₃ receptors agonists, which mimic ACh on postsynaptic end terminals.
- 5) M₂ and M₄ receptors antagonists, which regulate ACh release via negative feedback (auto receptors).
- 6) Nicotinic agonists, which should enhance ACh.

Acetylcholinesterase inhibitors seem to be the most effective strategy within the cholinergic approach in the treatment of AD.

1.2.2. Acetylcholinesterase

In 1914, Dale postulated an enzyme system responsible for terminating the physiological role of ACh at the cholinergic synapses. He differentiated between the muscarine- and nicotine-like actions of choline esters on different tissues and so he proposed: “it seems not improbable that an esterase contributes to the removal of acetylcholine from the circulation”. It was not until 1926 that Loewi and Navratil experimentally demonstrated acetylcholinesterase existence and in 1932 Stedman prepared a crude extract of an “ACh-splitting” enzyme from horse serum, which he called “choline esterase”. We now know that two enzymes efficiently hydrolyze ACh, acetylcholinesterase and butyrylcholinesterase (BuChE), also known as pseudocholinesterase or non specific cholinesterase. Those enzymes, which preferentially hydrolyze acetyl esters such as ACh, are called AChE and those which prefer other types of esters such as butyrylcholine (BuCh) are termed BuChE.

1.2.3. Localization and function

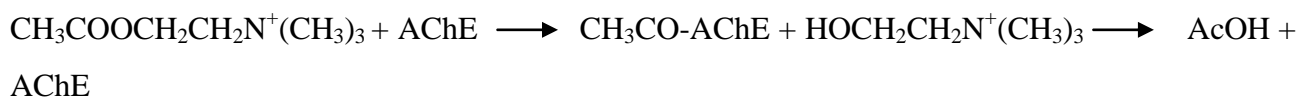
The principal biological role of AChE is the termination of impulse transmission at cholinergic synapses, by rapid hydrolysis of the neurotransmitter acetylcholine, within both the central and the peripheral nervous system; hence its location is related to cholinergic system. It has been reported that AChE is able to hydrolyze substance P and enkephalins too. Moreover, AChE shows peptidase and amidase activities. BuChE is found not only in association with neuronal cells in brain, but also with glial cells, in particular at the blood-brain barrier (BBB) level.

	AChE	BuChE
Brain	- Cholinergic Neuron	- Glial Cells
Blood-Brain Barrier		
	- Neuromuscular Junct.	- Heart
Periphery	- Heart - Liver	- Liver

Table 1. Localization of AChE and BuChE

The main function of AChE is the rapid hydrolysis of the neurotransmitter ACh at the cholinergic synapses: its catalytic mechanism is among the most efficient known, rate approaches that of a diffusion-controlled reaction, the substrate turnover is 25000 molecules sec^{-1} , and each turnover lasts about 40 μs . The hydrolysis reaction proceeds by nucleophilic attack of the carbonyl carbon,

involving acylation of the enzyme and release of choline. This is followed by a rapid hydrolysis of the acylated enzyme yielding acetic acid, and restoring the esteratic site.



The function of BuChE remains to be fully elucidated in both the brain and the systemic circulation, to date any specific natural substrate is known though is able to hydrolyze ACh. BuChE is found in association with the dopaminergic system where it may have a modulator role and is found in high concentrations in liver, suggesting a role in lipid metabolism, as well as in the cardiac muscle. Its massive presence in serum suggests a critical role in degradation of drugs such as succinyl choline, heroine, cocaine and physostigmine and activation of certain others like bambuterol. Recently it has been found that BuChE is a co-regulator of ACh levels in the advanced stage of AD, suggesting that its inhibition may play an important role for the therapeutic strategies.

	Brain	Peripheral Organs
AChE	-Brain cholinergic -Neurotransmission -Memory	-Peripheral cholinergic neurotransmission -Cardiovascular regulation -Neuromuscular activity -Papillary control
BuChE	-Modulation of dopamine neurotransmission	- Drug metabolism - Antitoxin

Table 2. Functions of AChE and BuChE

1.2.4. Structure

Knowledge of the three dimensional (3D) structure of AChE is essential for understanding its remarkable catalytic efficacy, for rational drug design and for developing new therapeutic approaches. The various oligomeric forms of AChE in the electric organ of certain fish, *Electrophorus* and *Torpedo*, are structurally homologous to those in vertebrate muscle and nerve. Highly purified preparations from this abundant sources of AChE facilitated research on this enzyme. The traditional view of the active site of AChE was initially considered to consist of two

subsites: an electron rich “anionic” site, to which the positively charged quaternary nitrogen moiety binds, and an esteratic site containing the catalytic residues. A second “anionic” site, which is known as the peripheral “anionic” site (PAS) was later proposed on the basis of binding of bis-quaternary compounds.

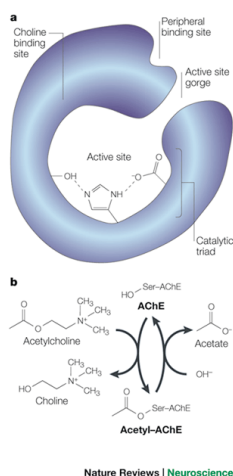


Fig. 2. Schematic representation of the binding sites of AChE: esteratic site, anionic binding site as well as the peripheral anionic binding site are shown

The nucleophile was assumed to be a serine residue, with a histidine residue enhancing its nucleophilicity. AChE was classified as a serine hydrolase, and therefore assumed to contain a catalytic triad of Glu-His-Ser at the esteratic site. A great leap forward in the understanding of catalytic mechanism, and mode of action of inhibitors, came in 1991 with the determination of the three dimensional structure of dimeric *Torpedo californica* AChE (*TcAChE*). The structure was determined to a resolution of 2.8 Å, which has more recently been refined to 2.2 Å by Sussman himself. According to the agreement adopted at the Oholo Conference in 1992, residues are numbered from the first one of the mature protein. The enzyme monomer is an α/β protein (MW 65612) containing 537 amino acids. The molecule possesses an ellipsoidal shape with dimensions of about 45 Å by 60 Å by 65 Å. It consists of a 12-stranded central mixed β -sheet surrounded by 14 α -helices and bears a striking resemblance to several hydrolases. The position of the active residue serine in *TcAChE* was established by irreversibly labeling it with [^3H]isopropyl fluorophosphate, followed by tryptic digestion and analysis of the tryptic peptides localizing it to Ser²⁰⁰. Both kinetic and chemical studies implicate a His residue in the active site. Mutagenesis studies identified the catalytic Histidine with His⁴⁴⁰. The glutamic group of the catalytic triad was confirmed to be Glu³²⁷ by site-directed mutagenesis on the related *Torpedo marmorata* AChE. The active site was found to be located 20 Å from the enzyme surface at the bottom of a narrow gorge, lined with 14

aromatic residues which may be important in guiding the substrate to the active site. There is not discernable “anionic” site, the quaternary nitrogen of choline binds chiefly through interactions with the π electrons of the Trp⁸⁴ residue. It is interesting to compare the structure of AChE and BuChE, since they possess 53% sequence homology, which has permitted the modeling of BuChE on the basis of 3D structure of *TcAChE*. Six aromatic residues, which are conserved in AChE and line the gorge leading to the active site, are absent in BuChE. Computer modeling has shown that two of these residues, Phe²⁸⁸ and Phe²⁹⁰, which are replaced in BuChE by leucine and valine, respectively, may prevent bulky esters of choline from entering into the acyl binding pocket of AChE. Mutagenesis experiments have confirmed this model. In addition to the subsite of the catalytic centre, AChE possesses one more additional binding site for ACh and other quaternary ligands. Such peripheral anionic binding site is located at the lip of the gorge. In BuChE Trp²⁷⁹ is missing.

1.2.5. Mechanism of action

The catalytic triad has been termed “charge relay system”. In human AChE (*huAChE*), the triad includes Ser²⁰³, the imidazole ring of His⁴⁴⁷ and the carboxylic group of Glu³³⁴. During the binding of ACh to AChE, the charge relay system causes electron shifts yielding to the acylation of the enzyme. The tetrahedral intermediate collapses to the acylated enzyme by acid catalyzed expulsion of choline by His⁴⁴⁷. The acylated enzyme complex is finally rapidly hydrolyzed, regenerating active enzyme by releasing acetic acid.

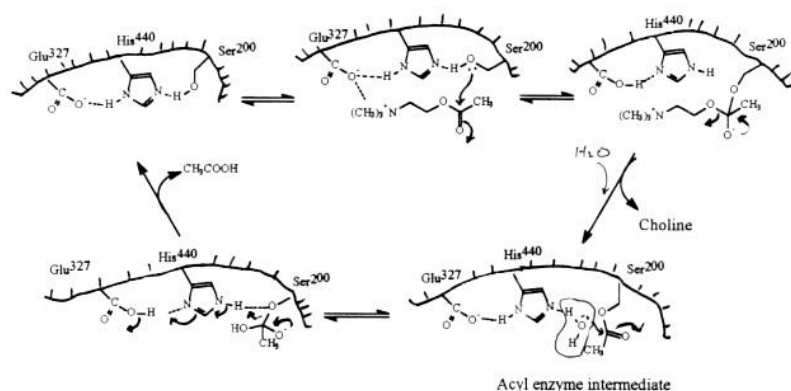


Fig. 3. Schematic mechanism of ACh metabolism by AChE

The inhibition of AChE by excess substrate is one of the key features that distinguishes it from BuChE. It's not known if the substrate inhibition has a biological role or it is just a consequence of AChE structure and mechanism. Various explanations have been proposed AChE could be allosterically regulated by the binding of ACh to the peripheral anionic site through conformational

changes at the active centre. The importance of the peripheral site in substrate inhibition has also been supported by Radic in 1991, based on studies of competition of the substrate with the peripheral site ligand propidium. However, studies on chicken AChE, which lacks the Tyr⁷⁰ and Trp²⁷⁹ residues found in *Torpedo californica* peripheral site, reveal substrate inhibition characteristics similar to those of TcAChE.

1.2.6. Amyloid- β peptide hypothesis

Two of the major markers^(8,9) of AD are the extracellular deposition of fibrous protein aggregates called senile or amyloid plaques, and NFTs in brain regions responsible for high cognitive function, such as hippocampus and association cortices.

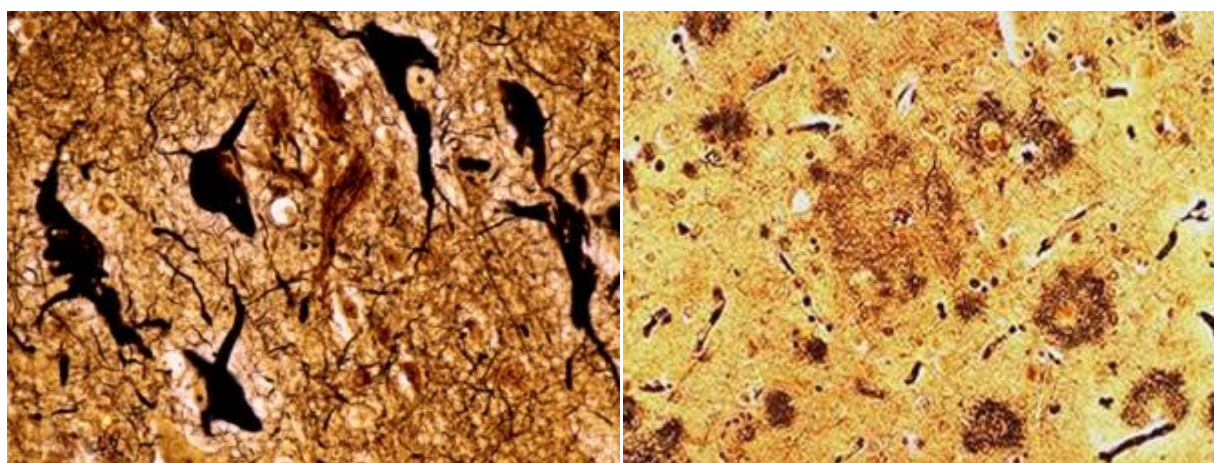


Fig. 4. Neurofibrillary tangles (left) and A β plaques (right)

The amyloid plaque as described by Alzheimer was isolated by Glenner and Wong in 1984. It is composed of an approximately 4 KDa peptide, that aggregates into a fibrillar, β -pleated structure. On the basis of its size and secondary structural characteristic, the peptide has been referred to by a variety of names including A4 peptide, β -peptide and β A4. According to accepted amyloid nomenclature, the peptide is now referred to as amyloid- β or A β . Even though a casual link between plaque formation and AD has not been firmly established, increasing evidences suggest that amyloid deposition may play a critical role in the neurodegenerative process. The plaque are primarily composed of aggregates of 39-43 amino acids (A β), of which the 42 amino acid peptide is the most prone to aggregation and thus, plaque formation. The “amyloid hypothesis” postulates that A β ₄₂, in particular, is casual in the disease process. This hypothesis is supported primarily by genetic evidence from individuals who greatly overproduce A β ₄₂. A growing effort is directed towards therapeutic strategies, which target the effects of A β as treatment for the cause of AD.

These strategies are complimentary to symptomatic cognition-improvement therapies based on AChE inhibitors and M₁ agonists. The A β strategies take three forms:

- 1) Disruption of A β production from its precursor protein (APP)
- 2) Protection from neurotoxicity of the A β aggregates
- 3) Inhibition of the aggregation of A β monomer into the neurotoxic aggregates that constitute the plaques

1.2.7. Amyloid- β peptide formation⁽⁹⁾

It is presently thought that A β is generated after sequential cleavage of the amyloid precursor protein, a transmembrane glycoprotein of undetermined function. APP can be processed by α -, β - and γ -secretases; A β protein is generated by successive action of the β (BACE) and γ secretases. The γ secretase, which produces the C-terminal end of the A β peptide, cleaves within the transmembrane region of APP and can generate a number of isoforms of 39-43 amino acid residues in length. The most common isoforms are A β ₄₀ and A β ₄₂; the shorter form is typically produced by cleavage that occurs in the endoplasmic reticulum, while the longer form is produced by cleavage in the trans-Golgi network. The A β ₄₀ form is the more common of the two, but A β ₄₂ is the more fibrillogenic and is thus associated with disease states. Mutations in APP associated with early-onset Alzheimer's have been noted to increase the relative production of A β ₄₂, and thus one suggested avenue of Alzheimer's therapy involves modulating the activity of β (BACE) and γ secretases to produce mainly A β ₄₀.

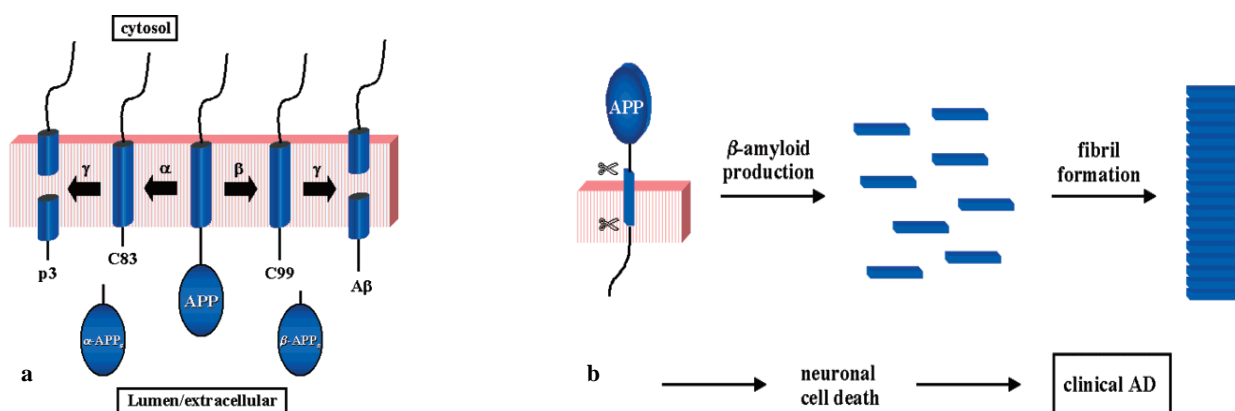


Fig. 5 a) Schematic representation of a possible processing pathway of the amyloid precursor protein (APP) by α -, β and γ secretases; b) representation of the amyloid- β theory.

Particularly, the proteolysis takes place just outside the membrane, releasing soluble APP (β -APPs) and leaving behind a 99 residue membrane-associated C-terminal fragment, C99. Alternatively, APP is cut by α -secretase, a membrane-bound metallo-protease, to produce α -APPs and an 83

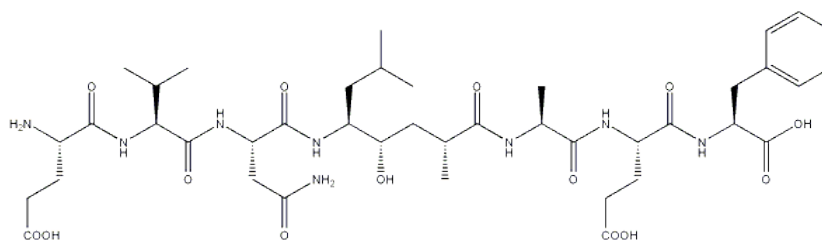
residue membrane-associated C-terminal fragment, C83. Both C99 and C83 are substrates for γ -secretase, an enzyme that carries out an unusual proteolysis in the middle of the transmembrane domain of APP, resulting in formation of the 4 kDa $A\beta$ from C99 and p3, a 3 kDa N-terminally truncated form of $A\beta$, from C83. AChE may also fulfill non-cholinergic roles. In AD brains, cortical AChE activity is associated predominantly with the amyloid core of mature senile plaques, pre-amyloid diffuse deposits and cerebral blood vessels. Previous studies have indicated that AChE binds to $A\beta$ and induces $A\beta$ fibril formation, forming macromolecular complexes with the growing fibrils. These studies suggested that a specific motif, located close to the rim of the active site gorge of the enzyme, may be involved in accelerating fibril formation. This motif, as elucidated by Inestrosa and co-workers^(15,16), matches with the PAS since both PAS inhibitors and a monoclonal antibody directed toward the PAS, blocked the amyloidogenic effect of AChE.

1.2.8. BACE (beta amyloid cleaving enzyme)⁽⁹⁾

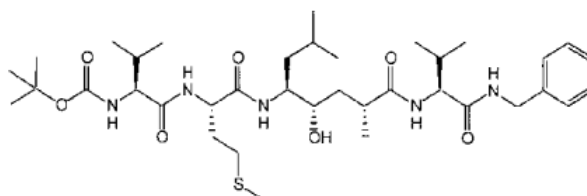
β -Secretase (BACE) is a proteolytic enzyme involved in the processing of an integral membrane protein known as amyloid precursor protein, or APP. The proteolysis of APP by BACE, followed by subsequent C-terminal cleavage(s) by γ -secretase, results in the formation of the amyloid β ($A\beta$) peptide. $A\beta$ is a neurotoxic and highly aggregatory peptide segment of APP that is the principal component of the neuritic plaque found in the brains of Alzheimer's disease (AD) patients. Because of the apparent causal relationship between $A\beta$ and AD, the so-called "secretases" (especially BACE) that produce $A\beta$ have been targeted.

1.2.9. BACE inhibitors⁽⁹⁾

Peptidomimetic BACE Inhibitors. Substrate based inhibitors of BACE were designed using the knowledge of the specificity and kinetics of BACE. Tang and co-workers at the University of Oklahoma have reported on the development of peptidic hydroxyethylene-based BACE inhibitor OM99-2, which has a BACE IC₅₀ of 0.002 μ M.⁽¹⁰⁾ They have further reported on using X-ray structure-based modification of the lead **1** that led to the discovery of a series of potent and considerably low molecular weight peptidomimetic BACE inhibitors such as **2**.



Peptidic hydroxyethylene BACE inhibitor **1** (OM99-2) $IC_{50} = .002 \mu M$



Hydroxyethylene BACE inhibitor **2** $IC_{50} = 0.002 \mu M$

Nonpeptidomimetic BACE Inhibitors. The most detailed account of nonpeptidomimetic BACE inhibitors to date comes from Vertex, via a published patent application. In late 2002, Vertex disclosed⁽¹¹⁾ several hundred compounds along with associated K_i ranges of BACE inhibition; these compounds spanned multiple classes of heterocyclic templates. Among the more potent classes reported (BACE $K_i < 3 \mu M$) were the halogen-substituted biarylnaphthalenes represented by **3**. From these results, Vertex proposed⁽¹²⁾ the first 3-D pharmacophore map of BACE to guide the design and optimization of inhibitors, wherein HB represents hydrogen-bonding moiety interactions with the active site and other key residues of BACE and HPB represents hydrophobic moiety interactions with BACE subsites.

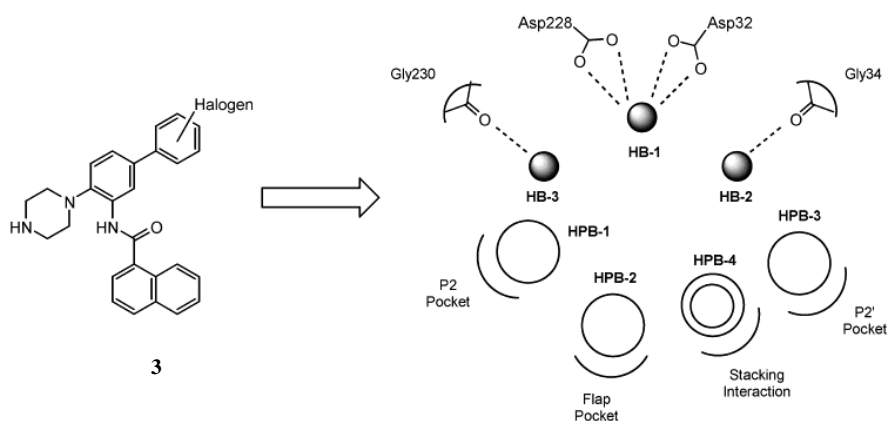


Figure 6. Vertex inhibitor and 3-D BACE pharmacophore map.

1.2.10. Tau protein theory⁽⁶⁾

Tau proteins are microtubule-associated proteins that are abundant in neurons in the central nervous system and are less common elsewhere. They were discovered in 1975 in Marc Kirschner's laboratory at Princeton University. Tau proteins interact with tubulin to stabilize microtubules and promote tubulin assembly into microtubules. Tau has two ways of controlling microtubule stability: isoforms and phosphorylation. Six tau isoforms exist in brain tissue, and they are distinguished by their number of binding domains. Three isoforms have three binding domains and the other three have four binding domains. The binding domains are located in the carboxy-terminus of the protein and are positively-charged (allowing it to bind to the negatively-charged microtubule). The isoforms with four binding domains are better at stabilizing microtubules than those with three binding domains. The isoforms are a result of alternative splicing in exons 2,3, and 10 of the *tau* gene. Phosphorylation of tau is regulated by a host of kinases, for example, PKN, a serine/threonine kinase. When PKN is activated, it phosphorylates tau, resulting in disruption of microtubule organization. Hyperphosphorylation of the tau protein (tau inclusions), however, can result in the self-assembly of tangles of paired helical filaments and straight filaments, which are involved in the pathogenesis of Alzheimer's disease. In fact, the observation that deposition of amyloid plaques does not correlate well with neuron loss has supported the *tau hypothesis*. In this model, hyperphosphorylated tau begins to pair with other threads of tau. Eventually, they form neurofibrillary tangles inside nerve cell bodies. When this occurs, the microtubules disintegrate, leading to collapse of the neuron's transport system. This may first result in malfunctions in biochemical communication between neurons, and later in the death of the cells.

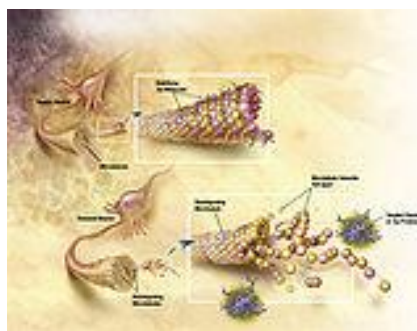


Fig. 7. Intracellular neurofibrillary tangles made of hyperphosphorylated tau protein

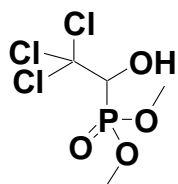
1.3. Acetylcholinesterase inhibitors⁽¹³⁾

Inhibition can be either reversible, by competitively preventing the substrate from reaching the active site; pseudo-irreversible, by covalent reaction with the active site serine, inactivating the catalytic ability of the enzyme or irreversible. Competitive inhibitors act by blocking substrate at the active site, non competitive inhibitors by binding to the peripheral site.

Organophosphorus compounds

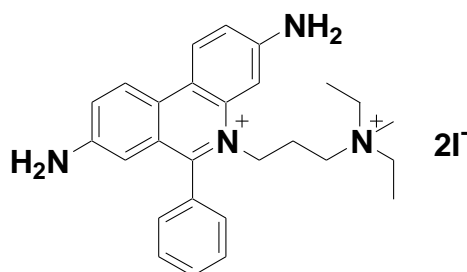
Organophosphorus compounds such as diisopropyl fluorophosphates (DFP) are very potent inhibitors of AChE and are used as agricultural insecticides or as nerve gases in chemical warfare. These compounds react with the active site serine, forming a very stable covalent phosphoryl-enzyme complex.

Metriphonate



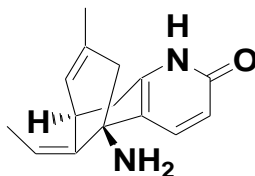
Metriphonate is a natural AChE inhibitor, which irreversibly phosphorylates the enzyme. This drug is unique among ChEIs for AD treatment; since in aqueous solution it spontaneously transforms in the active metabolite 2,2-dichlorovinyl dimethyl phosphate. The reaction doesn't require enzymatic activation; the inhibition is mediated by a competitive drug interaction at the catalytic site, followed by dimethylphosphorylation of a serine residue located in the active site of the enzyme.

Propidium



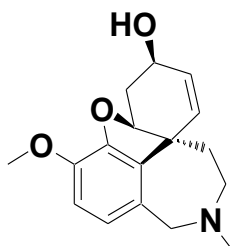
Propidium is a reversible AChE inhibitor. Its bulky structure doesn't allow the molecule to penetrate into the gorge. It is the reference compound for the determination of the inhibition at the PAS.

(-) *Huperzine A*



(-) Huperzine A (Hup A) is a natural origin alkaloid isolated from *Huperzia serrata*. This alkaloid inhibits the enzyme by forming reversible complexes with it and it is able to reduce neuronal cells death caused by glutamate. This double action and the very low toxicity indicate Hup A as a promising drug for the treatment of AD. The crystal structure of Hup A complexed with *TcAChE* reveals an unexpected orientation of the ligand within the active site, as well as an unusual protein-ligand interaction and a significant change in the main chain conformation of the protein. The orientation of Hup A within the active site gorge appears to be almost orthogonal to the ACh molecule. Binding of Hup A to the PAS, near to Trp²⁷⁹ was also predicted by docking studies, but no evidence of this was seen in the crystallography studies.

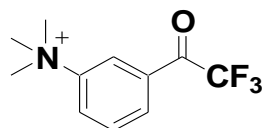
Galantamine



Alkaloid galantamine⁽¹⁴⁾ was primarily studied for botanic purposes and only in 1986 for the treatment of AD. It is a reversible inhibitor that shows CNS selectivity and despite its less potency compared with tacrine and E2020, it has excellent pharmacological and pharmacokinetic profiles exhibiting very low hepatotoxicity and side effects. Galantamine is also a representative member of a class of ligands acting as noncompetitive nicotinic receptor agonist. Its action is exerted via an allosteric binding site on nAChR, distinct from the site for acetylcholine, improving the nicotinic response induced by ACh and competitive agonists. The cost of obtaining galanthamine from natural sources is very high slowing down studies about this drug. Total synthesis procedures developed so far, still have to be improved for large-scale industrial preparation. Galantamine (Reminyl[®]) has now been approved for AD treatment in many countries among which Italy.

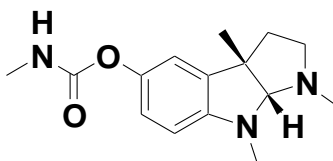
Trifluoromethyl ketons

Of particular interest are inhibitors, which act as transition-state mimics, such as trifluoromethyl ketons.



Trimethyl-[3-(2,2,2-trifluoro-acetyl)-phenyl]-ammonium (TMTFA) is a substrate-like inhibitor of AChE of this class, and it is one of the most potent reversible AChE inhibitors reported in the literature. Sussman and co-workers confirmed the nature of the binding mode of TMTFA with *TcAChE* by X-ray analysis. The active site serine covalently binds to the activated carbonyl of the trifluoroacetyl group, while the quaternary ammonium group favorably interacts with the adjacent aromatic residues Trp⁸⁴ and Phe³³⁰ among others.

Physostigmine

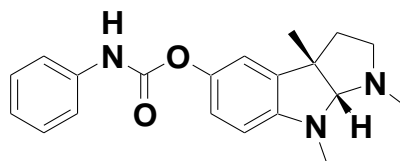


The longest known AChE inhibitor is the natural alkaloid physostigmine (PHY), which is extracted from the Calabar Beans. This carbamylates the active site serine residue, greatly slowing the acylenzyme hydrolysis reaction compared with the acetylated enzyme. The AChE IC₅₀ is 14.1 nM but it is not selective for AChE versus BuChE and its half life (t_{1/2}) is 15-30 minutes; for these reasons in November 1998 the U.S. Food and Drug Administration (FDA) issued a non approval letter for PHY's Alzheimer's indication based mainly on a lack of efficacy as shown from results in Clinical Phase II and Phase III studies.

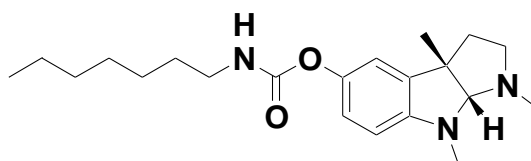
Physostigmine analogues

Derivatives of the alkaloid physostigmine, as well as physostigmine itself, inhibit the enzyme by carbamoylating the serine residue of the catalytic triad in a pseudoirreversible manner. Sequestration of AChE in its carbamoylated form precludes any further hydrolysis of ACh for an extended period of time. To ameliorate pharmacokinetic properties of PHY, the carbamic substituent has been modified increasing the duration of action and maintaining the acetylcholinesterase

activity. *Phenserine*, the phenyl carbamate of (-)-eseroline, was prepared in 1916 from natural physostigmine by Polonovsky.

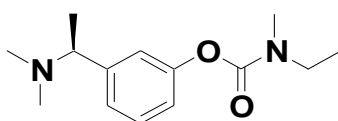


It's a long acting drug and it inhibits AChE selectively, being more than 50 times more active on AChE than BuChE. *Eptastigmine*, a more recent physostigmine analogue, is the heptyl carbamate of (-)-eseroline.



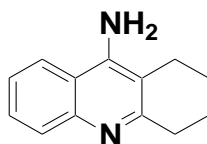
Compared to physostigmine this compound has a longer duration of action ($t_{1/2} = 10$ hours) and the drug inhibits red blood cells AChE in a dose-dependent manner. Although clinical phase III studies showed a positive effect of eptastigmine compared to placebo, in particular in the more severely impaired patients, they were subsequently dropped because of toxicity problems.

Rivastigmine



Rivastigmine (SDZ-ENA-713/Exelon[®]) is a miotine derivative. It is a carbamic AChE inhibitor with a short half-life and duration of action of about 10 hours. This drug inhibits AChE by carbamoylating the serine residue of the catalytic triad in a pseudoirreversible manner. Based on Phase III clinical studies conducted in the U.S. a regimen of increasing dosage seems to be necessary in order to achieve maximum clinical benefits with minimal side effects. Rivastigmine under the name of Exelon[®] has been launched worldwide: Europe, South America, Asia, Africa and more recently also in the United States.

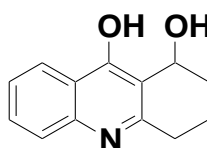
Tacrine



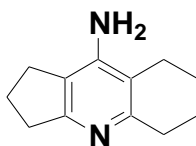
Tacrine (THA, Cognex[®]) was launched in 1993 as the first drug for the symptomatic treatment of AD. THA (9-amino-1,2,3,4-tetrahydroacridine) is a centrally active reversible inhibitor of AChE that shows a moderately long duration of action. The rationale for its use was related to the elevation of the acetylcholine levels that can compensate for the cholinergic deficit associated to the brain lesions present in mild to moderate AD. In the Tacrine-AChE complex, the tacrine moiety is staked against Trp⁸⁴, with the nitrogen in the ring forming a hydrogen bond with the main chain carbonyl oxygen of His⁴⁴⁰; its amino nitrogen binds to a water molecule. The Phe³³⁰ ring rotates to lie parallel to tacrine, which is sandwiched between the Phe³³⁰ and Trp⁸⁴ rings. Because of the positive effects observed with THA, this compound has been used as a reference drug in the clinical development of other AChE inhibitors for both clinical efficacy and side effects.

Tacrine analogues

Several THA analogues are under preclinical or clinical evaluation, among them are amiridine and velnacrine. *Velnacrine* is an hydroxyl metabolite of tacrine, with a shorter half-life.



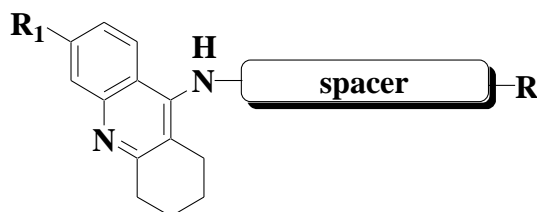
Pharmacodynamics trials with single doses of this inhibitor demonstrated statistically significant cognitive improvements compared with placebo, however about 20-30% of patients developed hepatotoxicity. *Amiridine* is now under phase III clinical studies in Japan.



Beneficial effects are produced at both the initial and marked stages of the disease, although the most significant results are obtained in patients with unmarked dementia. Some recent studies are addressed to tacrine-huperzine A hybrids and other alkylene-linked tacrine dimers.

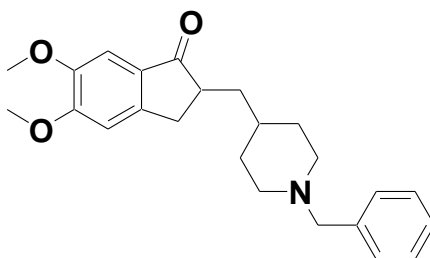
Tacrine dimers

Since bis(7)-tacrine, a heptamethylene-linked dimer of the first marketed anti-Alzheimer drug tacrine, was developed 1 decade ago,⁽¹⁵⁻¹⁸⁾ the search for inhibitors of acetylcholinesterase able to simultaneously bind to its catalytic and peripheral binding sites has become an area of very active research. Several classes of dual binding site AChE inhibitors have been developed by connecting through a suitable linker the two interacting units, which are generally derived from known AChE inhibitors either commercialized or under development.⁽¹⁹⁻²¹⁾ The success of the dual binding site strategy is evidenced by the large increase in AChE inhibitory potency of these dimers or hybrids relative to the parent compounds from which they have been designed. Further interest comes from the fact that some of these dual binding site AChE inhibitors have been shown to inhibit the aggregation of β -amyloid peptide ($A\beta$),⁽⁹⁻¹⁸⁾ which is a key event in the neurotoxic cascade of Alzheimer's disease (AD).^(19,20) This effect, which has been related to the blockade of the AChE peripheral site⁽¹⁶⁾ by dual binding site AChE inhibitors, makes these compounds very promising disease-modifying anti-Alzheimer drug candidates. The general structure of tacrine dimers can be represented as follows:



Two 9-amino-1,2,3,4-tetrahydroacridine moieties are linked one to another through an opportune spacer that most of the times happens to be an heptyl chain. There have been also heterodimers linking THA to different kinds of chemical motifs (mainly trimethoxy substituted benzenes, lipoic acid, melatonin, NO donor) sometimes through spacers other than alkyl-chains such as hydrazide-, amide- and triazole-based linkers. In these structures the 9-amino-1,2,3,4-tetrahydroacridine moiety is sometimes found to carry a chlorine substituent at C 6 position.

Donepezil



Donepezil hydrochloride (E2020, Aricept[®]) is the second drug approved by the U.S. FDA for the treatment of mild to moderate AD. This class of *N*-benzylpiperidines emerges from Eisai Company; through a random screening they found a *N*-benzylpiperazine derivative showing a promising AChE inhibitory activity. When *N*-benzylpiperazine was replaced with *N*-benzylpiperidines a dramatic increase in anti-acetylcholinesterase activity was detected. After various modifications they obtained Donepezil. They studied the possible interaction of the new compound with the enzyme finding multiple modes of binding, but only few years later Sussman and co-workers reported the crystal structure of a complex of donepezil with *Tc*AChE. The X-ray structure shows that the elongated donepezil molecule spans the entire length of the active-site gorge of the enzyme. It thus interact with both the anionic subsite at the bottom of the gorge, and with the peripheral anionic site, near its entrance, via aromatic stacking interactions with conserved aromatic residues. E2020 doesn't directly interact with either the catalytic triad or with the "oxyanion hole".

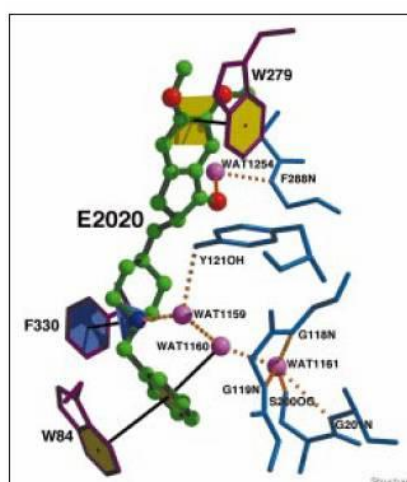


Fig. 8. E2020 (in green) binds along the active site and interacts with the PAS at the top and with the AS at the bottom of the gorge

Donepezil shows superior efficacy, minimal side effects, and high brain selectivity compared to THA and PHY. E2020 and related compounds are shown to reversibly and specifically inhibit AChE by forming a complex in which the *N*-benzylpiperidine group presumably interacts with the anionic site, which recognizes the quaternary ammonium group of ACh. Clinical trials have shown that the inhibition of BuChE may be linked with side effects. *N*-benzylpiperidine compounds are highly selective for AChE over BuChE demonstrating an exceptional safety profile (IC₅₀ for AChE is 5.7 nM while for BuChE is about 7000 nM).

1.4. Therapeutic Approaches

Four drugs are currently approved by regulatory agencies such as the U.S. Food and Drug Administration (FDA) and the European Medicines Agency (EMA) to treat the cognitive manifestations of AD: three are acetylcholinesterase inhibitors and the other one is memantine, an NMDA receptor antagonist. No drug has an indication for delaying or halting the progression of the disease. Since reduction in the activity of the cholinergic neurons is a well-known feature of Alzheimer's disease, acetylcholinesterase inhibitors are employed to reduce the rate at which acetylcholine (ACh) is broken down, thereby increasing the concentration of ACh in the brain and combating the loss of ACh caused by the death of cholinergic neurons. As of 2008, the cholinesterase inhibitors approved for the management of AD symptoms are donepezil (brand name *Aricept*[®]), galantamine (*Reminyl*[®]), and rivastigmine (branded as *Exelon*[®] and *Exelon Patch*[®]). There is evidence for the efficacy of these medications in mild to moderate Alzheimer's disease, and some evidence for their use in the advanced stage. Only donepezil is approved for treatment of advanced AD dementia. The use of these drugs in mild cognitive impairment has not shown any effect in a delay of the onset of AD. The most common side effects are nausea and vomiting, both of which are linked to cholinergic excess. These side effects arise in approximately ten to twenty percent of users and are mild to moderate in severity. Less common secondary effects include muscle cramps, decreased heart rate (bradycardia), decreased appetite and weight, and increased gastric acid production. Glutamate is a useful excitatory neurotransmitter of the nervous system, although excessive amounts in the brain can lead to cell death through a process called excitotoxicity, which consists of the overstimulation of glutamate receptors. Excitotoxicity was shown to occur in Alzheimer's disease, but also in other neurological diseases such as Parkinson's disease and multiple sclerosis. Memantine (brand names *Akatinol*[®], *Axura*[®], *Ebixa/Abixa*[®], *Memox*[®] and *Namenda*[®]), is a noncompetitive NMDA receptor antagonist, first used as an anti-influenza agent. It acts on the glutamatergic system by blocking NMDA receptors and inhibiting their overstimulation by glutamate. Memantine has been shown to be moderately efficacious in the

treatment of moderate to severe Alzheimer's disease. Its effects in the initial stages of AD are unknown. Reported adverse events with memantine are infrequent and mild, including hallucinations, confusion, dizziness, headache and fatigue. The combination of memantine and donepezil has been shown to be "of statistically significant, but clinically marginal effectiveness". Antipsychotic drugs are modestly useful in reducing aggression and psychosis in Alzheimer's patients with behavioural problems, but are associated with serious adverse effects, such as cerebrovascular events, movement difficulties or cognitive decline, that do not permit their routine use. When used in the long-term, they have been shown to associate with increased mortality.

1.5. New research's directions

As of 2008, the safety and efficacy of more than 400 pharmaceutical treatments are being investigated in clinical trials worldwide, and approximately one-fourth of these compounds are in Phase III trials, which is the last step prior to review by regulatory agencies. One area of clinical research is focused on treating the underlying disease pathology. Reduction of amyloid beta levels is a common target of compounds under investigation. Immunotherapy or vaccination for the amyloid protein is one treatment modality under study. Unlike preventative vaccination, the putative therapy would be used to treat people already diagnosed. It is based upon the concept of training the immune system to recognise, attack, and reverse deposition of amyloid, thereby altering the course of the disease. An example of such a vaccine under investigation was ACC-001, although the trials were suspended in 2008. Another similar agent is bapineuzumab, an antibody designed as identical to the naturally-induced anti-amyloid antibody. Other approaches are neuroprotective agents, such as AL-108, and metal-protein interaction attenuation agents, such as PBT2. A TNF α receptor fusion protein, etanercept has showed encouraging results. In 2008, two separate clinical trials showed positive results in modifying the course of disease in mild to moderate AD with methylthioninium chloride (trade name *rember*), a drug that inhibits tau aggregation, and dimebon, an antihistamine.

1.6. The Multi Target Directed Ligands (MTDL) paradigm

For much of the past century, drug discovery largely has relied on the use of animal models of disease as the first-line screen for testing the compounds produced by medicinal chemists. This *in vivo* pharmacology approach had the benefit of highlighting compounds that exhibited both desirable pharmacokinetic and pharmacodynamic profiles. A major disadvantage of this approach was that an animal model was essentially a "black box". When compounds were inactive, it was

unclear whether this was because they no longer interacted with a molecular target or simply because they had failed to reach the site of action. In many cases, the molecular target(s) driving the desired pharmacological effect had not been identified, and inevitably many older generation drugs cross-reacted with targets that caused detrimental side effects. Inexorably, the drug discovery paradigm shifted toward a reductionist “one-target, one-disease” approach that continues to dominate the pharmaceutical industry today. Many successful drugs have emerged from this strategy, and it will no doubt remain dominant for many years to come. However, despite the best efforts of drug discoverers, many diseases remain inadequately treated. There is an increasing readiness to challenge the current paradigm and to consider developing agents that modulate multiple targets simultaneously (polypharmacology), with the aim of enhancing efficacy or improving safety relative to drugs that address only a single target. There are three possible approaches to polypharmacology (Figure 9)^(48,49).

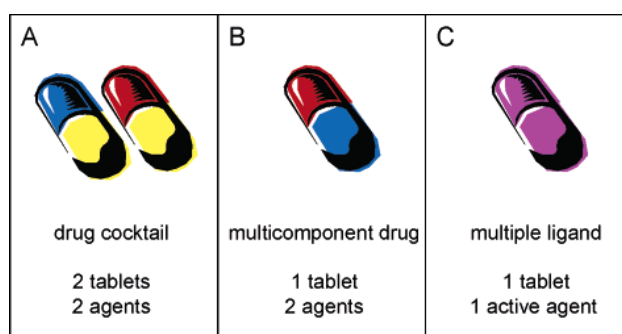


Fig. 9. Three main clinical scenarios for multitarget therapy

Traditionally, clinicians have treated unresponsive patients by combining therapeutic mechanisms with cocktails of drugs. Most frequently, the cocktail is administered in the form of two or more individual tablets (scenario A). However, the benefits of this approach are often compromised by poor patient compliance, particularly for treating asymptomatic diseases such as hypertension. Recently, there has been a move toward multicomponent drugs whereby two or more agents are coformulated in a single tablet to make dosing regimes simpler and thereby to improve patient compliance (scenario B). An alternative strategy is to develop a single chemical entity that is able to modulate multiple targets simultaneously (scenario C). Across the pharmaceutical industry, scenario B is increasingly providing an attractive opportunity for enhancing R&D output. Several multicomponent drugs have recently been launched, such as Caduet (amlodipine/ atorvastatin) and Vytorin (ezetimibe/simvastatin) that were approved in 2004 for the treatment of cardiovascular disease. However, there are significant risks involved in the development of multicomponent drugs. There is the commercial uncertainty arising from the risk that clinicians might still prefer

prescribing combinations of existing monotherapies that may offer greater dose flexibility and lower cost treatment, particularly in the case of generic drugs. Differences in the relative rates of metabolism between patients can produce highly complex pharmacokinetic (PK)/pharmacodynamic (PD) relationships for multicomponent drugs, leading to unpredictable variability between patients and calling for extensive and expensive clinical studies. Compared to multicomponent drugs, the multipleligand approach (scenario C) has a profoundly different risk-benefit profile. A downside is that it is significantly more difficult to adjust the ratio of activities at the different targets. However, this increased complexity in the design and optimization of such ligands is shifted toward the earlier and therefore less expensive stages of the drug discovery process. The clinical development of multiple ligands, in terms of the risks and costs involved, is in principle no different from the development of any other single entity. Another advantage is a lower risk of drug-drug interactions compared to cocktails or multicomponent drugs. While many currently marketed drugs are in essence multiple ligands, very few were rationally designed to be so.

1.6.1. Strategies for designing multiple ligands

Conceptually, there are two quite different methods of generating chemical matter with which to commence a DML project: *knowledge-based* approaches and *screening* approaches. Knowledge-based approaches rely on existing biological data from old drugs or other historical compounds, from either literature or proprietary company sources. Serendipitous approaches involve the screening of either diverse or focused compound libraries. Typically, diversity-based screening involves the high-throughput screening (HTS) of large, diverse compound collections at one target, and any actives are then triaged on the basis of activity at the second target. In focused screening, compound classes that are already known to provide robust activity at one of the targets of interest, A, are screened for signs of activity at a new target, B. Even if only weak activity is observed for target B, this can provide a useful baseline for increasing that activity by incorporating structural elements from more potent selective ligands for target B. For both the screening or knowledge-based approaches, the identification of a lead compound with appropriate activity at both targets A and B is unlikely. In reality, a lead generation, or “hit-to-lead” phase, will be required. In one scenario, two compounds that bind with very high selectivity to their respective targets are used as the starting points. To incorporate activity at both targets into a single molecule (“designing in”), structural elements from the two selective ligands are combined. Incorporating a second activity into a compound that has no measurable affinity for that target, while retaining affinity for the original target, is not an easy task. However, many literature examples testify to the fact that it can often be achieved. Perhaps a more tractable scenario is to first identify a compound that has at least

minimal activity at both targets. In this case, the activity at both targets must be modulated to achieve an optimal ratio. In a third scenario, a compound is identified that possesses activity at both targets A and B but also possesses undesirable activity at another target C. The optimization strategy must then focus on “*designing out*” this cross-reactivity. In some cases, a compound may possess more than one undesired activity, and this will inevitably increase the complexity of the task. By far the most common trajectory for generating leads is to convert a ligand with a single activity into a dual ligand. The conversion of single ligands into triple ligands is more challenging and is much rarer. As the number of targets in a profile increases, the “designing in” philosophy will become less attractive compared to the “designing out” approach starting from a nonselective ligand. The lead candidate will usually lack the optimal ratio of in vitro activities. In lead optimization, the ratio is adjusted so that both targets are modulated to an appropriate degree in vivo at similar plasma or brain concentrations. In most examples, the aim has been to obtain in vitro activities within an order of magnitude of each other, with the assumption that this will lead to similar levels of receptor occupancy in vivo. However, this may not necessarily be the case, and assuming a validated animal model is available, the testing of a lead candidate in vivo may help to clarify the required ratio of in vitro activities. Ultimately, feedback from clinical studies will be required to identify the optimal ratio that can be used to drive the design of “follow-up” compounds. In addition to adjusting the ratio of activities, optimizing wider selectivity against a broad panel of targets is often required. This will be particularly intricate for targets for which a large number of subtypes or isozymes exist. Many publications do not discuss the key issue of global selectivity, so it is frequently difficult to judge whether real selectivity for the disease-relevant targets has been achieved. Again, animal models and subsequent clinical studies will provide essential feedback on the level of cross-reactivity that can be tolerated. A particular challenge in lead optimization is to optimize the PK profile and to obtain physicochemical properties that are consistent with good oral absorption.

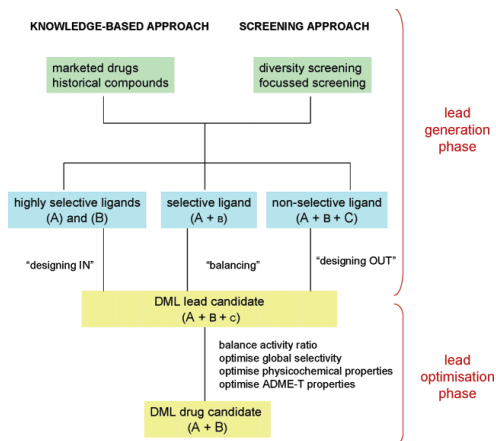


Figure 10. Different strategies for DML projects. In the lead generation phase, knowledge-based or screening approaches are used to provide starting compounds that may be highly selective (little or no activity at a second target), moderately selective, or nonselective (with undesired activity). The subsequent strategy involves “designing in”, “balancing”, or “designing out” activities, respectively. As well as balancing the activity ratio, lead optimization provides other major challenges, in particular adsorption, distribution, metabolism, excretion, and toxicity (ADME-T) optimization. In this schematic, activity at targets A and B is desired and activity at target C is undesired. The size of the target letter illustrates the affinity for that target.

1.6.2 Classification of designed multiple ligands

“Conjugates” are DMLs in which the molecular frameworks, which contain the underlying pharmacophore elements for each target, are well separated by a distinct linker group that is not found in either of the selective ligands (Figure 11). Most conjugates contain a metabolically stable linker. “Cleavable conjugates” employ a linker that is designed to be metabolized to release two ligands that interact independently with each target.



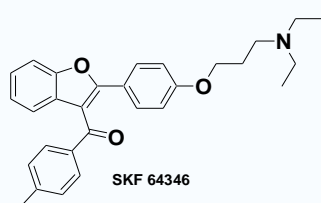
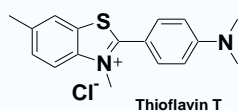
Fig. 11

As the size of the linker decreases, a point is reached where the frameworks are essentially touching, and these DMLs can be regarded as “fused”. In the most common type of DML, the frameworks are “merged” by taking advantage of commonalities in the structures of the starting compounds. In reality, the degree of merger of the frameworks forms a continuum, with high molecular weight conjugates with lengthy linker groups representing one extreme. At the other extreme are examples where the frameworks, and underlying pharmacophores, are highly merged, giving rise to smaller and simpler molecules.

2. Aim of the thesis

The multi target directed ligand theory (MTDL) is becoming an interesting approach in the field of medicinal chemistry, being particularly used to combat multi-factorial diseases such as Alzheimer's. Our research group⁽⁵¹⁻⁵⁴⁾ has been involved in this topic for several years designing and synthesizing dual binding compounds addressed against this terrible neurodegenerative disease. With the aim of continuing this work, we have developed a series of "oxa" and "aza" heterocycles able to simultaneously improve the cholinergic system through the inhibition of AChE and BuChE and to slow down the self and the AChE-induced A β aggregation. Additionally, compounds with β -secretase (BACE) inhibitory activity have been developed with the aim of blocking A β formation. The thesis can be divided in two parts: part A, dealing with compounds having a benzofuran related motif, and part B, with THA related compounds.

PART A



The benzofuran moiety is abundant both in natural and synthetic molecules possessing potent biological activities. Compounds carrying the mentioned motif are known for having a good binding affinity for A β ₍₁₋₄₂₎, being an isosteric analogue of Thioflavin-T (the dye used to visualize plaques composed of A β found in the brains of Alzheimer's disease patients). A series of benzofuran derivatives⁽⁵⁵⁾ was synthesized by scientists of Smith Kline Beecham Pharmaceuticals

that are able to block A β self-aggregation at μ M concentration. According to the MTDL approach, we decided to synthesize a series of hybrid compounds (see chart 1A) carrying the benzofuran motif of SKF-64346 linked through an appropriate heptyloxy spacer to a *N*-methylbenzylamine moiety, that in our previous works^(52,54,56-57) resulted good at contacting the anionic binding site within the AChE gorge, inhibiting ACh breakdown by means of cation- π interactions with Trp⁸⁶. Afterwards, we performed SAR studies on our lead compound **4c** modifying both the furan ring and the alkyloxy chain. In the first case a series of Friedel & Craft acylations at C₃ of the benzofuran ring led to derivatives able to modulate A β self-aggregation measured on the A β ₂₅₋₃₅ fragment (**11-28**, **35-37**, **39-40**). A methoxy substituent was introduced at C₆ position to evaluate the effect on the anti-aggregatory activity (**62**) Furthermore, a methylene insertion at C₂ has been made to evaluate whether the coplanarity between the two aromatic rings plays a role towards the biological activity or not (**66**). In the second case, we have tried to optimize the cholinesterase activity by shortening and lengthening the alkyloxy spacer chain (**4a-b**, **4d-e** and **6-10**), and moving this latter from the

para to the *meta* position of the phenyl ring searching for the optimal orientation within the gorge of AChE (**4f**, **21-28**). A carbamic derivative (**30**) has been synthesized to evaluate a different inhibitory mechanism involving the catalytic triad.

Chart 1A

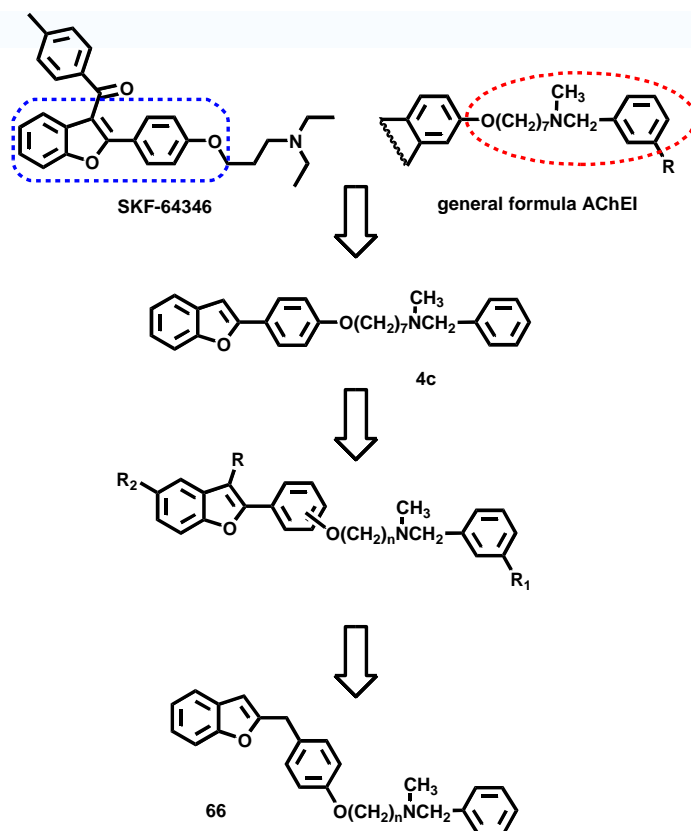
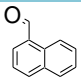
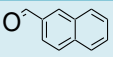
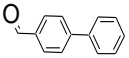
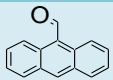


Fig. 12. Representation of the rationale underlying part A. Linking two different moieties, each one addressing to a different target, results in the realization of hybrid compounds with combined activity.

Compound	R	R ₁	R ₂	n	Chain position
4a	H	H	H	3	para
4b	H	H	H	5	para
4c	H	H	H	7	para
4d	H	H	H	8	para
4e	H	H	H	9	para
4f	H	H	H	7	meta
6	COC ₆ H ₄ - <i>p</i> -OCH ₃	H	H	3	para
7	COC ₆ H ₄ - <i>p</i> -OCH ₃	H	H	5	para
8	COC ₆ H ₄ - <i>p</i> -OCH ₃	H	H	7	para
9	COC ₆ H ₄ - <i>p</i> -OCH ₃	H	H	8	para
10	COC ₆ H ₄ - <i>p</i> -OCH ₃	H	H	9	para
11	COCH ₃	H	H	7	para
12	COC ₆ H ₅	H	H	7	para

13	$\text{COC}_6\text{H}_4\text{-}m\text{-CH}_3$	H	H	7	para
14	$\text{COC}_6\text{H}_4\text{-}p\text{-CH}_3$	H	H	7	para
15	$\text{COC}_6\text{H}_4\text{-}m\text{-OCH}_3$	H	H	7	para
16	$\text{COC}_6\text{H}_4\text{-}m,p\text{-OCH}_3$	H	H	7	para
17		H	H	7	para
18		H	H	7	para
19		H	H	7	para
20		H	H	7	para
21	COC_6H_5	H	H	7	meta
22	$\text{COC}_6\text{H}_4\text{-}p\text{-CH}_3$	H	H	7	meta
23	$\text{COC}_6\text{H}_4\text{-}m\text{-CH}_3$	H	H	7	meta
24	$\text{COC}_6\text{H}_4\text{-}m\text{-OCH}_3$	H	H	7	meta
25	$\text{COC}_6\text{H}_4\text{-}o\text{-OCH}_3$	H	H	7	meta
26	$\text{COC}_6\text{H}_4\text{-}m,p\text{-OCH}_3$	H	H	7	meta
27	$\text{COC}_6\text{H}_4\text{-}o,m\text{-OCH}_3$	H	H	7	meta
28	$\text{COC}_6\text{H}_4\text{-}3,5\text{-OCH}_3$	H	H	7	meta
30	$\text{COC}_6\text{H}_4\text{-}p\text{-CH}_3$	OCONHCH_3	H	7	para
35	$\text{COC}_6\text{H}_4\text{-}p\text{-O}(\text{CH}_2)_2\text{NEt}_3$	H	H	7	para
36	$\text{COC}_6\text{H}_4\text{-}m\text{-O}(\text{CH}_2)_2\text{NEt}_3$	H	H	7	para
37	$\text{COC}_6\text{H}_4\text{-}p\text{-O}(\text{CH}_2)_2\text{morpholine}$	H	H	7	para
39	$\text{COC}_6\text{H}_4\text{-}p\text{-CH}_2\text{NEt}_3$	H	H	7	para
40	$\text{COC}_6\text{H}_4\text{-}m\text{-CH}_2\text{NEt}_3$	H	H	7	para
62	H	H	OCH_3	7	para

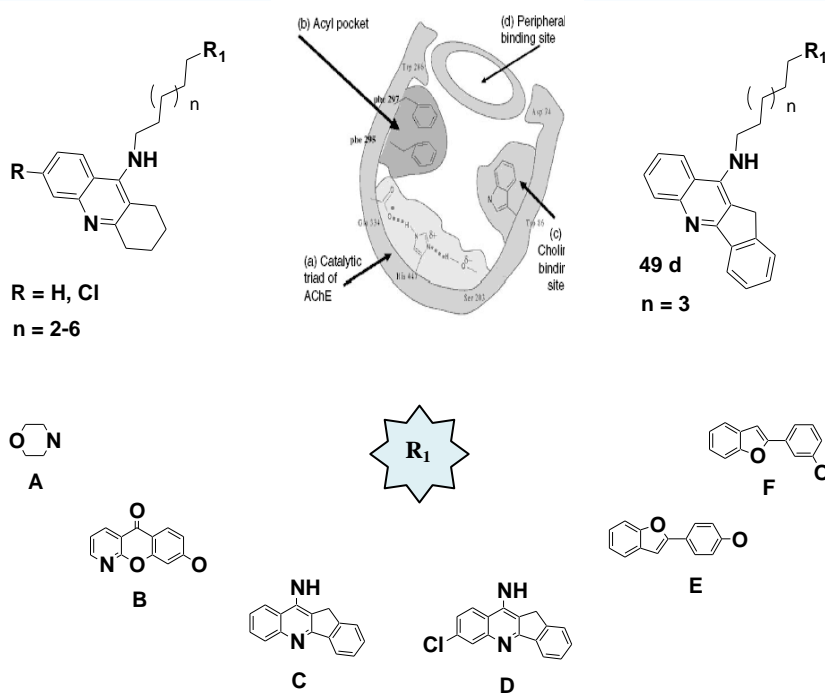
Tab. 3. Summary of compounds synthesized within part A with the exception of **66** previously shown in chart 1A

PART B

Despite several reports about modifications of the tetrahydroaminoacridine nucleus (THA) and the structure-activity relationships studies (SAR) of this class of compounds, the study of tacrine analogues is still of interest to medicinal chemists dealing with AD research worldwide. In particular, following the MTDL paradigm, heterodimeric structures have led to very interesting compounds designed with the aim of conferring, two or even more biological activities, implicated in the selected pathology to the same molecule. Here follows our contribute to the topic. Part of the work was aimed at connecting through an alkyl tether of a variable length (6-10 carbons) the 1,2,3,4-tetrahydroacridine moiety (known for firmly being stacked against the aromatic rings of Trp⁸⁶ and Tyr³³⁷ at the catalytic site of human AChE) to a morpholinic ring, that could be able to interact with Trp²⁸⁶ at the PAS, inhibiting the AChE-induced A β aggregation. Morpholine has been chosen among other aliphatic bases because of its more favorable pharmacokinetic properties (**45a-**

e). We kept then the heptyl chain as the optimal spacer and replaced morpholine by different heterocyclic scaffolds previously reported by our research group (azaxanthone⁽⁵⁸⁾, indenoquinoline⁽⁵⁹⁻⁶¹⁾ and benzofuran⁽⁶²⁾ cores) obtaining compounds **52**, **49a**, **53a-b**. With the aim of improving the cholinesterase activity, a chlorine atom was introduced in position 6 of the THA ring on the tacrine-indenoquinoline hybrid compound **49b**, furthermore to selectively address the 6-Cl-THA moiety towards the catalytic site, an analogue of **49b** was synthesized carrying a further chlorine atom in position 7 of the indenoquinoline ring so that, because of the steric hindrance, this latter shouldn't penetrate within the gorge of the enzyme (**49c**). An indenoquinolinic homodimer (**49d**) was synthesized as well.

Chart 1B



Compound	R	R ₁	n
45a	H	A	2
45b	H	A	3
45c	H	A	4
45d	H	A	5
45e	H	A	6
49a	H	C	3
49b	Cl	C	3
49c	Cl	D	3
49d		C	3
52	H	B	3
53a	Cl	E	3
53b	Cl	F	3

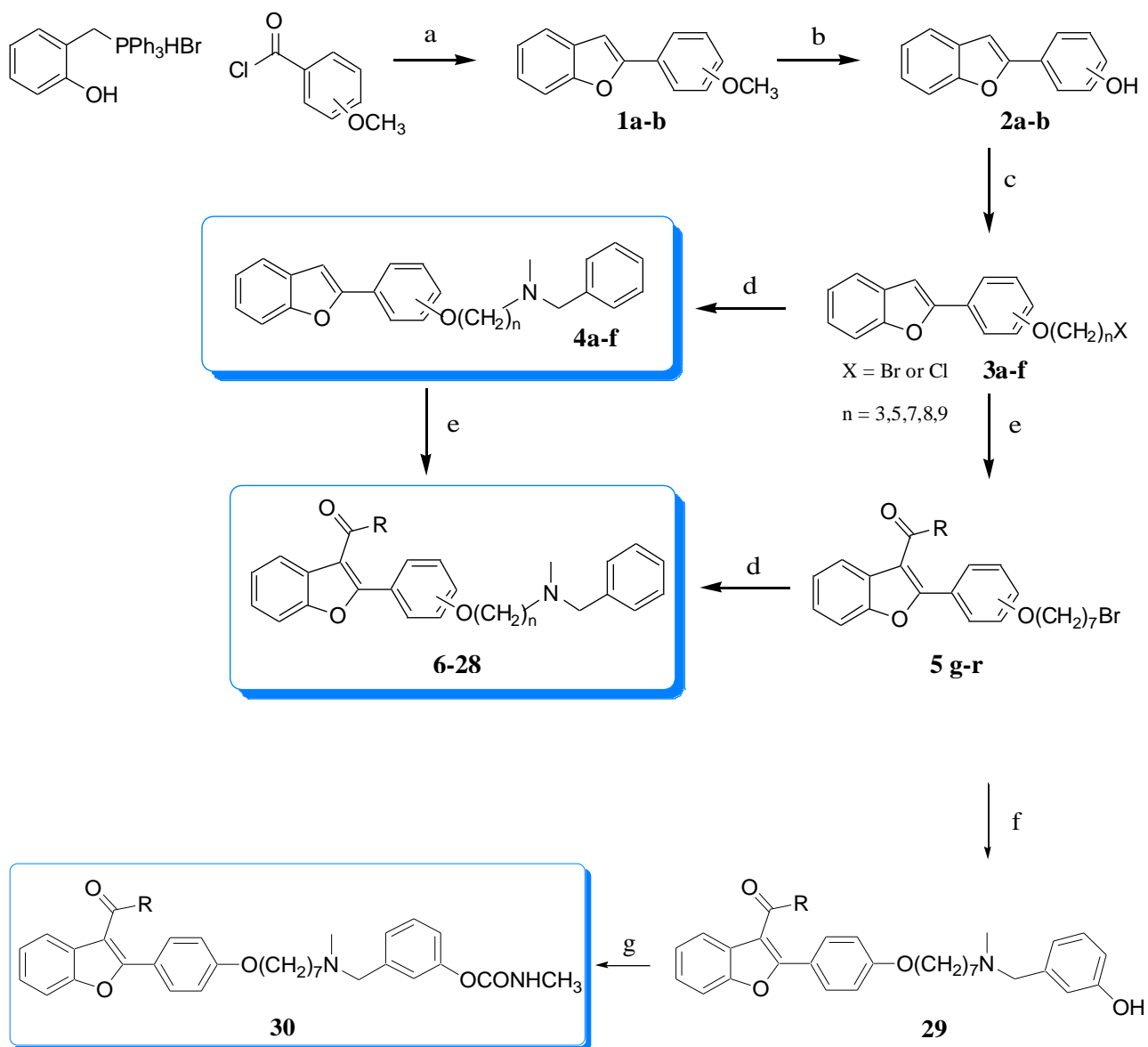
Fig. 13. Representation of the rationale underlying part B. **Tab. 4.** Summary of compounds synthesized within part B.

3. Chemistry

PART A

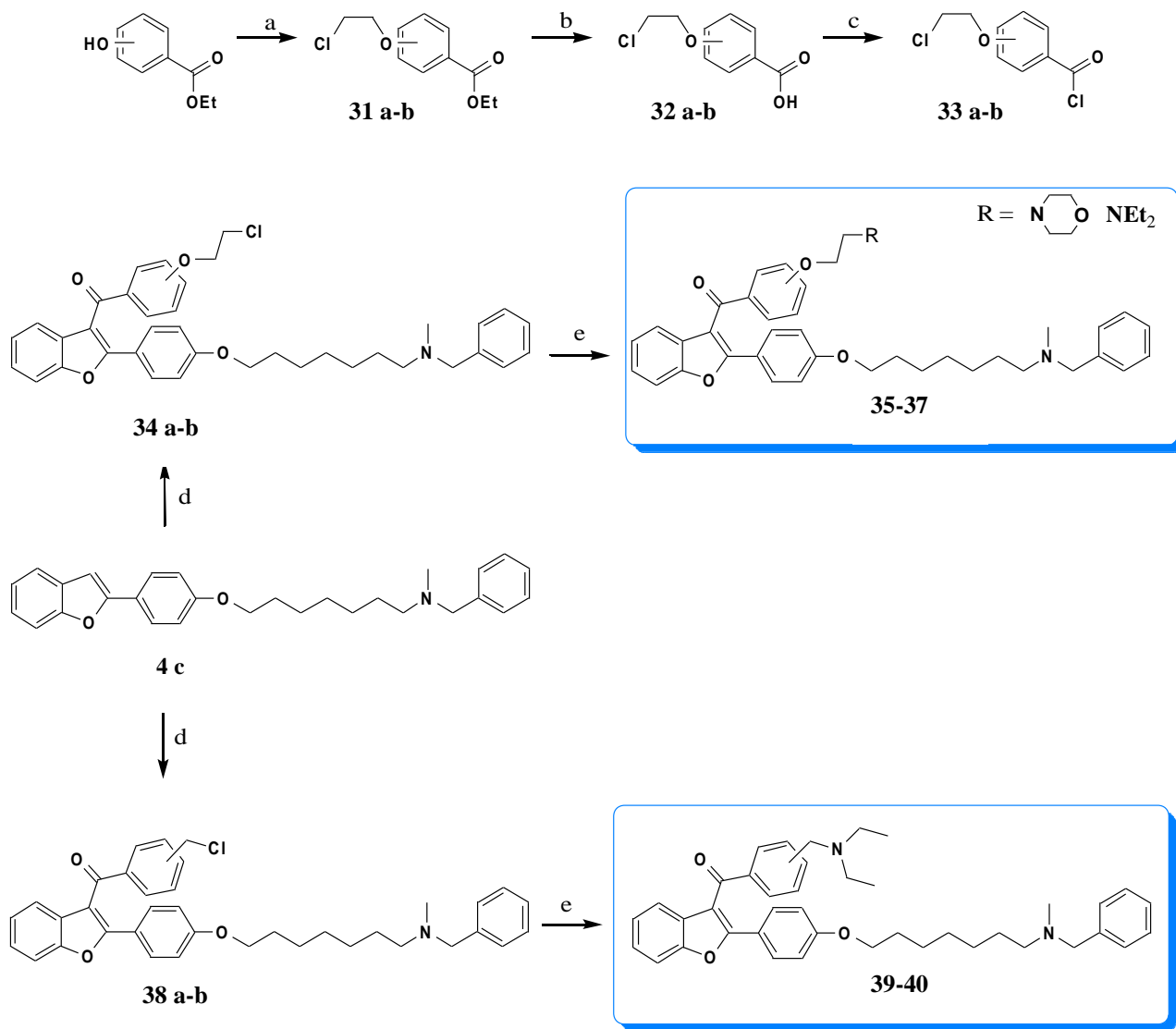
The reported benzofuran derivatives were prepared by conventional synthetic methods. In scheme 1A, the synthesis of compounds **6-28** and **30** is illustrated. The first step is a modified intramolecular Wittig reaction leading to the formation of the benzofuran rings in moderate-good yields (**1a-b**). Demethylation with BBr_3 proved to be very effective on this substrate affording, in almost quantitative yield, the corresponding phenols (**2a-b**), that subsequently underwent alkylation with di-alo-alkyl-chains of various length using K_2CO_3 as the base and affording alo-alkyloxy-derivatives in good to moderate yields (**3a-f**). Condensation with *N*-benzylmethylamine by refluxing in toluene afforded compounds **4a-f**, in low to moderate yields. A series of Friedel & Craft acylations, with selected acylchlorides, occurring at position 3 of the furanic ring, afforded compounds **6-20**, in generally poor yields. Performing F&C acylations prior than condensation with *N*-benzylmethylamine proved to be a better strategy affording compounds **21-28** in higher overall yields. The synthesis of **30** required condensation of {2-[4-(7-Bromoheptyloxy)phenyl] benzofuran-3-yl}-*p*-tolylmethanone with 3-Methyl amino methylphenol followed by carbamoylation using NaH and Methyl isocyanate in DCM. Scheme 2A illustrates the synthesis of compounds **35-37** and **39-40**. In these cases **4c** represents the key intermediate that underwent diversification by means of opportune F&C acylations, followed by condensations with selected amines, such as Et_3N and Morpholine. Scheme 3A illustrates the synthesis of compound **62**. In particular, it is necessary to first prepare the non commercial (2-Hydroxy-5-methoxy-benzyl)-triphenylphosphonium bromide (**55**) by reducing 2-Hydroxy-5-methoxy benzaldehyde to the corresponding benzylic alcohol (**54**) with NaBH_4 , and then treating **54** with Triphenylphosphonium bromide. **55** undergoes intramolecular Wittig reaction with 4-Benzyloxybenzoyl chloride (**58**). Removal of the protective group is conducted by hydrogenolysis leaving the phenolic function (**60**) available for the further sequence of reactions similar to those already described for the synthesis of **4c**. Scheme 4A illustrates the synthesis of **66** which follows the same route for preparing **4c** with the only difference of using 4-Methoxyphenylacetyl chloride as the starting material.

Scheme 1A



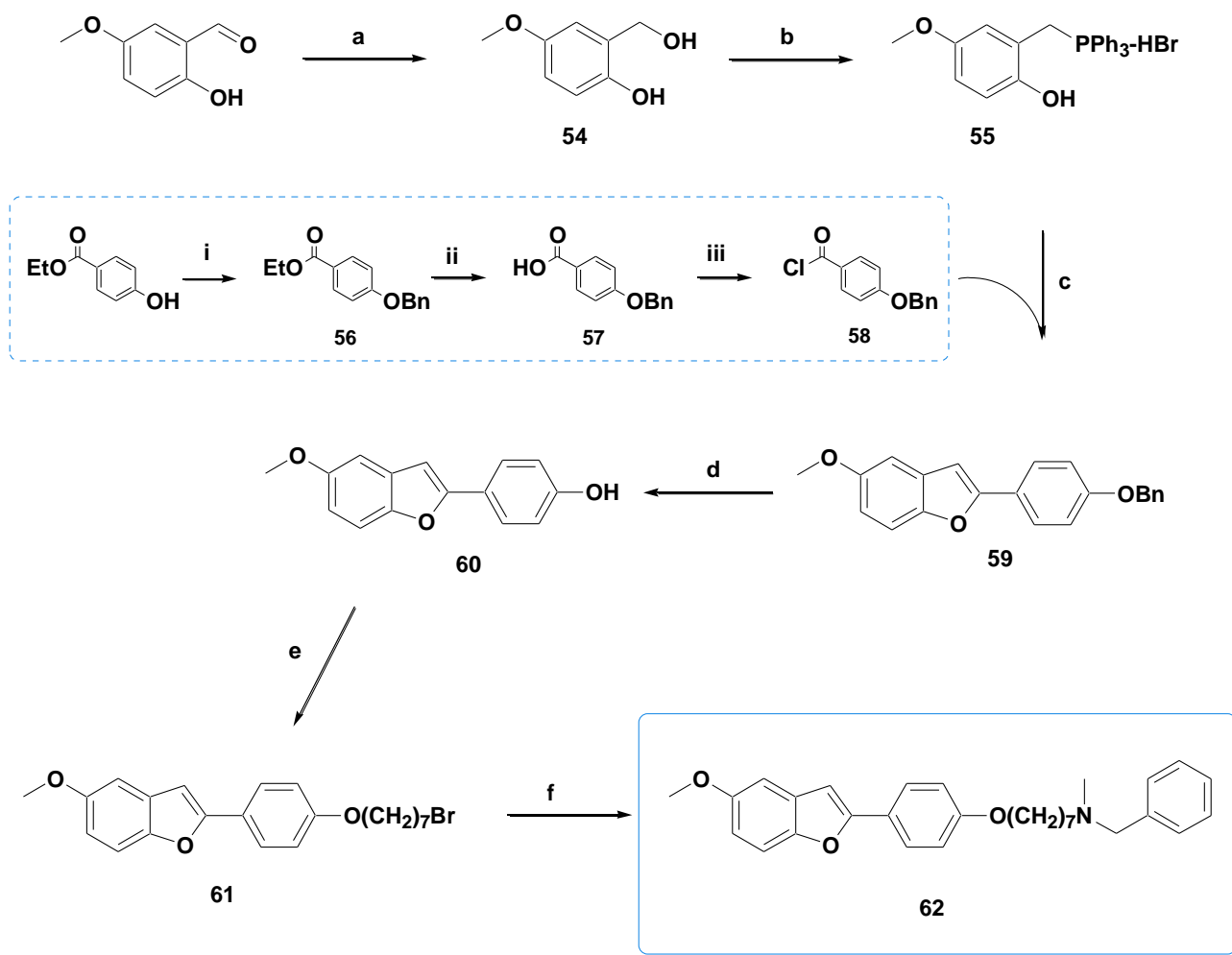
Reagents and conditions: a) Et_3N , Toluene, reflux; b) BBR_3 , DCM , r.t.; c) $\text{X}(\text{CH}_2)_n\text{X}$, K_2CO_3 , Acetone, reflux; d) *N*-benzylmethylamine, Toluene, reflux; e) selected acylchloride, SnCl_4 , DCM , r.t.; f) 2-[4-(7-Bromoheptyloxy)phenyl]benzofuran-3-yl]-*p*-tolylmethanone, 3-Methylamino methyl phenol, Toluene, reflux; g) Methylisocyanate, NaH , DCM , r.t.

Scheme 2A



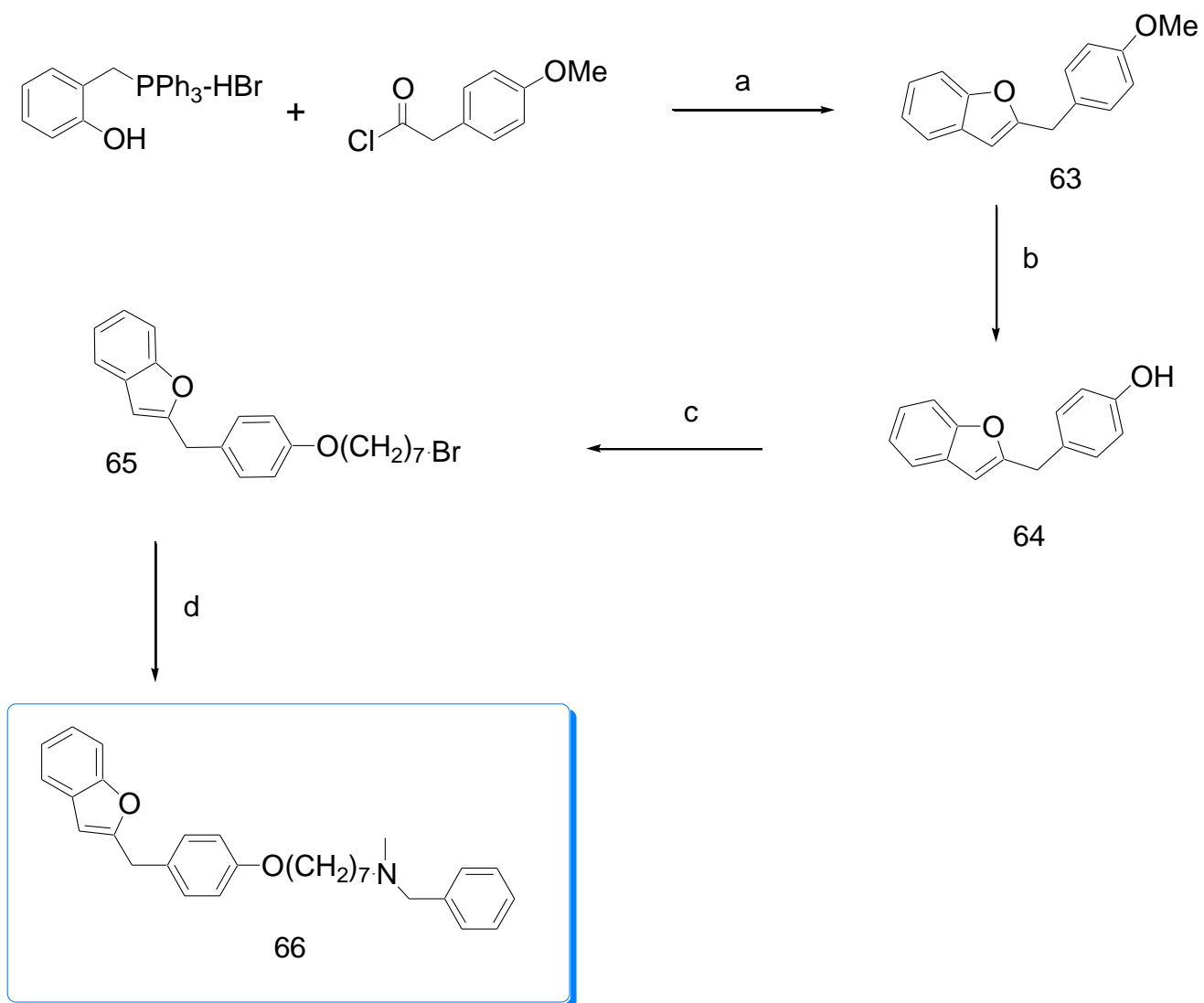
Reagents and conditions: a) Br(CH₂)₂Cl, K₂CO₃, Acetone, reflux; b) NaOH, EtOH, reflux; c) SOCl₂, reflux; d) selected acylchloride, SnCl₄, DCM, r.t.; e) selected amine, Toluene, reflux;

Scheme 3A



Reagents and conditions: a) NaBH_4 , EtOH, r.t.; b) $\text{PPh}_3\text{-HBr}$, acetonitrile, reflux; c) Et_3N , Toluene, reflux; d) H_2 , Pd/C, THF, r.t.; e) 1,7-Dibromoheptane, K_2CO_3 , Acetone, reflux; f) *N*-methylbenzylamine, Toluene, reflux. i) BnBr , K_2CO_3 , Acetone, reflux; ii) NaOH , EtOH, reflux; iii) SOCl_2 , reflux.

Scheme 4A

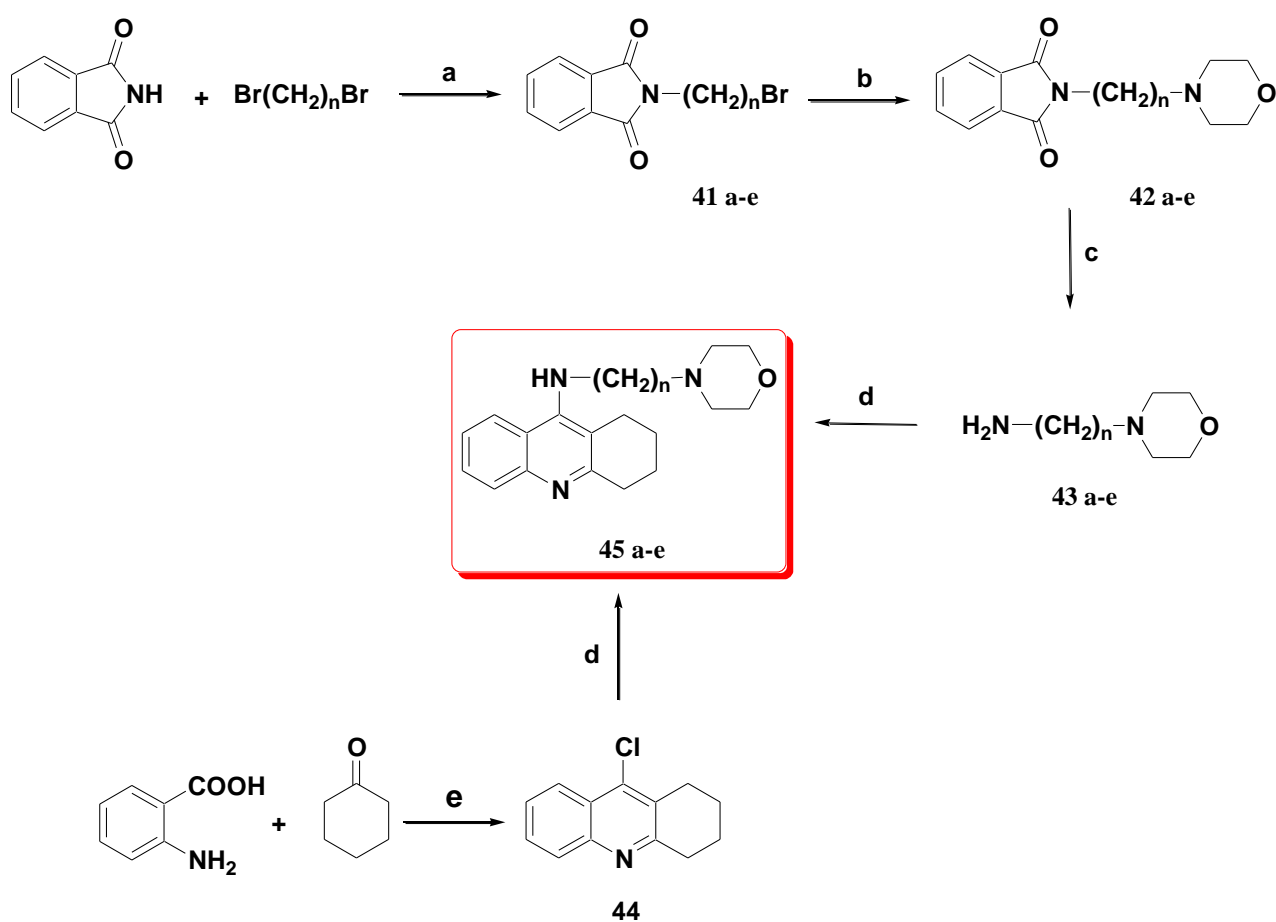


Reagents and conditions: a) Et₃N, Toluene, reflux; b) BBr₃, DCM, r.t.; c) Br(CH₂)₇Br, K₂CO₃, Acetone, reflux; d) *N*-benzylmethanamine, Toluene, reflux.

PART B

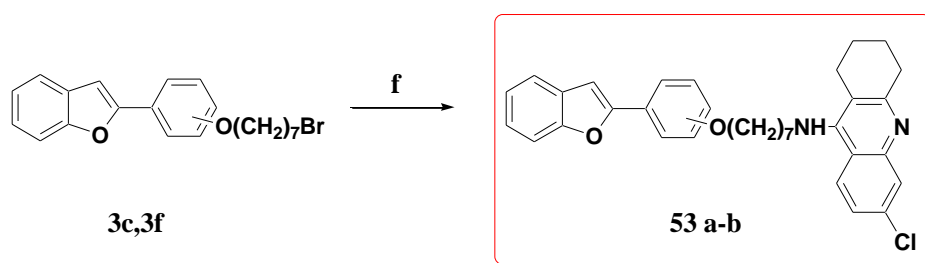
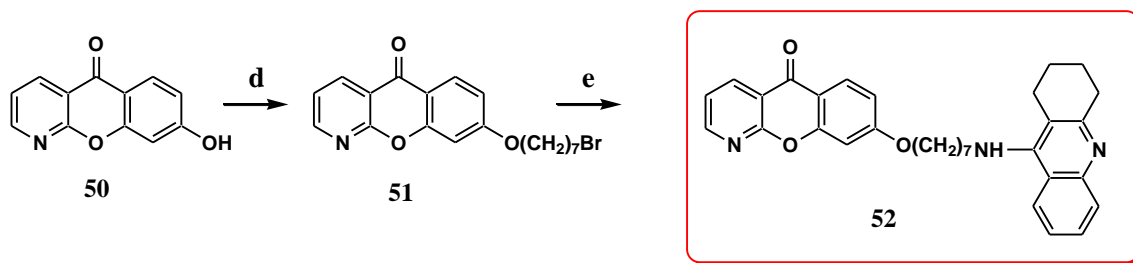
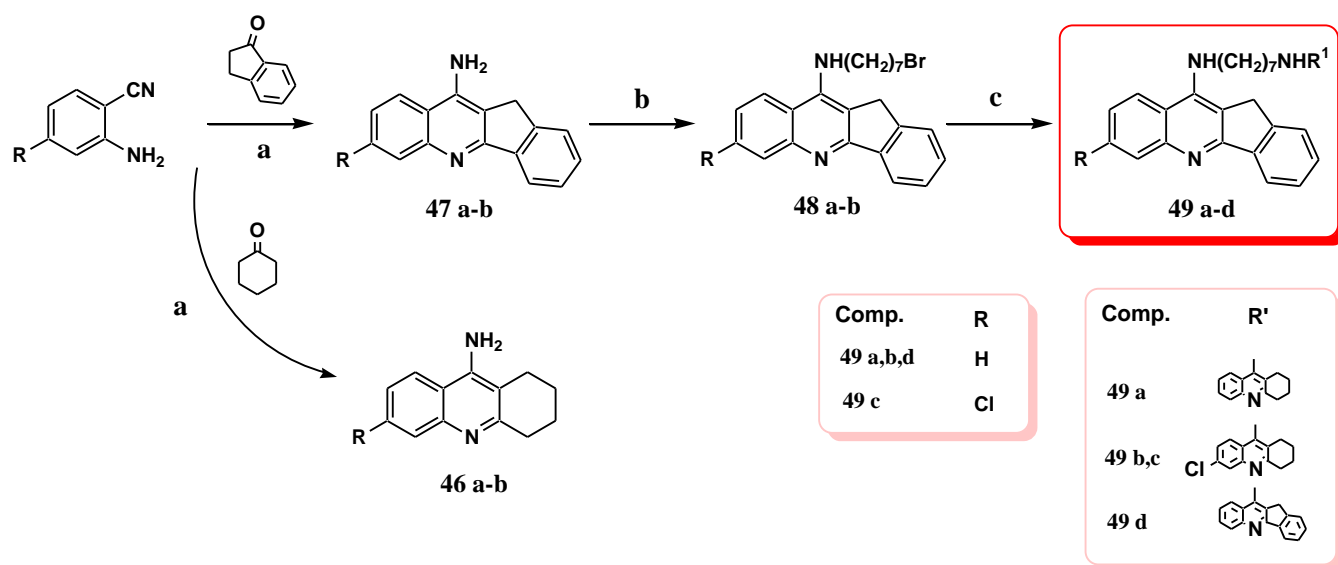
The reported tacrine derivatives were prepared by conventional synthetic methods. In scheme 1B, dibromoalkyl-chains of various length (6 to 10 carbons) were turned to primary amines using Gabriel's procedure. In particular, after creating the phthalic end, **41a-e** bromoalkyl derivatives were reacted with Morpholine, affording **42a-e** subsequently converted in **43a-e** using hydrazine. Aromatic substitution of **43a-e** with **44**, previously obtained by reacting anthranilic acid with cyclohexanone in POCl₃, afforded compounds **45a-e**. In scheme 2B, the synthesis of compounds **49a-d** started by building intermediates **46a-b** and **47a-b**, prepared by condensation of the selected anthranilonitrile with cyclohexanone or indanone, respectively in the presence of ZnCl₂. These latter were reacted with 1,7-dibromoheptane in DMSO made basic by KOH affording **48a-b**, subsequently condensed with **46a-b** and **47a** to give the desired compounds **49a-d**. Synthesis of **52** was accomplished starting from azaxanthone **50** which undergoes alkylation with 1,7-dibromoheptane giving the bromoheptyloxy-derivative (**51**), subsequently condensed with **46a** using a phase transfer catalyst in an heterogeneous medium made of DCM and 50% NaOH solution. Finally, compounds **53a-b** were obtained by reacting intermediates **3c** and **3f** with **46b** at room temperature in DMSO, using KOH as the base.

Scheme 1B



Reagents and conditions: a) DMF, reflux; b) Morpholine, Toluene, reflux; c) Hydrazine monohydrate, EtOH, reflux, then HCl; d) PhOH, 130 °C; e) POCl₃, reflux.

Scheme 2B



Reagents and conditions: a) ZnCl_2 , $130\text{ }^\circ\text{C}$; b) $\text{Br}(\text{CH}_2)_7\text{Br}$, KOH , DMSO , r.t.; c) **46a-b** or **47a** KOH , DMSO , r.t.; d) $\text{Br}(\text{CH}_2)_7\text{Br}$, K_2CO_3 , Acetone, reflux; e) **46a**, tetra-*n*-butyl ammonium hydrogen sulphate, NaOH/DCM 50%, r.t.; f) **46b**, KOH , DMSO , r.t.

4. Results and discussion

In this section, available biological data are shown and discussed. Parts A and B deal respectively with benzofuran and tacrine derivatives. A detailed description of analysis procedures used for testing the activity of our compounds is reported at the end of the experimental section.

PART A

The inhibitory activities of the newly synthesized compounds against both cholinesterases were studied using the method of Ellman⁽³³⁾ to determine the rate of acetylthiocholine or butyrylthiocholine hydrolysis in the presence of the inhibitor and are reported in Table 5, expressed as IC₅₀ values. The inhibitory activity of A β fibril formation was studied with an original in vitro assay that uses UV-vis measurements and electron microscopy⁽³⁴⁾ (Figure 14). The A β ₂₅₋₃₅ amino acid peptide, which preserves the properties of neurotoxicity and aggregation, was used.^(35,36) For the compounds exhibiting an inhibitory activity at least equal to that of curcumin (compound reported to have antiamyloidogenic properties⁽³⁷⁾), IC₅₀ values were calculated as reported in Table 5. The neuroprotective effects of the most interesting A β antiaggregating compounds were also determined against the A β ₂₅₋₃₅ peptide induced toxicity in human neuronal like SH-SY5Y cells using a colorimetric MTT assay^(38,39) (Table 6 and Figure 15).

C	R	R ₁	R ₂	n	Chain	AChE IC ₅₀ μ M	BuChE IC ₅₀ μ M	A β ₂₅₋₃₅ IC ₅₀ μ M
4a	H	H	H	3	para	>10	136 \pm 10	
4b	H	H	H	5	para	215 \pm 1	6.60 \pm 0.23	
4c	H	H	H	7	para	32.6 \pm 11.9	0.28\pm0.02	7.0
4d	H	H	H	8	para	>10	7.47 \pm 0.34	
4e	H	H	H	9	para	>10	55.6 \pm 7.4	5.5
4f	H	H	H	7	meta	>10	3.00 \pm 0.17	3.9
8	COC ₆ H ₄ - <i>p</i> -OCH ₃	H	H	7	para	281 \pm 95	89.1 \pm 1.6	
11	COCH ₃	H	H	7	para	17.4 \pm 1.0	1.83\pm0.12	
12	COC ₆ H ₅	H	H	7	para	40.7 \pm 3.5	38.1 \pm 2.2	12.5
13	COC ₆ H ₄ - <i>m</i> -CH ₃	H	H	7	para	127 \pm 42	40.9 \pm 1.1	

14	$\text{COC}_6\text{H}_4\text{-}p\text{-CH}_3$	H	H	7	para	10.5±1.3	1.82±0.09	13.0
15	$\text{COC}_6\text{H}_4\text{-}m\text{-OCH}_3$	H	H	7	para	127±10	21.7±1.6	
16	$\text{COC}_6\text{H}_4\text{-}m,p\text{-OCH}_3$	H	H	7	para	177±43	74.1±0.2	
30	$\text{COC}_6\text{H}_4\text{-}m\text{-CH}_3$	OCONHCH ₃	H	7	para		0.34±0.03	
35	$\text{COC}_6\text{H}_4\text{-}p\text{-O(CH}_2)_2\text{NEt}_3$	H	H	7	para	24.3		
36	$\text{COC}_6\text{H}_4\text{-}m\text{-O(CH}_2)_2\text{NEt}_3$	H	H	7	para	37.1±6.0		
37	$\text{COC}_6\text{H}_4\text{-}p\text{-O(CH}_2)_2\text{morpholine}$	H	H	7	para	39.9±0.5		
39	$\text{COC}_6\text{H}_4\text{-}p\text{-CH}_2\text{NEt}_3$	H	H	7	para	100		
40	$\text{COC}_6\text{H}_4\text{-}m\text{-CH}_2\text{NEt}_3$	H	H	7	para	52.9		
Rivastigmine							3.03±0.21	0.30±0.01
Curcumine								10

Tab. 5. Available data within the benzofuran derivatives series

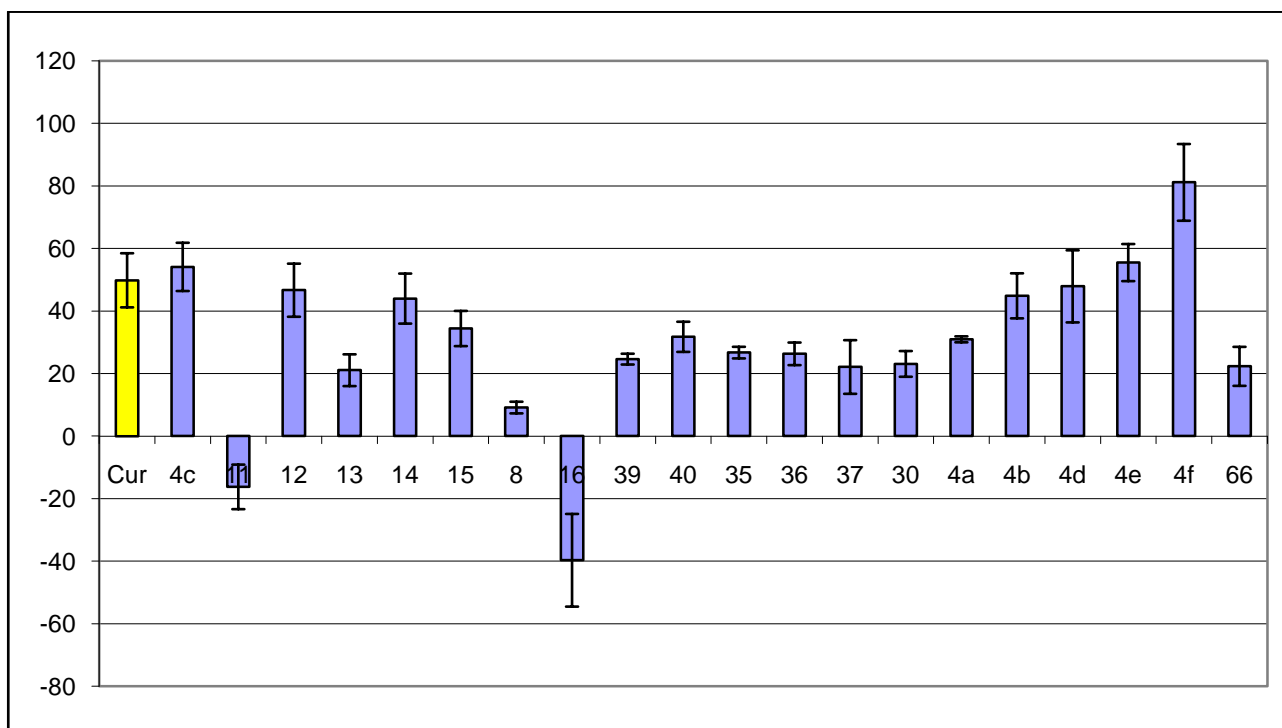
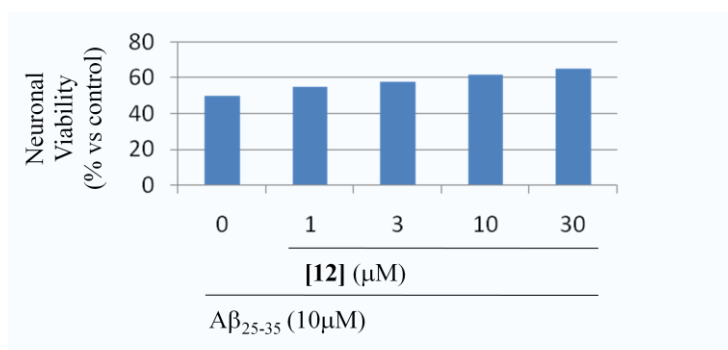


Fig. 14. β_{25-35} fibril inhibition compared to that of curcumin. The mean \pm SD values from three independent experiments are shown.

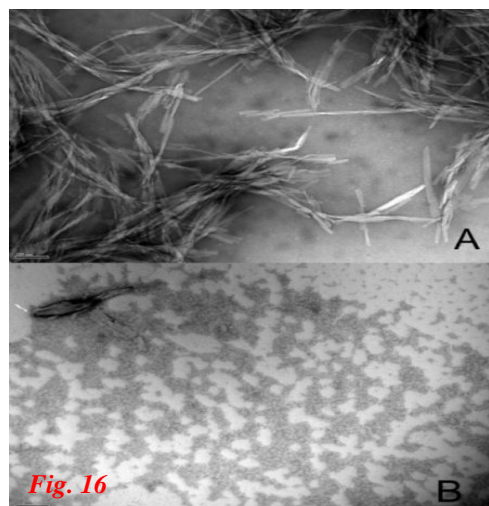


Compound	$A\beta_{25-35}$ IC_{50} μM (human neuronal SH-SY5Y cells)
4c	nd
12	5.6

Fig.15. Compound **12** protects human neuronal SH-SY5Y cells $A\beta_{25-35}$ peptide induced toxicity. The neuronal viability was determined by the MTT assay (as described in Supporting Information) after 3 h of incubation with 10 μM $A\beta_{25-35}$ peptide in the presence or absence of various concentrations of **3**. The results are expressed as percentage of control cells. **Tab.6.** Neuroprotective activity of **12** on human neuronal cells SH-SY5Y

The anticholinesterase activity of the new molecules proved to be generally better toward BuChE than AChE. In detail, **11** and **14** showed the best AChE inhibitory activity of the series (17.4 and 10.5 μM , respectively), still keeping a fairly good BuChE inhibition (1.83 and 1.82 μM , respectively), probably as a consequence of a higher affinity. There are differences in terms of topology between AChE and BuChE, since in this latter enzyme Lys²⁸⁶ and Val²⁸⁸ line the gorge, compared to the large Phe of the corresponding residues of AChE, and this could allow bulky compounds to better fit inside the gorge of BuChE and to stabilize its occupancy probably by means of hydrophobic interactions. In particular **4c**, the lead compound, was found to possess a good BuChE inhibitory activity (0.28 μM), about 100-fold higher than its activity toward AChE. Several lines of evidence indicate that BuChE might be a co-regulator of the activity of the neurotransmitter ACh⁽⁴⁰⁾ and that it might be important to inhibit this enzyme in the treatment of AD. Several drugs that proved to be selective BuChE inhibitors have been evaluated; for example, rivastigmine showed clinical efficacy without remarkable side effects.⁽⁴¹⁾ It is intriguing that specific BuChE inhibitors not only improve cognition, presumably through an increase in acetylcholine concentration, but also reduce levels of APP, which is the source of $A\beta$ peptide, the main component of plaques in AD. The effect of these compounds on APP seems to be independent of their ability to inhibit BuChE enzymatic activity, and it has been suggested that it involves interactions with interleukin-1, a proinflammatory molecule that has also been implicated in the pathogenesis of AD.⁽⁴²⁾ Compounds bearing a second amine moiety, such as **35-37** and **39-40**, were not able to improve AChE inhibition. Compound **30** bearing a methylcarbamic group (acting as a pseudo-irreversible inhibitor), showed an higher activity ($IC_{50} = 0.34 \pm 0.029$ μM) compared to the

reference rivastigmine ($IC_{50} = 3.03 \pm 0.21 \mu M$) toward AChE (Data for BuChE not available). Compared to **4c**, compounds with shorter or longer spacer-chains such as **4a-b** and **4d-e** showed no activity toward AChE ($IC_{50} > 10 \mu M$), while **4b** and **4d** kept a fairly good activity toward BuChE ($IC_{50} = 6.60 \pm 0.23 \mu M$ and 7.47 ± 0.34 respectively). Moving the heptyloxy chain from para to meta position of the phenyl ring (**4f**) lowered the activity toward BuChE, losing AChE inhibition compared to our lead compound. Regarding $A\beta$ fibril inhibition, **4c** showed a higher potency compared to that of the standard curcumin ($IC_{50} = 7$ and $10 \mu M$, respectively). Acylation of **4c** with acetylchloride led to **11**, whose activity was surprisingly proaggregatory, whereas acylation of **4c** with benzoyl chloride retained the activity (**12**, $IC_{50} = 12.5 \mu M$), suggesting that the introduction of an aryl moiety in position 3 of the benzofuran ring was tolerated. Modifications of **12** by the introduction of a methyl group in the meta or para position on the aryl group led respectively to **13** and **14** and resulted in a lower activity for **13**, whereas **14** retained the potency of the unsubstituted **12**. In the opposite direction, the introduction of a methoxy group in the meta position (**15**) resulted in a slightly lower but still remarkable activity, though moving the methoxy group from the meta to the para position (**16**) was considerably detrimental for the activity. Moreover, the acylation of **4c** with 3,4-dimethoxybenzoyl chloride led to **16**, which surprisingly proved to have remarkable proaggregating activity. Compounds **30**, **35-37** and **39-40** proved to weakly inhibit amyloid aggregation. The chain length turned out to play a role too, since the propyloxy derivative **4a** had a poor inhibition, while moving through the homologous series the activity rose. Pentyloxy (**4b**) and octyloxy (**4d**) derivatives showed their selves being equactive with the standard curcumin, while nonyloxy derivative was more active (**4e**, $IC_{50} = 5.5 \mu M$). The most potent inhibitor of the series (**4f**, $IC_{50} = 3.9 \mu M$) was obtained by moving the heptyloxy chain to the meta position. The assembly of $A\beta$ aggregates, derived from $A\beta$ oligomers, into fibrils is toxic to neurons. The formation of $A\beta$ is related to protein misfolding, since the conformational transition to β -sheet leads



to a faster formation of aggregates.⁽⁴³⁾ Thus, compounds that are able to slow or block the amyloid polymerization process could be considered potential drugs for inhibition of AD progression. During incubation of $A\beta$ in the presence of **4c**, only small bulk aggregates were visible and no characteristic $A\beta$ fibrils were observed in the electron micrographs (Figure 16). Interestingly, **12** also showed a marked neuroprotective effect against $A\beta_{25-35}$ peptide induced neurotoxicity (Tab. 6). As reported in Figure 15,

treatment of SH-SY5Y cells with **12** at 10 and 30 μM significantly reduced the neuronal viability loss evoked by $A\beta_{25-35}$ peptide, in a dose-dependent manner, with a maximum of inhibition of 63%. Since the same trend was not observed with **4c**, these results prove that the modification of **4c** by introduction of an aryl moiety in the benzofuran ring is crucial for the observed neuroprotective effects. $A\beta_{25-35}$ peptide contains a number of hydrophobic residues (i.e., Ile³¹, Ile³², and Met³⁵) that are critical for neurotoxicity and aggregation processes.^(44,45) In this regard, recent studies have suggested that unaggregated $A\beta_{25-35}$ and $A\beta_{31-35}$ peptides could initiate a cascade of events leading to neurotoxicity solely after their internalization within the neuronal cells.⁽⁴⁶⁾ Neuroprotective effects of **12** against $A\beta_{25-35}$ toxicity could be ascribed to its hydrophobic properties (compare **12** with **4c**: 8.00 vs 6.80 log *P*) and its ability to block the interaction of $A\beta_{25-35}$ with the lipid bilayer of the neuronal plasma membrane. It is therefore reasonable to predict that there are adequate opportunities for functionally important hydrophobic interactions between **12** and the $A\beta_{25-35}$ peptide. Thus, these preliminary results could encourage further studies to elucidate the neuroprotective mechanisms of **12**.

PART B

The inhibitory activities of the newly synthesized compounds against both cholinesterases were studied using the method of Ellman⁽³³⁾ to determine the rate of acetylthiocholine or butyrylthiocholine hydrolysis in the presence of the inhibitor and are reported in Table 7, expressed as IC₅₀ values together with data from BACE 1 inhibition obtained by spectrofluorometric analyses. Docking simulations were carried out by means of the GOLD software 6 (v.3.0.1) and using the crystal structure of human AChE (figure 17).

Compound	R	R ₁	n	AChE IC ₅₀ (nM)	BuChE IC ₅₀ (nM)	BACE % inib	BACE IC ₅₀ (μM)
45a	H	A	2	68.9 \pm 3.8	101 \pm 4		
45b	H	A	3	44.5 \pm 3.1	90.5 \pm 0.4		
45c	H	A	4	16.5 \pm 0.8	42.8 \pm 1.5		
45d	H	A	5	34.0 \pm 1.6	38.1 \pm 0.9		
45e	H	A	6	28.4 \pm 1.8	14.7 \pm 1.5		
49a	H	C	3	13.9 \pm 2.1	24.8 \pm 0.8	36.12	
49b	Cl	C	3	1.22\pm0.13		78.16	0.97

49c	Cl	D	3	4.59±0.87	
49d		C	3	45.5±2.6	28.6±1.5
52	H	B	3	283±6	101±6
53a	Cl	E	3	242±12	
53b	Cl	F	3	146±8	
Tacrine				250±10	50±2.0

Tab. 7. Available data for the tacrine derivatives series

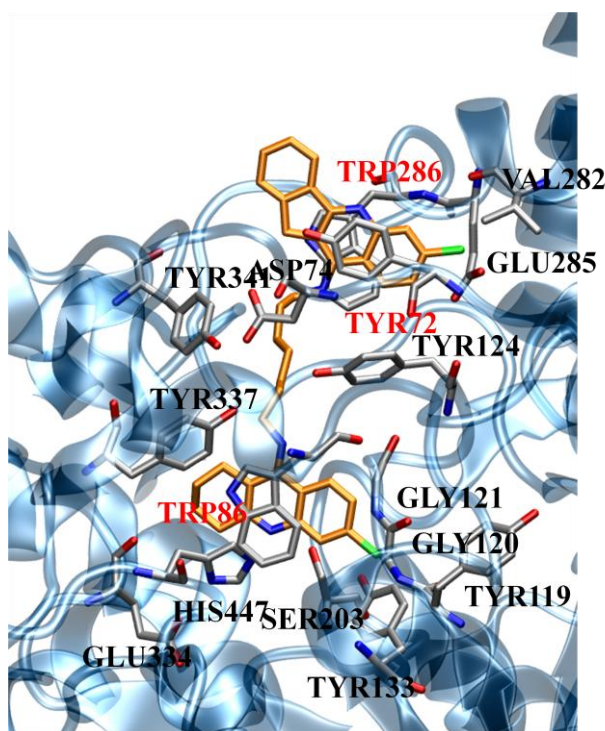


Fig. 17. Docking simulation of compound **49c** within the human AChE gorge.

With regard to the AChE inhibition, all the new molecules (with the exception of **52**) proved to be more active compared to the standard tacrine. Compounds **49b** and **49c** were the most active of the series at AChE inhibition ($IC_{50} = 1.22 \pm 0.13 \mu\text{M}$ and $4.59 \pm 0.87 \mu\text{M}$ respectively). In light of this increased activity, a docking study of **49c** was performed, (figure 17) pointing out the existence of favorable interactions within the *hAChE* gorge. Particularly, the indenoquinolinic moiety is suggested to establish interactions with Trp²⁸⁶ and Tyr⁷² in a “sandwich-like” manner. The tacrine motif, addressed toward the central anionic site (CAS), is shown to interact with Trp⁸⁶ by means of

a π - π interaction. The chlorine atom at position 6 is meant to fill a lipophilic pocket, close to the CAS (central anionic site), via hydrophobic interactions. All the compounds showed a good inhibition of BuChE with generally poor selectivity with regard to BuChE/AChE ratio. Rivastigmine also inhibits BuChE, providing dual AChE and BuChE inhibition. It has been suggested that dual inhibition may afford several advantages, including greater and broader symptomatic effects, particular behavioural benefits and the absence of AChE upregulation. These benefits are likely to increase with time, because, as AD progresses, AChE activity decreases by up to 45%, while BuChE activity increases by 40-90%. The gradual shift in the enzyme responsible for degrading ACh from AChE to BuChE during AD progression could be responsible for the inefficacy of AChE inhibitors, that do not achieve dual inhibition. Consequently, there is a rationale for switching from a selective AChE inhibitor to an inhibitor of both AChE and BuChE⁽⁵⁰⁾. Furthermore compounds **49a** and **49b** were tested for the inhibition of BACE1 and **49b** showed a remarkable activity (78.16% of inhibition at 4.75 μ M with IC₅₀ = 0.97 μ M).

5. Conclusions

In conclusion, because of the multifactorial nature of AD, molecules that modulate the activity of a single protein target are unable to significantly modify the progression of the disease. With regard to part A of the thesis, we have reported a new series of hybrid molecules based on the frame works of our AChE/BuChE inhibitors and of SKF-64346. Promising hits proved to be **4c**, with very good inhibitory activity of BuChE and $A\beta$ aggregation, and **12**, which turned out to inhibit AChE/BuChE enzymes and showed remarkable inhibition of $A\beta$ aggregation and $A\beta$ neurotoxicity. Compounds **4e** and **4f** were able to potently inhibit $A\beta$ aggregation while **17-20** are expected to possess a good inhibition of $A\beta$ neurotoxicity because of their bigger lipophilicity which probably makes these compounds more prone to penetrate through cellular barriers. With regard to part B a series of heterodimers structurally related to tacrine has been developed which possesses a very good activity at cholinesterase inhibition. Compounds **49b** and **49c** turned out to be very potent reversible inhibitors of AChE. Particularly, **49c** showed a good inhibition of BACE1 and a mode of docking within AChE gorge which is going to probably give the compound the ability of blocking AChE-induced β -amyloid aggregation by interactions with the PAS. These evidences make **49c** a very promising lead compound for the development of new potent MTDL's for the treatment of AD.

6. Experimental section

Chemistry.

General Methods. Melting points were measured in glass capillary tubes on a Büchi SMP-20 apparatus and are uncorrected. Direct infusion ES-MS spectra were recorded on a Waters Micromass ZQ 4000 apparatus. ^1H and ^{13}C NMR experiments were recorded in CDCl_3 , unless differently indicated, on Varian VXR 300 MHz instrument. Chemical shifts are reported in parts per million (ppm) relative to tetramethylsilane (TMS), and spin multiplicities are given as s (singlet), d (doublet), t (triplet), m (multiplet) or br (broad). Wherever analyses are only indicated with elements symbols, analytical results obtained for those elements are within 0.4 % of the theoretical values. Chromatographic separations were performed on silica gel columns (Kieselgel 40, 0.040-0.063 mm; Merck) by flash chromatography. Compounds were named following IUPAC rules as applied by Beilstein-Institut AutoNom (version 2.1), a PC integrated software package for systematic names in organic chemistry.

2-(4-Methoxyphenyl)benzofuran (1a). A stirred suspension of 4-Methoxybenzoylchloride (5 g, 29 mmol), 2-Hydroxybenzyltriphenyl phosphonium bromide (12 g, 27 mmol) and Et_3N (11.1 mL, 80 mmol) in toluene (125 mL) was refluxed for 10 hours. The reaction mixture was filtered under vacuum and evaporated to dryness. EtOH (150 mL) was added to the oily residue and the flask kept in the freezer overnight. A yellowish solid formed which was filtered off and purified by flash chromatography on silica gel (Petroleum Ether/Ethyl Acetate 95:5), affording **1a** as a white solid (3.58 g, 55%). mp 153 °C. ^1H NMR (CDCl_3) δ : 3.85 (s, 3H), 6.86 (s, 1H), 6.92-7.01 (m, 2H), 7.18-7.28 (m, 2H), 7.32-7.60 (m, 2H), 7.75-7.85 (m, 2H).

2-(3-Methoxyphenyl)benzofuran (1b). A stirred suspension of 3-Methoxybenzoylchloride (5 g, 29 mmol), 2-Hydroxybenzyltriphenyl phosphonium bromide (12 g, 27 mmol) and Et_3N (11.1 mL, 80 mmol) in Toluene (125 mL), was refluxed for 10 hours. The reaction mixture was filtered under vacuum and evaporated to dryness. EtOH (150 mL) was added to the oily residue and the flask kept in the freezer overnight. A yellowish solid formed which was filtered off and purified by flash chromatography on silica gel (Petroleum Ether/Ethyl Acetate 96:4), affording **1b** as a colorless oil (3.00 g, 50%). ^1H NMR (CDCl_3) δ : 3.87 (s, 3H), 6.82-6.95 (m, 1H), 7.00 (s, 1H), 7.18-7.60 (m, 6H).

4-Benzofuran-2-yl-phenol (2a). To a cold (0 °C) solution of **1a** (3.50 g, 16 mmol) in DCM anhydrous (300 mL), BBr_3 (22 mL of 1M solution in DCM) was added slowly. The resulting

mixture was stirred overnight at room temperature. The reaction was quenched with ice/water and stirred for 30 minutes. The organic layer was washed with water (3 x 50 mL), then with brine (3 x 25 mL) and dried over Na₂SO₄. The solvent was removed affording **2a** (3.10 g, 93%) as a white solid. mp 142 °C. ¹H NMR (CDCl₃) δ: 4.87 (br, 1H), 6.86-6.94 (m, 3H), 7.21-7.25 (m, 2H), 7.42-7.56 (m, 2H), 7.69-7.84 (m, 2H). ES-MS *m/z*: 209 (*M* – 1).

3-Benzofuran-2-yl-phenol (2b). To a cold (0 °C) solution of **1b** (3 g, 13 mmol) in DCM anhydrous (250 mL), BBr₃ (18 mL of 1M solution in DCM) was added slowly. The resulting mixture was stirred overnight at room temperature. The reaction was quenched with ice/water and stirred for 30 minutes. The organic layer was washed with water (3 x 50 mL), then with brine (3 x 25 mL) and dried over Na₂SO₄. The solvent was removed by rotary evaporation affording **2b** (2.65 g, 97%) as a white solid. m.p. 123 °C. ¹H NMR (CDCl₃) δ: 4.92 (br, 1H), 6.83-6.97 (m, 3H), 7.18-7.28 (m, 2H), 7.43-7.58 (m, 2H), 7.70-7.79 (m, 2H). ES-MS *m/z*: 209 (*M* – 1).

2-[4-(3-Chloropropoxy)phenyl]benzofuran (3a). A stirred mixture of **2a** (1 g, 4.7 mmol), 1-Bromo-3-Chloropropane (0.94 mL, 9.5 mmol) and K₂CO₃ (1.2 g) was refluxed in acetone (100 mL) for 20 hours. The suspension was hot filtered and the solvent was removed. After adding Petroleum Ether, the residue was kept in the freezer overnight and the white solid that formed was filtered off, affording **3a** (0.93 g, 69 %). mp 137-138 °C. ¹H NMR (CDCl₃) δ: 2.23-2.31 (quintet, *J* = 6.0 Hz, 2H), 3.77–3.80 (m, 2H), 4.17-4.22 (t, *J* = 4.5 Hz, 2H), 6.87 (s, 1H), 6.94-6.98 (d, *J* = 12 Hz, 2H), 7.18-7.32 (m, 2H), 7.47-7.58 (m, 2H), 7.76-7.80 (d, *J* = 12 Hz, 2H).

2-[4-(5-Chloropentyloxy)phenyl]benzofuran (3b). Using the previous procedure and starting from **2a** (0.34 g, 1.6 mmol) and 1-Bromo-5-Chloropentane (0.42 mL, 3.2 mmol), **3b** (0.35 g, 69 %) was obtained as a white solid. mp 115 °C. ¹H NMR (CDCl₃) δ: 1.60-1.71 (m, 2H), 1.83–1.90 (m, 4H), 3.56-3.61 (t, *J* = 6.3 Hz, 2H), 4.01-4.05 (t, *J* = 6.0 Hz, 2H), 6.88 (s, 1H), 6.95-6.98 (d, *J* = 8.4 Hz, 2H), 7.21-7.26 (m, 2H), 7.48-7.56 (m, 2H), 7.77-7.80 (d, *J* = 12 Hz, 2H).

2-[4-(7-Bromoheptyloxy)phenyl]benzofuran (3c). Using the previous procedure and starting from **2a** (0.35 g, 1.6 mmol) and 1,7-Dibromoheptane (0.57 mL, 3.3 mmol), **3c** (0.34 g, 58 %) was obtained as a white solid. mp 92 °C. ¹H NMR (CDCl₃) δ: 1.25-1.60 (m, 6H), 1.71–1.98 (m, 4H), 3.39-3.44 (t, *J* = 5.0 Hz, 2H), 3.96-4.05 (t, *J* = 9.0 Hz, 2H), 6.87 (s, 1H), 6.90-6.93 (d, *J* = 8.4 Hz, 2H), 7.23-7.29 (m, 2H), 7.49-7.58 (m, 2H), 7.75-7.78 (d, *J* = 12 Hz, 2H).

2-[4-(8-Bromooctyloxy)phenyl]benzofuran (3d). Using the previous procedure and starting from **2a** (0.45 g, 2.1 mmol) and 1,8-Dibromooctane (0.79 mL, 4.3 mmol), **3d** (0.51 g, 61 %) was

obtained as a white solid. mp 112 °C. ¹H NMR (CDCl₃) δ: 1.37-1.58 (m, 8H), 1.76–1.92 (m, 4H), 3.39-3.44 (t, *J* = 5.0 Hz, 2H), 3.98-4.02 (t, *J* = 6.6 Hz, 2H), 6.88 (s, 1H), 6.95-6.97 (d, *J* = 6.9 Hz, 2H), 7.20-7.25 (m, 2H), 7.48-7.56 (m, 2H), 7.71-7.80 (dd, *J*₁ = 2.1 Hz; *J*₂ = 6.9 Hz, 2H).

2-[4-(9-Bromononyloxy)phenyl]benzofuran (3e). Using the previous procedure and starting from **2a** (0.57 g, 2.7 mmol) and 1,9-Dibromononane (1.1 mL, 5.4 mmol), **3e** (0.82 g, 73 %) was obtained as a white solid. mp 108 °C. ¹H NMR (CDCl₃) δ: 1.34-1.56 (m, 10H), 1.76-1.95 (m, 4H), 3.39-3.44 (t, *J* = 5.0 Hz, 2H), 3.98-4.02 (t, *J* = 6.6 Hz, 2H), 6.88 (s, 1H), 6.95-6.97 (d, *J* = 6.9 Hz, 2H), 7.20-7.25 (m, 2H), 7.48-7.56 (m, 2H), 7.71-7.80 (dd, *J*₁ = 2.1 Hz; *J*₂ = 6.9 Hz, 2H).

2-[3-(7-Bromoheptyloxy)phenyl]benzofuran (3f). Using the previous procedure and starting from **2b** (2.65 g, 13 mmol) and 1,7-Dibromoheptane (4.3 mL, 25 mmol), **3f** (4 g, 81%) was obtained as a white solid. mp 145 °C. ¹H NMR (CDCl₃) δ: 1.23-1.58 (m, 6H), 1.69–1.98 (m, 4H), 3.37-3.42 (t, *J* = 5.0 Hz, 2H), 3.97-4.06 (t, *J* = 9.0 Hz, 2H), 6.89 (s, 1H), 6.92-6.95 (d, *J* = 8.4 Hz, 2H), 7.24-7.31 (m, 2H), 7.50-7.56 (m, 2H), 7.78-7.81 (d, *J* = 12 Hz, 2H).

[3-(4-Benzofuran-2-yl-phenoxy)propyl]benzylmethylamine (4a). A stirred solution of **3a** (0.9 g, 3.1 mmol) and N-Benzylmethylamine (0.80 mL, 6.2 mmol) in toluene (100 mL) was refluxed in the presence of catalytic amount of NaI for 20 hours. The mixture was washed with water (3 x 25 mL) and the organic layer was dried over Na₂SO₄. The solvent was removed under reduced pressure and the residue was purified by flash chromatography on silica gel (Toluene/Acetone 96:4), affording **4a** as a yellowish solid (1.1 g, 95%). mp 84 °C. ¹H NMR (CDCl₃) δ: 1.96-2.04 (quintet, *J* = 6.0 Hz, 2H), 2.23 (s, 3H), 2.52-2.60 (t, *J* = 12.0 Hz, 2H), 3.51 (s, 2H), 4.05-4.13 (t, *J* = 12.0 Hz, 2H), 6.86 (s, 1H), 6.95-6.97 (d, *J* = 6.9 Hz, 2H), 7.15-7.30 (m, 7H), 7.45-7.55 (m, 2H), 7.75-7.80 (m, 2H). ES-MS *m/z*: 372 (M + 1).

[5-(4-Benzofuran-2-yl-phenoxy)pentyl]benzylmethylamine (4b). Using the previous procedure and starting from **3b** (0.34 g, 1.6 mmol), **4b** was obtained as a yellowish solid (0.26 g, 40%). mp 57 °C. ¹H NMR (CDCl₃) δ: 1.47-1.59 (m, 4H), 1.75-1.81 (m, 2H), 2.18 (s, 3H), 2.34-2.41 (t, *J* = 7.4 Hz, 2H), 3.47 (s, 2H), 3.92-3.99 (t, *J* = 6.2 Hz, 2H), 6.84 (s, 1H), 6.90-6.95 (d, *J* = 9.2 Hz, 2H), 7.18-7.31 (m, 7H), 7.46-7.51 (m, 2H), 7.73-7.78 (d, *J* = 8.8 Hz, 2H). ES-MS *m/z*: 400 (M + 1).

[7-(4-Benzofuran-2-yl-phenoxy)heptyl]benzylmethylamine (4c). Using the previous procedure and starting from **3c** (0.49 g, 1.3 mmol), **4c** was obtained as a yellowish solid (0.51 g, 92%). mp 57 °C. ¹H NMR (CDCl₃) δ: 1.27-1.59 (m, 8H), 1.75-1.85 (m, 2H), 2.19 (s, 3H), 2.32-2.39 (t, *J* = 7.4

Hz, 2H), 3.42 (s, 2H), 3.94-4.01 (t, $J = 6.2$ Hz, 2H), 6.84 (s, 1H), 6.91-6.96 (d, $J = 9.2$ Hz, 2H), 7.18-7.31 (m, 7H), 7.46-7.51 (m, 2H), 7.73-7.78 (d, $J = 8.8$ Hz, 2H). ES-MS m/z : 428 ($M + 1$).

[8-(4-Benzofuran-2-yl-phenoxy)octyl]benzylmethylamine (4d). Using the previous procedure and starting from **3d** (0.51 g, 1.3 mmol), **4d** was obtained as a white solid (0.2 g, 36%). mp 69-70 °C. $^1\text{H NMR}$ (CDCl_3) δ : 1.32-1.58 (m, 10H), 1.75-1.85 (m, 2H), 2.18 (s, 3H), 2.32-2.39 (t, $J = 7.4$ Hz, 2H), 3.47 (s, 2H), 3.97-4.03 (t, $J = 6.2$ Hz, 2H), 6.84 (s, 1H), 6.94-6.99 (d, $J = 9.2$ Hz, 2H), 7.19-7.32 (m, 7H), 7.47-7.54 (m, 2H), 7.76-7.81 (d, $J = 8.8$ Hz, 2H). ES-MS m/z : 442 ($M + 1$).

[9-(4-Benzofuran-2-yl-phenoxy)nonyl]benzylmethylamine (4e). Using the previous procedure and starting from **3e** (0.82 g, 2.0 mmol), **4e** was obtained as a white solid (0.53 g, 58%). mp 79 °C. $^1\text{H NMR}$ (CDCl_3) δ : 1.34-1.53 (m, 12H), 1.75-1.86 (m, 2H), 2.22 (s, 3H), 2.37-2.42 (t, $J = 7.8$ Hz, 2H), 3.51 (s, 2H), 4.02-4.06 (t, $J = 6.6$ Hz, 2H), 6.91 (s, 1H), 6.94-6.99 (d, $J = 9.2$ Hz, 2H), 7.24-7.36 (m, 7H), 7.52-7.58 (m, 2H), 7.80-7.84 (dd, $J_1 = 2.4$ Hz; $J_2 = 6.9$ Hz, 2H). ES-MS m/z : 456 ($M + 1$).

[7-(3-Benzofuran-2-yl-phenoxy)heptyl]benzylmethylamine (4f). Using the previous procedure and starting from **3f** (4 g, 10 mmol), **4f** was obtained as a yellowish oil (0.84 g, 20%). $^1\text{H NMR}$ (CDCl_3) δ : 1.20-1.59 (m, 8H), 1.69-1.87 (m, 2H), 2.17 (s, 3H), 2.32-2.39 (t, $J = 7.4$ Hz, 2H), 3.42 (s, 2H), 3.94-4.01 (t, $J = 6.2$ Hz, 2H), 6.84 (s, 1H), 6.91-6.96 (d, $J = 9.2$ Hz, 2H), 7.18-7.31 (m, 7H), 7.46-7.51 (m, 2H), 7.73-7.78 (d, $J = 8.8$ Hz, 2H). ES-MS m/z : 428 ($M + 1$).

Compounds 5 g-r were obtained according to the following general procedure:

SnCl_4 (1.2 eq.) was added dropwise to a mixture of **3f** (1 eq.) and the selected acylchloride (1.2 eq.) in dry dichloromethane and the resulting solution was stirred at room temperature overnight. The reaction was quenched with ice/water and stirred for 1 h. The organic layer was separated and the aqueous one was extracted with dichloromethane. The combined organic extracts were dried (Na_2SO_4), filtered and concentrated under reduced pressure to afford the desired 3-acylated benzofurans (**5 g-r**), generally as honey colored oils purified by flash chromatography.

{2-[3-(7-Bromoheptyloxy)phenyl]benzofuran-3-yl}phenylmethanone (5g). (0.09 g, 28%). (Petroleum ether/Ethyl acetate 98:2). $^1\text{H NMR}$ (CDCl_3) δ : 1.25-1.58 (m, 6H), 1.62-1.95 (m, 4H), 3.35-3.42 (t, $J = 6.6$ Hz, 2H), 3.80-3.86 (t, $J = 6.2$ Hz, 2H), 6.83-6.87 (dt, $J_1 = 1.0$ Hz, $J_2 = 7.6$ Hz, 1H), 7.11-7.40 (m, 7H), 7.47-7.58 (m, 2H), 7.76-7.80 (d, $J = 8.0$ Hz, 2H).

{2-[3-(7-Bromoheptyloxy)phenyl]benzofuran-3-yl}-*p*-tolylmethanone (5h). (0.09 g, 27%). (Petroleum ether/Ethyl acetate 98:2). ¹H NMR (CDCl₃) δ: 1.25-1.58 (m, 6H), 1.62-1.95 (m, 4H), 2.36 (s, 3H), 3.37-3.44 (t, *J* = 6.6 Hz, 2H), 3.79-3.85 (t, *J* = 6.2 Hz, 2H), 6.82-6.86 (dt, *J*₁ = 1.0 Hz, *J*₂ = 7.6 Hz, 1H), 7.12-7.38 (m, 7H), 7.48-7.59 (m, 2H), 7.75-7.79 (d, *J* = 8.0 Hz, 2H).

{2-[3-(7-Bromoheptyloxy)phenyl]benzofuran-3-yl}-*m*-tolylmethanone (5i). (0.06 g, 18%). (Petroleum ether/Ethyl acetate 98:2). ¹H NMR (CDCl₃): δ 1.41-1.59 (m, 6H), 1.70-1.95 (m, 4H), 2.28 (s, 3H), 3.38-3.45 (t, *J* = 6.6 Hz, 2H), 3.78-3.84 (t, *J* = 6.6 Hz, 2H), 6.81-6.87 (m, 1H), 7.14-7.40 (m, 7H), 7.56-7.67 (m, 4H).

{2-[3-(7-Bromoheptyloxy)phenyl]benzofuran-3-yl}-3-methoxyphenylmethanone (5j). (0.07 g, 21%). (Petroleum ether/Ethyl acetate 98:2). ¹H NMR (CDCl₃) δ: 1.40-1.58 (m, 6H), 1.60-1.95 (m, 4H), 3.38-3.45 (t, *J* = 6.6 Hz, 2H), 3.73 (s, 3H), 3.78-3.84 (t, *J* = 6.2 Hz, 2H), 6.82-6.88 (m, 1H), 7.01-7.06 (m, 1H), 7.15-7.41 (m, 8H), 7.56-7.62 (m, 2H).

{2-[3-(7-Bromoheptyloxy)phenyl]benzofuran-3-yl}-2-methoxyphenylmethanone (5k). (0.2 g, 59%). (Petroleum ether/Ethyl acetate 94:6). ¹H NMR (CDCl₃) δ: 1.42-1.58 (m, 6H), 1.62-1.98 (m, 4H), 3.38-3.45 (t, *J* = 6.6 Hz, 2H), 3.55 (s, 3H), 3.81-3.87 (t, *J* = 6.2 Hz, 2H), 6.67-6.71 (d, *J* = 8.4 Hz, 1H), 6.84-6.92 (m, 2H), 7.12-7.38 (m, 6H), 7.45-7.56 (m, 2H), 7.73-7.78 (m, 1H).

{2-[3-(7-Bromoheptyloxy)phenyl]benzofuran-3-yl}-3,5-dimethoxyphenylmethanone (5l). (0.07 g, 16%). (Petroleum ether/Ethyl acetate 90:10). ¹H NMR (CDCl₃) δ: 1.41-1.58 (m, 6H), 1.62-1.95 (m, 4H), 3.38-3.45 (t, *J* = 6.6 Hz, 2H), 3.68 (s, 6H), 3.78-3.84 (t, *J* = 6.2 Hz, 2H), 6.56-6.58 (t, *J* = 2.2 Hz, 1H), 6.83-6.90 (m, 1H), 6.98 (s, 1H), 6.99 (s, 1H), 7.13-7.41 (m, 5H), 7.56-7.66 (m, 2H).

{2-[3-(7-Bromoheptyloxy)phenyl]benzofuran-3-yl}-3,4-dimethoxyphenylmethanone (5m). (0.13 g, 36%). (Petroleum ether/Ethyl acetate 90:10). ¹H NMR (CDCl₃): δ 1.30-1.56 (m, 6H), 1.60-1.98 (m, 4H), 3.37-3.44 (t, *J* = 6.6 Hz, 2H), 3.80-3.90 (m, 8H), 6.72-6.88 (m, 2H), 7.16-7.59 (m, 9H).

{2-[3-(7-Bromoheptyloxy)phenyl]benzofuran-3-yl}-2,3-dimethoxyphenylmethanone (5n). (0.17 g, 47%). (Petroleum ether/Ethyl acetate 90:10). ¹H NMR (CDCl₃) δ: 1.42-1.51 (m, 6H), 1.72-1.92 (m, 4H), 3.37-3.44 (t, *J* = 6.6 Hz, 2H), 3.74 (s, 3H), 3.82 (s, 3H), 3.87-3.94 (t, *J* = 6.6 Hz, 2H), 6.81-6.93 (m, 4H), 7.13-7.40 (m, 5H), 7.51-7.65 (m, 2H).

{2-[4-(7-Bromoheptyloxy)phenyl]benzofuran-3-yl}naphthalen-1-yl-methanone (5o). (0.06 g, 16%). (Petroleum ether/Ethyl acetate 98:02). ¹H NMR (CDCl₃) δ: 1.25-1.58 (m, 6H), 1.62-1.95 (m,

4H), 3.37-3.44 (t, $J = 6.6$ Hz, 2H), 3.83-3.89 (t, $J = 6.6$ Hz, 2H), 6.60-6.64 (m, 2H), 7.20-7.38 (m, 4H), 7.50-7.65 (m, 7H), 7.84-7.90 (d, 2H), 8.55-8.60 (m, 1H).

{2-[4-(7-Bromoheptyloxy)phenyl]benzofuran-3-yl}naphthalen-2-yl-methanone (5p). (0.16 g, 47%). (Petroleum ether/Ethyl acetate 98:02). $^1\text{H NMR}$ (CDCl_3) δ : 1.56 (m, 6H), 1.64-1.92 (m, 4H), 3.37-3.44 (t, $J = 6.6$ Hz, 2H), 3.83-3.89 (t, $J = 6.6$ Hz, 2H), 6.73-6.78 (m, 2H), 7.21-7.38 (m, 3H), 7.42-7.63 (m, 4H), 7.64-7.90 (m, 4H), 7.95-8.01 (m, 1H), 8.34 (s, 1H).

Biphenyl-4-yl-{2-[4-(7-bromoheptyloxy)phenyl]benzofuran-3-yl}methanone (5q). (0.22 g, 58%). (Petroleum ether/Ethyl acetate 98:02). $^1\text{H NMR}$ (CDCl_3) δ : 1.58 (m, 6H), 1.62-1.95 (m, 4H), 3.36-3.43 (t, $J = 6.6$, 2H), 3.87-3.94 (t, $J = 6.6$ Hz, 2H), 6.78-6.82 (dd, $J_1 = 2.2$ Hz, $J_2 = 7.0$ Hz, 2H), 7.24-7.50 (m, 5H), 7.51-7.71 (m, 8H), 7.90-7.93 (m, 2H).

Anthracen-9-yl-{2-[4-(7-bromoheptyloxy)phenyl]benzofuran-3-yl}methanone (5r). (0.08 g, 18%). (Petroleum ether/Ethyl acetate 98:02). $^1\text{H NMR}$ (CDCl_3) δ : 1.61 (m, 6H), 1.62-1.95 (m, 4H), 3.40-3.47 (t, $J = 6.6$, 2H), 3.77-3.83 (t, $J = 6.2$ Hz, 2H), 6.29 (br, 2H), 6.72-7.82 (m, 10H), 7.84-8.12 (m, 4H), 8.34 (s, 1H).

2-{4-[3-(Benzylmethylamino)propoxy]phenyl}benzofuran-3-yl-(4-methoxyphenyl)methanone (6). To a cooled solution (0 °C) of **4a** (0.54 g, 1.4 mmol) and 4-Methoxybenzoylchloride (0.3 g, 1.7 mmol) in DCM anhydrous (25 mL), SnCl_4 (0.44 g, 1.7 mmol) was added dropwise with stirring. The mixture was allowed to reach room temperature then stirred overnight. The reaction was quenched with ice/water and stirred for 30 minutes. The organic layer was washed with water (3 x 10 mL) and brine (3 x 10 mL), then dried over Na_2SO_4 anhydrous and evaporated to dryness. The crude was purified by flash chromatography (Toluene/Acetone 96:4) affording **6** as a pale yellow oil (0.04 g, 6%). $^1\text{H NMR}$ (CDCl_3) δ : 1.94-2.02 (quintet, $J = 6.9$ Hz, 2H), 2.23 (s, 3H), 2.52-2.57 (t, $J = 6.9$ Hz, 2H), 3.53 (s, 2H), 3.82 (s, 3H), 3.98-4.03 (t, $J = 6.3$ Hz, 2H), 6.79-6.85 (m, 4H), 7.22-7.32 (m, 7H), 7.45-7.53 (m, 2H), 7.65-7.68 (dd, $J_1 = 2.1$ Hz; $J_2 = 6.9$ Hz, 2H), 7.86-7.89 (dd, $J_1 = 2.1$ Hz; $J_2 = 6.9$ Hz, 2H). ES-MS m/z : 528 ($M + 1$).

2-{4-[5-(Benzylmethylamino)pentyl]oxy]phenyl}benzofuran-3-yl-(4-methoxyphenyl)methanone (7). Following the previous procedure and starting from **4b** (0.13 g, 0.32 mmol), **7** was obtained as a colorless oil (0.03 g, 17%) after flash chromatography (from Toluene/Acetone 90:10 to Toluene/Acetone 20:80). $^1\text{H NMR}$ (CDCl_3) δ : 1.39-1.65 (m, 4H), 1.68-1.85 (m, 2H), 2.18 (s, 3H), 2.34-2.41 (t, $J = 7.4$ Hz, 2H), 3.47 (s, 2H), 3.82 (s, 3H), 3.92-3.99 (t, $J = 6.2$ Hz, 2H), 6.79-6.85 (m,

4H), 7.22-7.32 (m, 7H), 7.45-7.53 (m, 2H), 7.65-7.68 (dd, $J_1 = 2.1$ Hz; $J_2 = 6.9$ Hz, 2H), 7.86-7.89 (dd, $J_1 = 2.1$ Hz; $J_2 = 6.9$ Hz, 2H). ES-MS m/z : 534 (M + 1).

2-{4-[7-(Benzylmethylamino)heptyloxy]phenyl}benzofuran-3-yl-(4-methoxyphenyl)methanone (8). Following the previous procedure and starting from **4c** (0.18 g, 0.41 mmol), **8** was obtained as a colorless oil (0.09 g, 39%) after flash chromatography (from Toluene 100 to Toluene/Acetone 94:6). $^1\text{H NMR}$ (CDCl_3) δ : 1.21-1.45 (m, 6H), 1.68-1.81 (m, 4H), 2.18 (s, 3H), 2.42 (t, 2H), 3.60 (s, 2H), 3.82 (s, 3H), 3.95 (t, 2H), 6.78-6.97 (m, 4H, Ar), 7.10-7.60 (m, 9H, Ar), 7.68 (d, 2H, Ar), 7.87 (d, 2H, Ar). ES-MS m/z : 562 (M+1). Anal. $\text{C}_{37}\text{H}_{39}\text{NO}_4$ (C, H, N).

2-{4-[8-(Benzylmethylamino)octyloxy]phenyl}benzofuran-3-yl-(4-methoxyphenyl)methanone (9). Following the previous procedure and starting from **4d** (0.18 g, 0.41 mmol), **9** was obtained as a colorless oil (0.05 g, 21%) after flash chromatography (from Toluene 100 to Toluene/Acetone 94:6). $^1\text{H NMR}$ (CDCl_3) δ : 1.30-1.61 (m, 10H), 1.68-1.83 (m, 2H), 2.18 (s, 3H), 2.34-2.41 (t, $J = 7.4$ Hz, 2H), 3.47 (s, 2H), 3.82 (s, 3H), 3.92-3.99 (t, $J = 6.2$ Hz, 2H), 6.79-6.85 (m, 4H), 7.22-7.32 (m, 7H), 7.45-7.53 (m, 2H), 7.65-7.68 (dd, $J_1 = 2.1$ Hz; $J_2 = 6.9$ Hz, 2H), 7.86-7.89 (dd, $J_1 = 2.1$ Hz; $J_2 = 6.9$ Hz, 2H). ES-MS m/z : 576 (M + 1).

2-{4-[9-(Benzylmethylamino)nonyloxy]phenyl}benzofuran-3-yl-(4-methoxyphenyl)methanone (10). Following the previous procedure and starting from **4e** (0.48 g, 1.0 mmol), **10** was obtained as a pale yellow oil (0.03 g, 5%) after flash chromatography (Toluene/Acetone 96:4). $^1\text{H NMR}$ (CDCl_3) δ : 1.30-1.61 (m, 12H), 1.68-1.83 (m, 2H), 2.18 (s, 3H), 2.34-2.41 (t, $J = 7.4$ Hz, 2H), 3.47 (s, 2H), 3.82 (s, 3H), 3.92-3.99 (t, $J = 6.2$ Hz, 2H), 6.79-6.85 (m, 4H), 7.22-7.32 (m, 7H), 7.45-7.53 (m, 2H), 7.65-7.68 (dd, $J_1 = 2.1$ Hz; $J_2 = 6.9$ Hz, 2H), 7.86-7.89 (dd, $J_1 = 2.1$ Hz; $J_2 = 6.9$ Hz, 2H). ES-MS m/z : 590 (M + 1).

Compounds 11-16 were obtained according to the following general procedure:

SnCl_4 (1.2 eq.) was added dropwise to a mixture of **4c** (1 eq.) and the selected acylchloride (1.2 eq.) in dry DCM and the resulting solution was stirred at room temperature overnight. The reaction was quenched with ice/water and stirred for 1 h. The organic layer was separated and the aqueous one was extracted with DCM. The combined organic extracts were dried (Na_2SO_4), filtered and concentrated under reduced pressure to afford the desired 3-acylated benzofurans (**11-16**), generally as honey colored oils purified by flash chromatography. (Toluene/Acetone 90:10)

1-(2-{4-[7-(Benzylmethylamino)heptyloxy]phenyl}benzofuran-3-yl)ethanone (11). 15 % yield. $^1\text{H NMR}$ (CDCl_3) δ : 1.37-1.58 (m, 6H), 1.78-1.85 (m, 4H), 2.20 (s, 3H), 2.38 (t, 2H), 2.42 (s, 3H),

3.48 (s,2H), 4.05 (t, 2H), 7.02 (d, 2H, Ar), 7.20-7.40 (m, 7H, Ar), 7.43-7.52 (m, 1H, Ar), 7.68 (d, 2H, Ar),8.05-8.15 (m, 1H, Ar). ES-MS m/z : 470 (M+1). Anal. C₃₁H₃₅NO₃ (C, H, N).

(2-{4-[7-(Benzylmethylamino)heptyloxy]phenyl}benzofuran-3-yl)phenylmethanone (12). 55 % yield. ¹H NMR (CDCl₃) δ : 1.25-1.48 (m, 6H), 1.68-1.82 (m, 4H), 2.20 (s, 3H), 2.38 (t, 2H), 3.47 (s, 2H), 3.98 (t, 2H), 6.78 (d, 2H, Ar), 7.18-7.58 (m, 12H, Ar), 7.62 (d, 2H, Ar), 7.82 (d, 2H, Ar). ES-MS m/z : 532 (M+1). Anal. C₃₆H₃₇NO₃ (C, H, N).

(2-{4-[7-(Benzylmethylamino)heptyloxy]phenyl}benzofuran-3-yl)-*m*-tolylmethanone (13). 38 % yield. ¹H NMR (CDCl₃) δ : 1.25-1.45 (m, 6H), 1.62-1.82 (m, 4H), 2.20 (s, 3H), 2.25-2.42 (m, 5H), 3.47 (s, 2H), 3.98 (t, 2H), 6.80 (m, 2H, Ar), 7.16-7.58 (m, 11H, Ar), 7.62-7.80 (m, 4H, Ar). ES-MS m/z : 546 (M+1). Anal. C₃₇H₃₉NO₃ (C, H, N).

(2-{4-[7-(Benzylmethylamino)heptyloxy]phenyl}benzofuran-3-yl)-*p*-tolylmethanone (14). 41 % yield. ¹H NMR (CDCl₃) δ : 1.23-1.58 (m, 6H), 1.62-1.82 (m, 4H), 2.18 (s, 3H), 2.25-2.42 (m, 5H), 3.48 (s, 2H), 3.98 (t, 2H), 6.82 (d, 2H, Ar), 7.17-7.58 (m, 11H, Ar), 7.62-7.80 (m, 4H, Ar). ES-MS m/z : 546 (M+1). Anal. C₃₇H₃₉NO₃ (C, H, N).

(2-{4-[7-(Benzylmethylamino)heptyloxy]phenyl}benzofuran-3-yl)-(3-methoxyphenyl)-methanone (15). 37 % yield. ¹H NMR (CDCl₃) δ : 1.25-1.45 (m, 6H), 1.61-1.81 (m, 4H), 2.18 (s, 3H), 2.45 (t, 2H), 3.60 (s, 2H), 3.78 (s, 3H), 3.95 (t, 2H), 6.78-6.97 (m, 4H, Ar), 7.05-7.45 (m, 9H, Ar), 7.55- 7.68 (m, 4H, Ar). ES-MS m/z : 562 (M+1). Anal. C₃₇H₃₉NO₄ (C, H, N).

(2-{4-[7-(Benzylmethylamino)heptyloxy]phenyl}benzofuran-3-yl)-(3,4-dimethoxyphenyl)-methanone (16). 35 % yield ¹H NMR (CDCl₃) δ : 1.24-1.55 (m, 6H), 1.68-1.81 (m, 4H), 2.18 (s, 3H), 2.39 (t, 2H), 3.48 (s, 2H), 3.81 (s, 3H), 3.83 (s, 3H), 3.98 (t, 2H), 6.78-7.75 (m, 16H, Ar). ES-MS m/z : 592 (M+1). Anal. C₃₈H₄₁NO₅ (C, H, N).

Compounds 17-28 were obtained according to the following general procedure:

A stirred solution of the opportune **5 g-r** (1 eq.) and N-Benzylmethylamine (2 eq.) in toluene was refluxed for 48 hours. The mixture was washed with water. The organic layer was dried over Na₂SO₄ and the solvent was removed. The residue was purified by flash chromatography (Toluene/Acetone 98:2) to afford **17-28** generally as a yellowish oil.

(2-{4-[7-(Benzylmethylamino)heptyloxy]phenyl}benzofuran-3-yl)naphthalen-1-yl-methanone (17). (0.04 g, 62%). ¹H NMR (CDCl₃) δ : 1.21-1.62 (m, 8H), 1.63-1.79 (m, 2H), 2.18 (s, 3H), 2.32-2.39 (t, J = 7.2 Hz, 2H), 3.47 (s, 2H), 3.81-3.88 (t, J = 6.6 Hz, 2H), 6.59-6.64 (m, 2H), 7.16-7.35

(m, 8H), 7.52-7.63 (m, 7H), 7.83-7.88 (d, $J = 8.2$ Hz, 2H), 8.55-8.59 (d, $J = 7.8$ Hz, 1H). ES-MS m/z : 582 ($M + 1$).

(2-{4-[7-(Benzylmethylamino)heptyloxy]phenyl}benzofuran-3-yl)naphthalen-2-yl-methanone (18). (0.17 g, 99%). ^1H NMR (CDCl_3) δ : 1.25-1.60 (m, 8H), 1.64-1.80 (m, 2H), 2.18 (s, 3H), 2.31-2.39 (t, $J = 7.4$ Hz, 2H), 3.48 (s, 2H), 3.81-3.88 (t, $J = 6.6$ Hz, 2H), 6.73-6.77 (d, $J = 8.8$ Hz, 2H), 7.18-7.38 (m, 8H), 7.41-7.85 (m, 8H), 7.96-8.02 (m, 1H), 8.33 (s, 1H). ^{13}C NMR (CDCl_3) δ : 25.86, 27.19, 27.24, 28.95, 29.18, 42.15, 57.35, 62.24, 67.93, 111.04, 114.42, 114.93, 121.21, 121.73, 123.65, 124.84, 125.10, 126.55, 126.87, 127.67, 128.14, 128.31, 128.39, 128.73, 129.03, 129.52, 129.85, 132.04, 132.39, 135.21, 135.56, 138.97, 150.90, 153.56, 158.04, 160.31, 192.28, 197.95. ES-MS m/z : 582 ($M + 1$).

(2-{4-[7-(Benzylmethylamino)heptyloxy]phenyl}benzofuran-3-yl)biphenyl-4-yl-methanone (19). (0.18 g, 73%). ^1H NMR (CDCl_3) δ : 1.21-1.62 (m, 8H), 1.64-1.80 (m, 2H), 2.20 (s, 3H), 2.37-2.44 (t, $J = 7.4$ Hz, 2H), 3.50 (s, 2H), 3.87-3.93 (t, $J = 6.6$ Hz, 2H), 6.78-6.83 (d, $J = 8.8$ Hz, 2H), 7.19-7.45 (m, 11H), 7.54-7.68 (m, 7H), 7.89-7.93 (d, $J = 8.2$ Hz, 2H). ES-MS m/z : 608 ($M + 1$).

Anthracen-9-yl-(2-{4-[7-(benzylmethylamino)heptyloxy]phenyl}benzofuran-3-yl)methanone (20). (0.06 g, 70%). ^1H NMR (CDCl_3) δ : 1.25-1.62 (m, 8H), 1.64-1.80 (m, 2H), 2.22 (s, 3H), 2.37-2.44 (t, $J = 7.4$ Hz, 2H), 3.52 (s, 2H), 3.76-3.83 (t, $J = 6.6$ Hz, 2H), 6.18-6.40 (m, 2H), 7.25-7.52 (m, 15H), 7.89-7.93 (dd, $J_1 = 2.2$ Hz, $J_2 = 6.6$ Hz, 4H), 8.34 (s, 1H). ^{13}C NMR (CDCl_3) δ : 25.94, 27.20, 27.32, 28.96, 29.24, 42.13, 57.35, 62.22, 67.88, 110.97, 113.14, 118.73, 121.05, 122.55, 124.38, 124.90, 125.19, 125.25, 126.54, 126.66, 127.00, 128.20, 128.37, 128.49, 128.71, 129.12, 130.00, 130.99, 135.12, 153.82, 158.54, 160.18, 182.87, 194.44, 197.98. ES-MS m/z : 632 ($M + 1$).

(2-{3-[7-(Benzylmethylamino)heptyloxy]phenyl}benzofuran-3-yl)phenylmethanone (21). (0.09 g, 65%). ^1H NMR (CDCl_3) δ : 1.21-1.62 (m, 8H), 1.63-1.79 (m, 2H), 2.18 (s, 3H), 2.32-2.39 (t, $J = 7.2$ Hz, 2H), 3.47 (s, 2H), 3.81-3.88 (t, $J = 6.6$ Hz, 2H), 6.89-6.94 (m, 1H), 7.16-7.62 (m, 15H), 7.80-7.93 (m, 2H). ^{13}C NMR (CDCl_3) δ : 25.98, 27.33, 29.09, 29.27, 42.25, 56.88, 57.47, 62.33, 67.99, 111.20, 113.87, 116.13, 116.74, 120.73, 121.46, 123.81, 125.36, 126.85, 128.15, 128.41, 128.51, 129.05, 129.41, 129.79, 130.49, 133.14, 137.82, 139.18, 150.95, 153.76, 157.35, 158.97, 192.30. ES-MS m/z : 532 ($M + 1$).

(2-{3-[7-(Benzylmethylamino)heptyloxy]phenyl}benzofuran-3-yl)-*p*-tolylmethanone (22). (0.08 g, 82.3%). ^1H NMR (CDCl_3) δ : 1.25-1.62 (m, 8H), 1.64-1.80 (m, 2H), 2.19 (s, 3H), 2.35-2.40 (m,

5H), 3.48 (s, 2H), 3.77-3.84 (t, $J = 6.6$ Hz, 2H), 6.82-6.86 (m, 1H), 7.11-7.42 (m, 12H), 7.50-7.58 (t, $J = 9.2$ Hz, 2H), 7.75-7.79 (d, $J = 7.6$ Hz, 2H). ES-MS m/z : 546 ($M + 1$).

(2-{3-[7-(Benzylmethylamino)heptyloxy]phenyl}benzofuran-3-yl)-*m*-tolylmethanone (23). (0.05 g, 77%). $^1\text{H NMR}$ (CDCl_3) δ : 1.22-1.62 (m, 8H), 1.64-1.80 (m, 2H), 2.20 (s, 3H), 2.28 (s, 3H), 2.34-2.41 (t, $J = 7.6$ Hz, 2H), 3.50 (s, 2H), 3.77-3.83 (t, $J = 6.6$ Hz, 2H), 6.82-6.86 (d, $J = 7.8$ Hz, 1H), 7.16-7.42 (m, 12H), 7.56-7.67 (m, 4H). $^{13}\text{C NMR}$ (CDCl_3) δ : 21.14, 25.97, 27.23, 27.30, 29.09, 29.25, 29.66, 42.16, 57.40, 62.26, 67.97, 111.15, 113.79, 116.29, 116.73, 120.63, 121.47, 123.77, 125.30, 126.90, 127.14, 128.16, 128.27, 128.52, 129.07, 129.37, 130.19, 130.58, 133.89, 137.77, 138.20, 150.94, 153.73, 157.28, 158.92, 192.46, 197.98. ES-MS m/z : 546 ($M + 1$).

(2-{3-[7-(Benzylmethylamino)heptyloxy]phenyl}benzofuran-3-yl)-3-methoxyphenylmethanone (24). (0.05 g, 66%). $^1\text{H NMR}$ (CDCl_3) δ : 1.25-1.61 (m, 8H), 1.65-1.82 (m, 2H), 2.20 (s, 3H), 2.34-2.41 (t, $J = 7.6$ Hz, 2H), 3.49 (s, 2H), 3.73 (s, 3H), 3.77-3.84 (t, $J = 6.2$ Hz, 2H), 6.83-6.87 (m, 1H), 6.98-7.05 (m, 1H), 7.16-7.20 (m, 2H), 7.22-7.32 (m, 8H), 7.37-7.41 (m, 3H), 7.56-7.63 (m, 2H). ES-MS m/z : 562 ($M + 1$).

(2-{3-[7-(Benzylmethylamino)heptyloxy]phenyl}benzofuran-3-yl)-2-methoxyphenylmethanone (25). (0.15 g, 70%). $^1\text{H NMR}$ (CDCl_3) δ : 1.28-1.62 (m, 8H), 1.65-1.82 (m, 2H), 2.19 (s, 3H), 2.33-2.40 (t, $J = 7.6$ Hz, 2H), 3.48 (s, 2H), 3.53 (s, 3H), 3.79-3.86 (t, $J = 6.6$ Hz, 2H), 6.66-6.70 (d, $J = 8.0$ Hz, 1H), 6.80-6.91 (m, 2H), 7.10-7.35 (m, 11H), 7.44-7.55 (m, 2H), 7.75-7.80 (m, 1H). ES-MS m/z : 562 ($M + 1$).

(2-{3-[7-(Benzylmethylamino)heptyloxy]phenyl}benzofuran-3-yl)-3,4-dimethoxyphenylmethanone (26). (0.09 g, 65%). $^1\text{H NMR}$ (CDCl_3) δ : 1.25-1.62 (m, 8H), 1.69-1.80 (m, 2H), 2.20 (s, 3H), 2.34-2.41 (t, $J = 7.6$ Hz, 2H), 3.49 (s, 2H), 3.80-3.89 (m, 8H), 6.72-6.76 (d, $J = 8.6$ Hz, 1H), 6.83-6.88 (m, 1H), 7.23-7.39 (m, 10H), 7.43-7.60 (m, 4H). ES-MS m/z : 592 ($M + 1$).

(2-{3-[7-(Benzylmethylamino)heptyloxy]phenyl}benzofuran-3-yl)-2,3-dimethoxyphenylmethanone (27). (0.14 g, 77%). $^1\text{H NMR}$ (CDCl_3) δ : 1.27-1.61 (m, 8H), 1.65-1.83 (m, 2H), 2.18 (s, 3H), 2.33-2.40 (t, $J = 7.8$ Hz, 2H), 3.48 (s, 2H), 3.73 (s, 3H), 3.79 (s, 3H), 3.86-3.93 (t, $J = 6.6$ Hz, 2H), 6.80-6.95 (m, 4H), 7.12-7.34 (m, 10H), 7.51-7.55 (m, 1H), 7.63-7.68 (m, 1H). ES-MS m/z : 592 ($M + 1$).

(2-{3-[7-(Benzylmethylamino)heptyloxy]phenyl}benzofuran-3-yl)-3,5-dimethoxyphenylmethanone (28). (0.05 g, 67%). $^1\text{H NMR}$ (CDCl_3) δ : 1.25-1.61 (m, 8H), 1.64-1.81 (m, 2H), 2.20 (s, 3H), 2.34-2.42 (t, $J = 7.2$ Hz, 2H), 3.50 (s, 2H), 3.67 (s, 6H), 3.77-3.83 (t, $J = 6.2$ Hz, 2H), 6.57

(s, 1H), 6.84-6.88 (m, 1H), 6.98-6.99 (d, $J = 2.2$ Hz, 2H), 7.14-7.41 (m, 10H), 7.56-7.67 (m, 2H). ES-MS m/z : 592 ($M + 1$).

[2-(4-{7-[(3-Hydroxybenzyl)methylamino]heptyloxy}phenyl)benzofuran-3-yl]-p-tolylmethanone (29). A stirred solution of {2-[4-(7-Bromoheptyloxy)phenyl]benzofuran-3-yl}-p-tolylmethanone (0.7 g, 1.38 mmol) and 3-Methylaminomethylphenol (0.38 g, 2.77 mmol) in toluene (120 mL) was refluxed for 20 hours. The mixture was washed with water, the organic layer was dried over Na_2SO_4 and the solvent was removed. The residue was purified by flash chromatography (Toluene/Acetone 90:10), to afford **29** as a yellowish oil (0.16 g, 21%). ^1H NMR (CDCl_3) δ : 1.20-1.60 (m, 8H), 1.62- 1.83 (m, 2H), 2.19 (s, 3H), 2.23-2.41 (m, 5H), 3.42 (s, 2H), 3.83-3.97 (t, 2H), 6.63-6.87 (m, 4H), 7.11-7.38 (m, 6H), 7.39-7.58 (m, 2H), 7.62-7.81 (m, 4H).

Methylcarbamic acid 3-[[methyl-(7-{4-[3-(4-methylbenzoyl)benzofuran-2-yl]phenoxy}heptyl)-amino]methyl]phenyl ester (30). To a solution of **29** (0.1 g, 0.18 mmol) in DCM, NaH (0.004 g, 0.18 mmol) and methyl isocyanate (0.010 g, 0.18 mmol) were added. The mixture was stirred for 24 h then quenched with ice/water and extracted with DCM. The organic layer was dried and evaporated. The crude was purified by flash chromatography (Toluene/Acetone 60:40), affording **30** as a clear oil (0.06 g, 54%). ^1H NMR (CDCl_3) δ : 1.21-1.59 (m, 8H), 1.63- 1.82 (m, 2H), 2.18 (s, 3H), 2.23-2.41 (m, 5H), 2.82-2.91 (d, 3H), 3.45 (s, 2H), 3.83-3.97 (t, 2H), 4.91-5.02 (br, 1H), 6.62-6.85 (m, 4H), 7.09-7.41 (m, 6H), 7.47-7.59 (m, 2H), 7.61-7.84 (m, 4H). ES-MS m/z : 620 ($M + 1$).

4-(2-Chloroethoxy)benzoic acid ethyl ester (31a). A stirred mixture of Ethyl-4-hydroxybenzoate (3 g, 18 mmol), 1-Bromo-2-chloroethane (3 mL, 36 mmol) and K_2CO_3 (4.5 g) in acetone (150 mL) was refluxed for 20 hours and then hot filtered. The solvent was removed and the residue treated with Petroleum Ether (150 mL) and kept in the freezer overnight. The white solid that formed was filtered off affording **31a** (1.64 g, 40%). mp 73 °C. ^1H NMR (CDCl_3) δ : 1.25-1.70 (t, $J = 7.8$ Hz, 3H), 3.80-4.00 (t, $J = 6.2$ Hz, 2H), 4.22-4.60 (m, 4H), 6.95-7.15 (d, $J = 8.4$ Hz, 2H), 7.99-8.27 (d, $J = 8.4$ Hz, 2H).

3-(2-Chloroethoxy)benzoic acid ethyl ester (31b). A stirred mixture of Ethyl-3-hydroxybenzoate (3g, 18mmol), 1-Bromo-2-chloroethane (3 mL, 36 mmol) and K_2CO_3 (4.5 g) in acetone (150 mL) was refluxed for 20 hours and then hot filtered. The solvent was removed and the residue was purified by flash chromatography (Toluene/Acetone 90:10), affording **31b** as a colorless oil (1.22 g, 30%). ^1H NMR (CDCl_3) δ : 1.34-1.38 (t, $J = 6.00$ Hz, 3H), 3.75-3.82 (t, $J = 6.21$ Hz, 2H), 4.18-4.23 (t, $J = 6.42$ Hz, 2H), 4.32-4.38 (q, $J = 6.54$ Hz, 2H), 7.05-7.17 (d, $J = 7.4$ Hz, 1H), 7.29-7.47 (t, $J = 8.4$ Hz, 1H), 7.56 (s, 1H), 7.62-7.71 (d, $J = 7.2$ Hz, 1H).

4-(2-Chloroethoxy)benzoic acid (32a). To a stirred solution of **31a** (1.64 g, 7.2 mmol) in EtOH (50 mL), KOH (0.6 g, 10.8 mmol), previously solubilized in the minimum amount of water, was added dropwise. The reaction mixture was refluxed for 3 hours. The solvent was removed and the residue diluted with water and cooled to 0 °C. The solution was made acid by adding HCl 6N dropwise with stirring. The white solid that formed was filtered off affording **32a** (1.14 g, 79%). mp 177 °C. ¹H NMR (CDCl₃) δ: 3.79-3.99 (t, *J* = 6.2 Hz, 2H), 4.23-4.59 (m, 4H), 6.92-7.12 (d, *J* = 8.4 Hz, 2H), 8.05-8.32 (d, *J* = 8.4 Hz, 2H).

3-(2-Chloroethoxy)benzoic acid (32b). Using the previous procedure and starting from **31b** (1.22 g, 5.3 mmol), **32b** (0.93 g, 80%) was obtained as a white solid. mp 153 °C. ¹H NMR (CDCl₃) δ: 3.75-3.82 (t, *J* = 6.21 Hz, 2H), 4.18-4.23 (t, *J* = 6.42 Hz, 2H), 7.05-7.17 (d, *J* = 7.4 Hz, 1H), 7.29-7.47 (t, *J* = 8.4 Hz, 1H), 7.56 (s, 1H), 7.62-7.71 (d, *J* = 7.2 Hz, 1H).

4-(2-Chloroethoxy)benzoyl chloride (33a). **32a** (1.14 g, 5.7 mmol) was suspended in SOCl₂ (7 mL, 98 mmol), and refluxed with stirring for 12 hours. The excess of SOCl₂ was removed under vacuum and collected using a trap affording **33a** which was used for the next step without further purification. The yield was considered as quantitative.

3-(2-Chloroethoxy)benzoyl chloride (33b). Using the previous procedure and starting from **32b** (0.93 g, 4.6 mmol), **33b** was obtained and used for the next step without further purification. The yield was considered as quantitative.

(2-{4-[7-(Benzylmethylamino)heptyloxy]phenyl}benzofuran-3-yl)-[4-(2-chloroethoxy)phenyl]-methanone (34a). To a cooled solution (0 °C) of **4c** (1.2 g, 2.8 mmol) and **33a** (0.73 g, 3.4 mmol) in DCM anhydrous (50 mL), SnCl₄ (0.87 g, 3.4 mmol) was added dropwise with stirring. The mixture was allowed to reach room temperature then stirred overnight. The reaction was quenched with ice/water and stirred during 30 minutes. The organic layer was washed with water (3 x 10 mL) and brine (3 x 10 mL), then dried over Na₂SO₄ anhydrous and the solvent removed. The crude was purified by flash chromatography (Toluene/Acetone 20:80), affording **34a** as a dark yellow oil (0.92 g, 54%). ¹H NMR (CDCl₃) δ: 1.17-1.59 (m, 8H), 1.60-1.85 (m, 2H), 2.19 (s, 3H), 2.30-2.37 (t, *J* = 7.4 Hz, 2H), 3.45 (s, 2H), 3.70-3.85 (t, *J* = 6.2 Hz, 2H), 3.86-3.97 (t, *J* = 8.4 Hz, 2H), 4.15-4.26 (t, *J* = 8.4 Hz, 2H), 6.74-6.83 (m, 4H), 7.00-7.96 (m, 13H).

(2-{4-[7-(Benzylmethylamino)heptyloxy]phenyl}benzofuran-3-yl)-[3-(2-chloroethoxy)phenyl]-methanone (34b). Using the previous procedure and starting from **4c** (0.62 g, 1.45 mmol) and **33b** (0.38 g, 1.7 mmol), **34b** was obtained as a dark yellow oil (0.53 g, 60%). ¹H NMR (CDCl₃)

δ : 1.17-1.59 (m, 8H), 1.56-1.79 (m, 2H), 2.15 (s, 3H), 2.32-2.39 (t, $J = 7.4$ Hz, 2H), 3.47 (s, 2H), 3.73-3.88 (t, $J = 6.2$ Hz, 2H), 3.84-3.95 (t, $J = 8.4$ Hz, 2H), 4.16-4.27 (t, $J = 8.4$ Hz, 2H), 6.72-6.87 (m, 4H), 7.05-8.02 (m, 13H).

(2-{4-[7-(Benzylmethylamino)heptyloxy]phenyl}benzofuran-3-yl)-[4-(2-diethylaminoethoxy)phenyl]methanone (35). A stirred solution of **34a** (0.46 g, 0.75 mmol) and diethylamine (0.32 mL, 3.0 mmol) was refluxed in toluene (100 mL) for 20 hours in the presence of a catalytic amount of NaI. The mixture was washed with water (3 x 25 mL), then with brine (3 x 25 mL). The organic layer was collected and dried over Na₂SO₄ anhydrous. The solvent was removed and the residue was purified by flash chromatography (Toluene/Acetone 20:80), affording **35** as a dark yellow oil (0.04 g, 9%). ¹H NMR (CDCl₃) δ : 1.05-1.15 (t, $J = 8.4$ Hz, 6H), 1.18-1.62 (m, 8H), 1.63-1.85 (m, 2H), 2.19 (s, 3H), 2.32-2.43 (t, $J = 7.4$ Hz, 2H), 2.58-2.71 (q, $J = 8.2$ Hz, 4H), 2.82-2.94 (t, $J = 8.2$ Hz, 2H), 3.53 (s, 2H), 3.85-3.97 (t, $J = 6.2$ Hz, 2H), 4.05-4.12 (t, $J = 8.4$ Hz, 2H), 6.74-6.83 (m, 4H), 7.00-7.96 (m, 13H). ES-MS m/z : 647 (M + 1).

(2-{4-[7-(Benzylmethylamino)heptyloxy]phenyl}benzofuran-3-yl)-[3-(2-diethylaminoethoxy)phenyl]methanone (36). Using the previous procedure and starting from **34b** (0.46 g, 0.75 mmol), **36** was obtained as a dark yellow oil (0.03 g, 8%). ¹H NMR (CDCl₃) δ : 1.02-1.12 (t, $J = 8.4$ Hz, 6H), 1.17-1.61 (m, 8H), 1.62-1.86 (m, 2H), 2.21 (s, 3H), 2.35-2.46 (t, $J = 7.4$ Hz, 2H), 2.60-2.73 (q, $J = 8.2$ Hz, 4H), 2.80-2.92 (t, $J = 8.2$ Hz, 2H), 3.55 (s, 2H), 3.87-3.99 (t, $J = 6.2$ Hz, 2H), 4.02-4.09 (t, $J = 8.4$ Hz, 2H), 6.75-6.86 (m, 4H), 7.00-7.94 (m, 13H). ES-MS m/z : 647 (M + 1).

(2-{4-[7-(Benzylmethylamino)heptyloxy]phenyl}benzofuran-3-yl)-[4-(2-morpholinoethoxy)phenyl]methanone (37). Using the previous procedure and starting from **34a** (0.4 g, 0.57 mmol) and morpholine (0.1 g, 1.14 mmol), **37** was obtained as a dark yellow oil (0.08 g, 21%). ¹H NMR (CDCl₃) δ : 1.21-1.58 (m, 8H), 1.62-1.83 (m, 2H), 2.20 (s, 3H), 2.30-2.42 (t, $J = 6.23$ Hz, 2H), 2.50-2.62 (t, $J = 7.3$ Hz, 4H), 2.73-3.83 (t, $J = 6.4$ Hz, 2H), 3.43 (s, 2H), 3.65-3.80 (t, $J = 8.2$ Hz, 4H), 3.87-3.98 (t, $J = 6.3$ Hz, 2H), 4.08-4.19 (t, $J = 6.2$ Hz, 2H), 6.78-6.84 (d, $J = 6.2$ Hz, 2H), 7.12-7.41 (m, 10H), 7.50-7.62 (m, 4H), 7.83-7.95 (m, 2H). ES-MS m/z : 661 (M + 1).

(2-{4-[7-(Benzylmethylamino)heptyloxy]phenyl}benzofuran-3-yl)-[4-(chloromethyl)phenyl]methanone (38a). To a cool solution (0 °C) of **4c** (0.43 g, 1.0 mmol) and 4-chloromethylbenzoylchloride (0.24 g, 1.25 mmol) in DCM anhydrous (50 mL), SnCl₄ (0.32 g, 1.25 mmol) was added dropwise with stirring. The mixture was allowed to reach room temperature then stirred overnight. The reaction was quenched with ice/water and stirred during 30 minutes. The organic layer was washed with water (3 x 10 mL) and with brine (3 x 10 mL), then dried over

Na₂SO₄ anhydrous and the solvent removed. The crude was purified by flash chromatography (Toluene/Acetone 60:40), affording **38a** as a dark yellow oil (0.26 g, 43%). ¹H NMR (CDCl₃) δ: 1.02-1.60 (m, 8H), 1.62-1.88 (m, 2H), 2.20 (s, 3H), 2.33-2.44 (t, *J* = 7.4 Hz, 2H), 3.46 (s, 2H), 3.85-3.97 (t, *J* = 8.2 Hz, 2H), 4.58 (s, 2H), 6.77-6.83 (d, *J* = 6.2 Hz, 2H), 7.05-7.38 (m, 11H), 7.50-7.63 (m, 4H), 7.79-7.92 (m, 2H).

(2-{4-[7-(Benzylmethylamino)heptyloxy]phenyl}benzofuran-3-yl)[3-(chloromethyl)phenyl]methanone (38b). Using the previous procedure and starting from **4c** (0.43 g, 1.0 mmol) and 3-Chloromethylbenzoylchloride (0.24 g, 1.25 mmol), **38b** was obtained after flash chromatography (Toluene/Acetone 60:40), as a dark yellow oil (0.27 g, 45%). ¹H NMR (CDCl₃) δ: 1.00-1.58 (m, 8H), 1.64-1.90 (m, 2H), 2.19 (s, 3H), 2.35-2.46 (t, *J* = 7.4 Hz, 2H), 3.45 (s, 2H), 3.80-3.92 (t, *J* = 8.2 Hz, 2H), 4.59 (s, 2H), 6.76-6.82 (d, *J* = 6.2 Hz, 2H), 7.05-7.38 (m, 11H), 7.49-7.61 (m, 4H), 7.81-7.93 (m, 2H).

(2-{4-[7-(Benzylmethylamino)heptyloxy]phenyl}benzofuran-3-yl)[4-(diethylaminomethyl)phenyl]methanone (39). A stirred solution of **38a** (0.26 g, 0.45 mmol) and diethylamine (0.1 mL, 0.90 mmol) was refluxed in toluene (100 mL) for 20 hours in the presence of a catalytic amount of NaI. The mixture was washed with water (3 x 25 mL), then with brine (3 x 25 mL). The organic layer was collected and dried over Na₂SO₄ anhydrous. The solvent was removed and the residue purified by flash chromatography (Toluene/Acetone 60:40), affording **39** as a dark yellow oil (0.05 g, 18%). ¹H NMR (CDCl₃) δ: 0.98-1.05 (t, *J* = 8.2 Hz, 6H), 1.22-1.58 (m, 8H), 1.62-1.82 (m, 2H), 2.20 (s, 3H), 2.35-2.46 (m, 6H), 3.45 (s, 2H), 3.58 (s, 2H), 3.83-3.95 (t, *J* = 8.2 Hz, 2H), 6.78-6.84 (d, *J* = 6.2 Hz, 2H), 7.10-7.38 (m, 10H), 7.49-7.61 (m, 4H), 7.81-7.93 (m, 2H). ES-MS *m/z*: 617 (M + 1).

(2-{4-[7-(Benzylmethylamino)heptyloxy]phenyl}benzofuran-3-yl)-[3-(diethylaminomethyl)phenyl]methanone (40). Using the previous procedure and starting from **38b** (0.27 g, 0.47 mmol), **40** (0.06 g, 20%) was obtained as a dark yellow oil. ¹H NMR (CDCl₃) δ: 1.01-1.08 (t, *J* = 8.2 Hz, 6H), 1.21-1.57 (m, 8H), 1.59-1.79 (m, 2H), 2.19 (s, 3H), 2.37-2.48 (m, 6H), 3.47 (s, 2H), 3.56 (s, 2H), 3.82-3.94 (t, *J* = 8.2 Hz, 2H), 6.79-6.85 (d, *J* = 6.2 Hz, 2H), 7.11-7.39 (m, 10H), 7.50-7.62 (m, 4H), 7.83-7.95 (m, 2H). ES-MS *m/z*: 617 (M + 1).

2-(6-Bromoethyl)isoindole-1,3-dione (41a). A suspension of Phtalimide potassium salt (5.3 g, 28.6 mmol) and 1,6-Dibromohexane (13.98 g, 57.3 mmol) in DMF (16 mL) was refluxed for 2 hours. The reaction mixture was poured in ice/water and the formed solid was filtered under

vacuum, obtaining **41a** as a solid (5.37 g, 60%). mp 42-44 °C. ¹H NMR (CDCl₃) δ: 1.4 (m, 4H), 1.7 (m, 2H), 1.85 (m, 2H), 3.4 (m, 2H), 3.7 (t, 2H), 7.75 (m, 2H), 7.85 (m, 2H).

2-(7-Bromoheptyl)isoindole-1,3-dione (41b). Following the previous procedure and starting from 1,7-Dibromoheptane (6 mL), **41b** was obtained as a solid (40% yield). mp 23-25° C. ¹H NMR (CDCl₃) δ: 1.3 (m, 6H), 1.65 (m, 2H), 1.85 (m, 2H), 3.35 (m, 2H), 3.7 (t, 2H), 7.75 (m, 2H), 7.85 (m, 2H).

2-(8-Bromooctyl)isoindole-1,3-dione (41c). Following the previous procedure and starting from 1,8-Dibromooctane (8.12 mL), **41c** was obtained as a solid (60% yield). mp 39-41 °C. ¹H NMR (CDCl₃) δ: 1.4 (m, 8H), 1.7 (m, 2H), 1.85 (m, 2H), 3.5 (m, 2H), 3.7 (t, 2H), 7.7 (m, 2H), 7.8 (m, 2H).

2-(9-Bromononyl)isoindole-1,3-dione (41d). Following the previous procedure and starting from 1,9-Dibromononane (10.5 mL), **41d** was obtained as a solid (60% yield). mp 31-32 °C. ¹H NMR (CDCl₃) δ: 1.4 (m, 10 H), 1.7 (m, 2H), 1.85 (m, 2H), 3.4 (m, 2H), 3.7 (t, 2H), 7.75 (m, 2H), 7.85 (m, 2H).

2-(10-Bromodecyl)isoindole-1,3-dione (41e). Following the previous procedure and starting from 1,10-Dibromodecane (9 g), **41e** was obtained as a solid (65% yield). mp 34-36° C. ¹H NMR (CDCl₃) δ: 1.4 (m, 12 H), 1.7 (m, 2H), 1.85 (m, 2H), 3.4 (m, 2H), 3.7 (t, 2H), 7.75 (m, 2H), 7.85 (m, 2H).

2-(6-Morpholin-4-yl-hexyl)isoindole-1,3-dione (42a). A solution of **41a** (5.37 g, 17.3 mmol) and morpholine (3.03 mL, 34.6 mmol) in toluene was refluxed for 10 hours. The mixture was washed with water then extracted with diluted HCl. The extracts were made basic by K₂CO₃ and the alkaline solution was extracted with DCM. The organic layer was dried and evaporated affording **42a** as a solid (3.48 g, 70%). mp 47-51 °C. ¹H NMR (CDCl₃) δ: 1.3 (m, 4 H), 1.6 (m, 2H), 1.8 (m, 2H), 2.35 (m, 2H), 2.5 (m, 4H), 3.7 (m, 6H), 7.75 (m, 2H), 7.85 (m, 2H).

2-(7-Morpholin-4-yl-heptyl)isoindole-1,3-dione (42b). Starting from **41b** and following the previous procedure, **42b** was obtained as an oil (95% yield). ¹H NMR (CDCl₃) δ: 1.3 (m, 6 H), 1.5 (m, 2H), 1.75 (m, 2H), 2.35 (m, 2H), 2.45 (m, 4H), 3.7 (m, 6H), 7.75 (m, 2H), 7.85 (m, 2H).

2-(8-Morpholin-4-yl-octyl)isoindole-1,3-dione (42c). Starting from **41c** and following the previous procedure, **42c** was obtained as an oil (75% yield). ¹H NMR (CDCl₃) δ: 1.3 (m, 8 H), 1.5 (m, 2H), 1.75 (m, 2H), 2.35 (m, 2H), 2.45 (m, 4H), 3.8 (m, 6H), 7.75 (m, 2H), 7.85 (m, 2H).

2-(9-Morpholin-4-yl-nonyl)isoindole-1,3-dione (42d). Starting from **41d** and following the previous procedure, **42d** was obtained as a solid (60% yield). mp 47-51 °C. ¹H NMR (CDCl₃) δ: 1.3 (m, 10H), 1.5 (m, 2H), 1.7 (m, 2H), 2.35 (m, 2H), 2.45 (m, 4H), 3.7 (m, 6H), 7.75 (m, 2H), 7.85 (m, 2H).

2-(10-Morpholin-4-yl-decyl)isoindole-1,3-dione (42e). Starting from **41e** and following the previous procedure, **42e** was obtained as a solid (68% yield). mp 49-54 °C. ¹H NMR (CDCl₃) δ: 1.3 (m, 12H), 1.5 (m, 2H), 1.7 (m, 2H), 2.35 (m, 2H), 2.45 (m, 4H), 3.7 (m, 6H), 7.75 (m, 2H), 7.85 (m, 2H).

6-Morpholin-4-yl-hexylamine (43a). A stirred solution of **42a** (3.48 g) and hydrazine monohydrate (1.6 mL) in EtOH (38 mL) was refluxed for 3 hours. HCl (4 mL) was then added portion wise and the mixture was allowed to reflux for 30 minutes. The solvent was removed and the residue treated with water and made alkaline by K₂CO₃. The aqueous phase is extracted with DCM which is then dried over Na₂SO₄ and evaporated affording **43a** as a solid (1.74 g, 85%) mp 57-60 °C. ¹H NMR (CDCl₃) δ: 1.3 (m, 4H), 1.5 (m, 4H), 2.35 (t, 2H), 2.45 (m, 4H), 2.7 (t, H), 3.7 (m, 4H).

7-Morpholin-4-yl-heptylamine (43b). Starting from **42b** and following the previous procedure, **43b** was obtained as an oil in quantitative yield. ¹H NMR (CDCl₃) δ: 1.3 (m, 6H), 1.5 (m, 4H), 2.0 (br, 2H), 2.35 (t, 2H), 2.45 (m, 4H), 2.7 (t, H), 3.75 (m, 4H).

8-Morpholin-4-yl-octylamine (43c). Starting from **42c** and following the previous procedure, **43c** was obtained as a solid in 70% yield. mp 63-65 °C. ¹H NMR (CDCl₃) δ: 1.3 (m, 8H), 1.5 (m, 4H), 2.3 (t, 2H), 2.45 (m, 4H), 2.7 (t, H), 3.75 (m, 4H).

9-Morpholin-4-yl-nonylamine (43d). Starting from **42d** and following the previous procedure, **43d** was obtained as a solid in 70% yield. mp 36-39 °C. ¹H NMR (CDCl₃) δ: 1.3 (m, 10H), 1.5 (m, 4H), 2.3 (t, 2H), 2.45 (m, 4H), 2.65 (t, H), 3.7 (m, 4H).

10-Morpholin-4-yl-decylamine (43e). Starting from **42e** and following the previous procedure, **43e** was obtained as a solid in 75% yield. mp 42-45 °C. ¹H NMR (CDCl₃) δ: 1.3 (m, 12H), 1.5 (m, 4H), 2.3 (t, 2H), 2.45 (m, 4H), 2.65 (t, H), 3.7 (m, 4H).

9-Chloro-1,2,3,4-tetrahydroacridine (44). To a cooled mixture (ice bath) of 2-Aminobenzoic acid (2.00 g, 14.58 mmol) and cyclohexanone (1.5 mL, 14.58 mmol), POCl₃ (12 mL) was carefully added. The mixture was heated under reflux for 2 h, then cooled at room temperature, and concentrated to give a slurry. The residue was diluted with EtOAc, neutralized with aqueous

K_2CO_3 , and washed with brine. The organic layer was dried over anhydrous Na_2SO_4 and concentrated to furnish **45** as a pale brown solid (1.74 g, 55%); mp 85-87 °C. 1H NMR ($CDCl_3$) δ : 1.63-1.71 (m, 2H), 2.13-2.42 (t, 2H), 2.67-2.82 (s, 4H), 7.24-7.39 (m, 4H).

(6-Morpholin-4-yl-hexyl)-(1,2,3,4-tetrahydroacridin-9-yl)amine (45a). A stirred suspension of **44** (0.35 g, 2.76 mmol) and Phenol (1.50 mL) was heated at 85-90 °C until a solution was obtained. **43a** (0.6 g, 5.53 mmol) was then added and the reaction mixture heated to 130 °C for 4 hours. The crude was washed with NaOH 2N solution and extracted with EtOAc, dried over Na_2SO_4 and evaporated. Flash chromatography (DCM/MeOH/ NH_4OH 70:30:0.7) afforded **45a** as a brownish oil (0.26 g, 26%). 1H NMR ($CDCl_3$) δ : 1.20-1.58 (m, 6H), 1.60-1.75 (m, 2H), 1.80-1.99 (s, 4H), 2.20-2.38 (t, 2H), 2.39-2.45 (s, 4H), 2.60-2.68 (s, 2H), 2.98-3.17 (s, 2H), 3.40-3.57 (t, 2H), 3.60-3.79 (m, 4H), 3.81-4.01 (br, 1H), 7.22-7.38 (m, 1H), 7.42-7.60 (t, 1H), 7.80-8.00 (t, 2H).

(7-Morpholin-4-yl-heptyl)-(1,2,3,4-tetrahydroacridin-9-yl)amine (45b). Starting from **43b** and following the previous procedure, **45b** was obtained as a brownish oil. 1H NMR ($CDCl_3$) δ : 1.20-1.58 (m, 8H), 1.60-1.75 (m, 2H), 1.80-1.99 (s, 4H), 2.20-2.38 (t, 2H), 2.39-2.45 (s, 4H), 2.60-2.68 (s, 2H), 2.98-3.17 (s, 2H), 3.40-3.57 (t, 2H), 3.60-3.79 (m, 4H), 3.81-4.01 (br, 1H), 7.22-7.38 (m, 1H), 7.42-7.60 (t, 1H), 7.80-8.00 (t, 2H).

(8-Morpholin-4-yl-octyl)-(1,2,3,4-tetrahydroacridin-9-yl)amine (45c). Starting from **43c** and following the previous procedure, **45c** was obtained as a brownish oil. 1H NMR ($CDCl_3$) δ : 1.20-1.58 (m, 10H), 1.60-1.75 (m, 2H), 1.80-1.99 (s, 4H), 2.20-2.38 (t, 2H), 2.39-2.45 (s, 4H), 2.60-2.68 (s, 2H), 2.98-3.17 (s, 2H), 3.40-3.57 (t, 2H), 3.60-3.79 (m, 4H), 3.81-4.01 (br, 1H), 7.22-7.38 (m, 1H), 7.42-7.60 (t, 1H), 7.80-8.00 (t, 2H).

(9-Morpholin-4-yl-nonyl)-(1,2,3,4-tetrahydroacridin-9-yl)amine (45d). Starting from **43d** and following the previous procedure, **45d** was obtained as a brownish oil. 1H NMR ($CDCl_3$) δ : 1.20-1.58 (m, 12H), 1.60-1.75 (m, 2H), 1.80-1.99 (s, 4H), 2.20-2.38 (t, 2H), 2.39-2.45 (s, 4H), 2.60-2.68 (s, 2H), 2.98-3.17 (s, 2H), 3.40-3.57 (t, 2H), 3.60-3.79 (m, 4H), 3.81-4.01 (br, 1H), 7.22-7.38 (m, 1H), 7.42-7.60 (t, 1H), 7.80-8.00 (t, 2H).

(10-Morpholin-4-yl-decyl)-(1,2,3,4-tetrahydroacridin-9-yl)amine (45e). Starting from **43e** and following the previous procedure, **45e** was obtained as a brownish oil. 1H NMR ($CDCl_3$) δ : 1.20-1.58 (m, 12H), 1.60-1.75 (m, 2H), 1.80-1.99 (s, 4H), 2.20-2.38 (t, 2H), 2.39-2.45 (s, 4H), 2.60-2.68 (s, 2H), 2.98-3.17 (s, 2H), 3.40-3.57 (t, 2H), 3.60-3.79 (m, 4H), 3.81-4.01 (br, 1H), 7.22-7.38 (m, 1H), 7.42-7.60 (t, 1H), 7.80-8.00 (t, 2H).

1,2,3,4-Tetrahydroacridin-9-ylamine (46a). A stirred mixture of 2-Aminobenzonitrile (5 g, 42.4 mmol), Cyclohexanone (4.15 g, 42.4 mmol) and ZnCl₂ (11.44 g, 84.7 mmol) was heated neat at 130 °C for 3 hours. The reaction mixture was quenched with ice/water and made alkaline by NaHCO₃ saturated solution. The solid residue was filtered and crystallized from EtOH affording **46a** as a pale yellow solid (3.78 g, 58%). mp 284-286 °C. ¹H NMR (CDCl₃) δ: 1.87-1.89 (m, 4H), 2.84-2.87 (m, 2H), 3.01 (s, 2H), 7.30-7.34 (m, 2H), 7.80-7.85 (m, 2H).

6-Chloro-1,2,3,4-tetrahydro-acridin-9-ylamine (46b). Following the previous procedure and starting from 2-Amino-4-chlorobenzonitrile (5 g, 32.9 mmol), **46b** was obtained as a pale yellow solid (3.58 g, 47%). mp 172-173 °C. ¹H NMR (CDCl₃) δ: 1.85-1.87 (m, 4H), 2.83-2.85 (m, 2H), 3.06 (s, 2H), 7.28-7.33 (m, 1H), 7.76-7.82 (m, 2H).

11H-Indeno[1,2-b]quinolin-10-ylamine (47a). Following the previous procedure and starting from 2-Aminobenzonitrile (5 g, 42.4 mmol) and indanone, **47a** was obtained as a pale yellow solid (2.5 g, 25%). mp 264-265 °C. ¹H NMR (CDCl₃) δ: 4.07 (s, 2H), 7.42-7.63 (m, 4H), 7.70-7.81 (t, 1H), 8.18-8.31 (m, 3H).

7-Chloro-11H-indeno[1,2-b]quinolin-10-ylamine (47b). Following the previous procedure and starting from 2-Amino-4-chlorobenzonitrile (5 g, 32.9 mmol) and indanone, **47b** was obtained as a pale yellow solid (1.4 g, 16%). mp 124-125 °C. ¹H NMR (CDCl₃) δ: 4.09 (s, 2H), 7.51-7.64 (m, 4H), 8.17-8.26 (m, 3H).

(7-Bromoheptyl)-(11H-indeno[1,2-b]quinolin-10-yl)amine (48a). A suspension of **47a** (0.65 g, 2.8 mmol), 1,7-dibromoheptan (0.57 mL, 3.4 mmol) and KOH (0.25 g, 4.5 mmol) in dry DMSO (10 mL) was stirred for 16 hours at room temperature under nitrogen in the presence of freshly activated 4 Å molecular sieves (100 mg). The mixture was filtered through Celite[®] and the filtrate diluted with water (250 mL), extracted with EtOAc (3 x 30 mL), anhydriified over Na₂SO₄ and concentrated to dryness. Flash chromatography (DCM/MeOH 98:2) afforded 0.11 g of **48a** as a yellowish oil (10%). ¹H NMR (CDCl₃): δ 1.38-1.60 (m, 6H), 1.62-1.83 (m, 4H), 3.60-3.78 (m, 4H), 4.12 (s, 2H), 7.40-7.61 (m, 4H), 7.72-7.83 (t, 1H), 8.16-8.29 (m, 3H).

(7-Bromoheptyl)-(7-chloro-11H-indeno[1,2-b]quinolin-10-yl)amine (48b). Following the previous procedure and starting from **47b** (0.5 g, 1.88 mmol), **48b** was obtained as a brownish oil (0.18 g, 22%). ¹H NMR (CDCl₃): δ 1.37-1.59 (m, 6H), 1.63-1.85 (m, 4H), 3.58-3.76 (m, 4H), 4.11 (s, 2H), 7.42-7.63 (m, 4H), 7.71-7.82 (t, 1H), 8.15-8.32 (m, 2H).

***N*-(11H-Indeno[1,2-b]quinolin-10-yl)-*N'*-(1,2,3,4-tetrahydroanthracen-9-yl)heptane-1,7-diamine (49a).** Following the previous procedure and starting from **48a** (0.1 g, 0.24 mmol) and **46a** (0.048 g, 0.24 mmol) **49a** was obtained as a pale brown oil (0.03 g, 24%). ¹H NMR (CDCl₃): δ 1.20-1.60 (m, 8H), 1.62-1.97 (m, 6H), 2.59-2.67 (m, 2H), 3.02-3.18 (m, 2H), 3.60 (t, 2H), 3.80 (t, 2H), 4.08 (s, 2H), 5.60 (br, 1H), 7.20-7.60 (m, 7H), 7.85-8.17 (m, 4H), 8.32-8.41 (m, 1H). ES-MS *m/z*: 527 (M + 1).

***N*-(6-Chloro-1,2,3,4-tetrahydroanthracen-9-yl)-*N'*-(11H-indeno[1,2-b]quinolin-10-yl)heptane-1,7-diamine (49b).** Following the previous procedure and starting from **48a** (0.1 g, 0.24 mmol) and **46b** (0.055 g, 0.24 mmol) **49b** was obtained as a pale brown oil (0.07 g, 51%). ¹H NMR (CDCl₃): δ 1.27-1.58 (m, 6H), 1.59-1.80 (m, 4H), 1.81-1.96 (m, 4H), 2.57-2.65 (m, 2H), 3.00-3.11 (m, 2H), 3.55 (t, 2H), 3.70 (t, 2H), 3.98 (s, 2H), 7.20-7.60 (m, 6H), 7.85-8.17 (m, 4H), 8.32-8.41 (m, 1H). ES-MS *m/z*: 561 (M + 1).

***N*-(3-Chloro-11H-indeno[1,2-b]quinolin-10-yl)-*N'*-(6-chloro-1,2,3,4-tetrahydroanthracen-9-yl)heptane-1,7-diamine (49c).** Following the previous procedure and starting from **48b** (0.15 g, 0.34 mmol) and **46b** (0.078 g, 0.34 mmol) **49c** was obtained as a pale brown oil (0.03 g, 15%). ¹H NMR (CDCl₃): δ 1.27-1.58 (m, 6H), 1.59-1.80 (m, 4H), 1.81-1.96 (m, 4H), 2.57-2.65 (m, 2H), 3.00-3.11 (m, 2H), 3.55 (t, 2H), 3.70 (t, 2H), 3.98 (s, 2H), 7.20-7.60 (m, 6H), 7.85-8.17 (m, 4H). ES-MS *m/z*: 595 (M + 1).

***N,N'*-Bis-(11H-indeno[1,2-b]quinolin-10-yl)heptane-1,7-diamine (49d).** Following the previous procedure and starting from **48a** (0.1 g, 0.24 mmol) and **47a** (0.056 g, 0.24 mmol), **49d** was obtained as a pale brown oil (0.05 g, 37%). ¹H NMR (CDCl₃): δ 1.35-1.59 (m, 6H), 1.60-1.77 (m, 4H), 3.59-3.72 (m, 4H), 4.11 (s, 2H), 4.80 (br, 2H), 7.05-7.71 (m, 12H), 8.00-8.17 (m, 2H), 8.20-8.32 (m, 2H). ES-MS *m/z*: 561 (M + 1).

7-(7-Bromoheptyloxy)-9-oxa-1-azaanthracen-10-one (51). A stirred suspension of **50** (0.8 g, 3.7 mmol), 1,7-Dibromoheptane (1.2 mL, 7.5 mmol) and K₂CO₃ (0.97 mg) in acetone (30 mL) was refluxed for 20 h. The reaction mixture was hot filtered and the filtrate evaporated. The residue was purified by flash chromatography (toluene/acetone 90:10), affording **51** as an oil (0.65 g, 45%). ¹H NMR (CDCl₃): δ 1.35-1.57 (m, 6H), 1.79-1.97 (m, 4H), 3.38-3.50 (t, 2H), 4.05-4.17 (t, 2H), 6.91-7.03 (m, 2H), 7.39-7.45 (m, 1H), 8.16-8.23 (m, 1H), 8.60-8.75 (m, 2H).

7-[7-(1,2,3,4-Tetrahydroanthracen-9-ylamino)heptyloxy]-9-oxa-1-azaanthracen-10-one (52). A mixture of **46a** (0.078 g, 0.39 mmol), **51** (0.31 g, 0.79 mmol) and a catalytic amount of tetra-*n*-

butylammoniumhydrogensulphate (0.0195 g) were stirred at room temperature for 4 hours in a biphasic mixture of DCM/NaOH 50% (7.5 / 5 mL). The organic layer was separated and washed with water, then dried and evaporated. The crude was purified by flash chromatography (DCM/MeOH 97:3) affording **52** as a brownish oil (0.015 g, 7.6%). ¹H NMR (CDCl₃): δ 1.42-1.65 (m, 6H), 1.77-2.05 (m, 8H), 2.60 (t, 2H), 3.30 (t, 2H), 3.90 (t, 2H), 4.15 (t, 2H), 5.80 (br, 1H), 7.05-7.71 (m, 8H), 8.00-8.17 (m, 2H). ES-MS *m/z*: 508 (M + 1).

[7-(4-Benzofuran-2-yl-phenoxy)heptyl]-(6-chloro-1,2,3,4-tetrahydroacridin-9-yl)amine (53a).

A solution of **46b** (0.15 g, 0.65 mmol), **3c** (0.3 g, 0.78 mmol) and KOH (0.06 g, 1.04 mmol) in dry DMSO (8 mL) was stirred for 16 hours at room temperature under nitrogen in the presence of freshly activated 4 Å molecular sieves (100 mg). The mixture was filtered through Celite[®] and the filtrate diluted with water (300 mL), extracted with EtOAc (3 × 25 mL) anhydriified over Na₂SO₄ and concentrated to dryness giving 0.26 g of crude. Flash chromatography (DCM/MeOH 98:2) afforded **53a** as a yellowish oil (0.18 g, 51%). ¹H NMR (CDCl₃) δ : 1.28-1.52 (m, 6H), 1.54-1.92 (m, 8H), 2.52-2.68 (m, 2H), 2.92-3.12 (m, 2H), 3.38-3.45 (t, *J* = 7.0 Hz, 2H), 3.89-3.95 (t, *J* = 6.2 Hz, 2H), 5.24 (s, 1H), 6.82 (s, 1H), 6.88- 6.92 (d, *J* = 8.8 Hz, 2H), 7.18-7.25 (m, 3H), 7.45-7.49 (m, 2H), 7.71-7.75 (d, *J* = 8.8 Hz, 2H), 7.83-7.88 (d, *J* = 10.6 Hz, 2H). ¹³C NMR (CDCl₃) δ : 22.48, 22.74, 24.37, 25.79, 26.66, 28.93, 31.52, 33.90, 40.77, 49.33, 67.72, 99.41, 110.76, 114.56, 115.50, 118.23, 120.38, 122.66, 122.93, 123.54, 123.93, 124.49, 126.18, 127.41, 129.32, 133.71, 148.00, 150.57, 150.79, 154.48, 155.89, 159.31. ES-MS *m/z*: 539 (M + 1).

[7-(3-Benzofuran-2-yl-phenoxy)heptyl]-(6-chloro-1,2,3,4-tetrahydroacridin-9-yl)amine (53b).

Following the previous procedure and starting from **46b** (0.15 g, 0.65 mmol) and **3f** (0.3 g, 0.78 mmol), **53b** was obtained as a yellowish oil (0.05 g, 14%). ¹H NMR (CDCl₃) δ : 1.38-1.58 (m, 6H), 1.60-1.93 (m, 8H), 2.60-2.65 (m, 2H), 2.98-3.10 (m, 2H), 3.45-3.52 (t, 7.0 Hz, 2H), 3.99-4.06 (t, 6.6 Hz, 2H), 5.28 (s, 1H), 6.81-6.92 (m, 1H), 7.00 (s, 1H), 7.21-7.59 (m, 8H), 7.87-7.91 (m, 2H).

2-Hydroxymethyl-4-methoxyphenol (54). A stirred solution of 2-Hydroxy-5-methoxy benzaldehyde (5 g, 32.86 mmol) in EtOH (66 mL, 0.5 M) was cooled to 0 °C and NaBH₄ (1.24 g, 32.86 mmol) was added portionwise. The resulting suspension was then allowed to reach room temperature and stirred for about 1 hour. The solvent was removed and the residue was cooled to 0 °C, made acid with HCl 1N and extracted with Et₂O. The organic layers were collected, dried over Na₂SO₄ and concentrated to afford **54** as a white crystalline solid (5 g, 99%). (R.f. 0.18; petroleum ether/ethyl acetate 60:40 as eluent). mp 76 °C. ¹H NMR (CDCl₃) δ : 3.99 (s, 3H), 5.28 (s, 2H), 6.81-6.92 (m, 1H), 7.00 (s, 1H), 7.21-7.59 (m, 1H).

(2-Hydroxy-5-methoxybenzyl)-triphenylphosphonium bromide (55). To stirred solution of **54** (0.47 g, 3.05 mmol) in acetonitrile (325 mL, 0.1 M), triphenyl-phosphonium bromide (1.05 g, 3.05 mmol) was added. The resulting mixture was refluxed for 1 hour until the formation of an heavy white precipitate. The solid was filtered off and washed with cold acetonitrile affording **55** as a white solid (1.14 g, 78%). mp 298 dec. $^1\text{H NMR}$ ($d_6\text{DMSO}$) δ : 3.99 (s, 3H), 5.68 (s, 2H), 6.97-7.15 (m, 8H), 7.32-7.54 (m, 3H), 8.35-8.59 (m, 2H), 8.85-8.91 (m, 5H).

4-Benzyloxybenzoic acid ethyl ester (56). A stirred suspension of Ethyl-*p*-hydroxybenzoate (5 g, 30 mmol), K_2CO_3 (8.30 g, 60 mmol) and benzylbromide (5.35 mL, 45 mmol) in acetone (60 mL, 0.5 M) was refluxed for 10 hours, then hot filtered. The filtrate was concentrated to dryness. To the residue, petroleum ether was added and the flask kept in the freezer overnight. The formed white solid was filtered off affording **56** (6.06 g, 79%). mp 43-44 °C. $^1\text{H NMR}$ (CDCl_3) δ : 1.56-1.87 (t, 3H), 4.05 (q, 2H), 5.23(s, 2H), 6.78-6.90 (m, 3H), 7.01-7.12 (d, 2H), 7.23-7.42 (d, 2H), 8.02-8.14 (m, 2H).

4-Benzyloxybenzoic acid (57). To a stirred solution of **56** (6.06 g, 24 mmol) in EtOH (50 mL), NaOH (1.42 g, 0.035 mmol) previously solubilized in 2.5 mL of water was added. The mixture was refluxed for 3 hours, then cooled to room temperature. EtOH was removed under vacuum and the residue was diluted with water then cooled to 0 °C and made acid with HCl 6N. The white solid that formed was filtered off affording **57** (5.24 g, 96%). mp 189-190 °C. $^1\text{H NMR}$ (CDCl_3) δ : 4.98 (s, 2H), 6.77-6.92 (m, 3H), 7.03-7.15 (d, 2H), 7.26-7.43 (d, 2H), 7.98-8.10 (m, 2H).

4-Benzyloxybenzoyl chloride (58). **57** (5.24 g, 23 mmol) was refluxed in SOCl_2 (16.67 mL, 230 mmol) with stirring for 3 hours. The resulting solution is cooled to room temperature and the excess of SOCl_2 removed under vacuum affording **58** as a greyish solid (5.65 g, 100%). mp 99-100 °C. The intermediate is used for the next step without any further characterization.

2-(4-Benzyloxyphenyl)-5-methoxybenzofuran (59). A stirred suspension of **55** (10 g, 20.8 mmol), **58** (5.6 g, 22.9 mmol) and Et_3N (8.7 mL, 62.6 mmol) in Toluene (208 mL) was refluxed for 10 hours. The reaction mixture was cooled to room temperature and filtered. The filtrate was concentrated to dryness, EtOH was added to the residue and the flask kept in the freezer overnight. The solid that formed was filtered off affording 2.35 g of crude which upon flash chromatography (DCM/petroleum ether 50:50) gave **59** as a white crystalline solid (0.74 g, 11 %). mp 76 °C. $^1\text{H NMR}$ (CDCl_3): δ 3.85 (s, 3H), 5.12 (s, 2H), 6.82 (s, 1H), 6.86-6.87 (d, 2.6 Hz, 1H), 7.02-7.06 (m, 3H), 7.35-7.43 (m, 6H), 7.74-7.79 (d, 8.8 Hz, 2H).

4-(5-Methoxybenzofuran-2-yl)phenol (60). **59** (0.2 g, 0.61 mmol) was dissolved in THF (100 mL) and Pd/C 10% was added catalytically. The flask was purged and filled with H₂. The reaction was stirred under H₂ (1 atm) at room temperature for 5 h. The catalyst was then removed by filtration through a pad of Celite[®] and the filtrate concentrated to dryness affording 0.19 g of crude. Flash chromatography (DCM/petroleum ether/acetone 50:45:5), afforded **60** (0.1 g, 69%) as a white solid. mp 189 °C. ¹H NMR (CD₃COCD₃): δ 3.81 (s, 3H), 6.82-7.09 (m, 5H), 7.37-7.41 (d, 8.4 Hz, 1H), 7.73-7.77 (d, 8.8 Hz, 2H), 8.73 (br, 1H OH) .

2-[4-(7-Bromoheptyloxy)phenyl]-5-methoxybenzofuran (61). A stirred suspension of **60** (0.07 g, 0.29 mmol), K₂CO₃ anhydrous (0.08 g, 0.58 mmol) and 1,7-dibromoheptan (0.1 mL, 0.58 mmol) in acetone (20 mL) was refluxed for 10 hours, then filtered when hot. The filtrate was concentrated and petroleum ether was added to the resulting residue. After cooling overnight in a freezer a white solid formed which was filtered off affording **61** (0.07g, 58%). mp 123 °C. ¹H NMR (CDCl₃): δ 1.15-1.32 (m, 6H), 1.75-1.89 (q, 7.2 Hz, 4H), 3.37-3.44 (t, 6.6 Hz, 2H), 3.83 (s, 3H), 3.94-4.00 (t, 6.6 Hz, 2H), 6.80-7.00 (m, 5H), 7.34-7.39 (d, 8.8 Hz, 1H), 7.72-7.76 (d, 8.8 Hz, 2H); ¹³C NMR (CDCl₃): δ 25.83, 28.03, 28.47, 29.07, 32.65, 33.89, 55.83, 67.88, 99.73, 103.09, 111.29, 112.16, 114.69, 123.15, 126.25, 130.02, 149.65, 153.07, 155.94, 156.86, 159.43, 197.95.

Benzyl-{7-[4-(5-methoxybenzofuran-2-yl)phenoxy]heptyl}methyl-amine (62). A stirred solution of **61** (0.07 g, 0.17 mmol) and *N*-Benzylmethylamine (0.04 mL, 0.34 mmol) in toluene (20 mL) was refluxed for 20 hours. The mixture was washed with water and the organic layer dried over Na₂SO₄ and concentrated. The crude was then purified by flash chromatography (toluene/acetone 96:4), affording **62** as a white solid (0.05 g, 65%). mp 122 °C. ¹H NMR (CDCl₃): δ 1.25-1.52 (m, 8H), 1.75-1.82 (m, 2H), 2.18 (s, 3H), 2.32-2.39 (t, 7.2 Hz, 1H), 3.47 (s, 2H), 3.84 (s, 3H), 3.94-4.01 (t, 6.4 Hz, 2H), 6.80- 6.87 (m, 2H), 6.92-7.00 (m, 3H), 7.24-7.39 (m, 6H), 7.72-7.77 (d, 8.4 Hz, 2H). ¹³C NMR (CDCl₃): δ 25.98, 27.31, 29.17, 29.28, 42.25, 55.85, 57.46, 62.32, 68.02, 99.71, 103.12, 111.30, 112.15, 114.72, 123.14, 126.27, 126.82, 128.13, 129.01, 130.05, 139.25, 149.67, 155.96, 156.92, 158.51, 159.50.

2-(4-Methoxy-benzyl)-benzofuran (63). Following the same procedure for the synthesis of **1a** and starting from 4-Metoxybenzoylchloride (5 g, 27 mmol), **63** was obtained as a colorless oil. (2.97 g, 46%). ¹H NMR (CDCl₃) δ: 2.47 (s, 2H), 3.93 (s, 3H), 6.89 (s, 1H), 6.91-6.99 (m, 2H), 7.21-7.32 (m, 2H), 7.33-7.61 (m, 2H), 7.72-7.83 (m, 2H).

4-Benzofuran-2-ylmethyl-phenol (64). Following the same procedure for the synthesis of **2a** and starting from **63** (2.5 g, 11 mmol), **64** was obtained as a white solid (2.11 g, 90%). mp 137 °C.

¹H NMR (CDCl₃) δ : 2.45 (s, 2H), 6.86 (s, 1H), 6.89-6.97 (m, 2H), 7.18-7.29 (m, 2H), 7.34-7.62 (m, 2H), 7.71-7.85 (m, 2H).

2-[4-(7-Bromo-heptyloxy)-benzyl]-benzofuran (65). Following the same procedure for the synthesis of **3c** and starting from **64** (2.0 g, 8.9 mmol), **65** was obtained as a white solid (2.57 g, 72%). mp 165 °C. ¹H NMR (CDCl₃) δ : 1.27-1.59 (m, 6H), 1.71-1.98 (m, 4H), 2.34-2.67 (s, 2H), 3.42-3.46 (t, 2H), 4.01-4.07 (t, 2H), 6.86 (s, 1H), 6.92-6.97 (d, 2H), 7.25-7.32 (m, 2H), 7.45-7.59 (m, 2H), 7.73-7.75 (d, 2H).

[7-(4-Benzofuran-2-ylmethyl-phenoxy)-heptyl]-benzyl-methyl-amine (66). Following the same procedure for the synthesis of **4c** and starting from **65** (0.23 g, 0.57 mmol), **66** was obtained as a brownish oil. ¹H NMR (CDCl₃) δ : 1.26-1.61 (m, 8H), 1.72-1.87 (m, 2H), 2.20 (s, 3H), 2.32-2.43 (m, 4H), 3.45 (s, 2H), 3.96-4.05 (t, 2H), 6.82 (s, 1H), 6.92-6.98 (d, 2H), 7.21-7.34 (m, 7H), 7.42-7.53 (m, 2H), 7.74-7.79 (d, 2H). ES-MS *m/z*: 442 (M + 1).

Biology

Inhibition of AChE and BuChE activity.

The capacity of compounds to inhibit AChE activity was assessed using the Ellman's method⁽³³⁾ Initial rate assays were performed at 37 °C with a Jasco V-530 double beam Spectrophotometer: the rate of increase in the absorbance at 412 nm was followed for 5 min. AChE stock solution was prepared by dissolving human recombinant AChE (E.C.3.1.1.7) lyophilized powder (Sigma, Italy) in 0.1 M phosphate buffer (pH = 8.0) containing Triton X-100 0.1 %. Stock solution of BuChE (E.C. 3.1.1.8) from human serum (Sigma Italy) was prepared by dissolving the lyophilized powder in an aqueous solution of gelatine 0.1 %. Stock solutions of inhibitors (1 or 2 μM) were prepared in methanol. Five increasing concentrations of the inhibitor were used, able to give an inhibition of the enzymatic activity in the range of 20-80 %. The assay solution consisted of a 0.1 M phosphate buffer pH 8.0, with the addition of 340 μM 5,5'-dithio-bis(2-nitrobenzoic acid), 0.02 unit/mL of human recombinant AChE, or BuChE from human serum and 550 μM of substrate (acetylthiocholine iodide, ATCh or butyrylthiocholine iodide, BTCh, respectively). 50 μL aliquots of increasing concentration of the tested compound were added to the assay solution and preincubated for 20 min at 37 °C with the enzyme followed by the addition of substrate. Assays were carried out with a blank containing all components except AChE or BuChE in order to account for the non-enzymatic reaction. The reaction rates were compared and the percent inhibition due to the presence of tested inhibitor at increasing concentration was calculated. Each concentration was analyzed in duplicate, and IC50 values were determined graphically from log concentration–inhibition curves (GraphPad Prism 4.03 software, GraphPad Software Inc.).

Inhibition of β-amyloid aggregation.

Preparation of solutions: Stock solution of 1 μM was prepared by solubilizing the lyophilized Aβ_{25–35} peptide by brief vortexing in sterile water at 4 °C, then by sonication for 1 min. The peptide stock solution was aliquoted and stored at -20 °C. All steps were carried out at 4 °C to prevent Aβ_{25–35} polymerization. The new compounds were solubilized in MeOH solution to a concentration S5 of 1 M. The stock solution was diluted to obtain aliquots with concentrations between 0.1-50 μM, then stored at -20 °C.

Measurement of inhibitory activity by UV-Visible Spectroscopy: To study the kinetic of Aβ_{25–35} polymerization alone, experiments were carried out by using a reaction mixture containing 80 μL phosphate buffer (10 mM final concentration) and 10 μL Aβ_{25–35} (100 μM final concentration), pH

7.2. When A β_{25-35} was added to the buffer solution, we performed sonication for 1 min to avoid any peptide aggregation. 10 μ L MeOH were added to the solution to have the same conditions for the experiments with the new compounds. To study the inhibitory activity of the new compounds, experiments were carried out by using a reaction mixture containing 80 μ L phosphate buffer (10 mM final concentration), 10 μ L MeOH containing 10 μ M final concentration of one of the new compounds or 10 μ L MeOH containing 0.1, 1, 10, 20 and 50 μ M final concentration for IC₅₀ determination and 10 μ L A β_{25-35} (100 μ M final concentration), pH 7.2. All steps were carried out at 4 °C to prevent A β_{25-35} polymerization. UV-Visible spectroscopy was performed on a Cary 300 bio UV-Visible spectrophotometer. Polymerization kinetics were monitored in the range of 190–380 nm between 0 and 6 hours. Data were collected 5 hours after incubation. For each inhibition experiment, one sample containing A β_{25-35} alone and another containing the new compound alone were used in parallel as controls in the same experimental conditions. Moreover, to rule out any influence due to the new compounds absorbance, their UV-visible spectra were subtracted from the A β_{25-35} absorption spectra. At least three independent measurements were made for all cases. All results are presented with means and standard deviation. IC₅₀ was calculated by using a least-square fitting technique to match the experimental data with a sigmoidal curve. IC₅₀ was the concentration of the new compound inhibiting the formation of A β fibrils to 50 % of the control value.

Electron Microscopy: The samples are taken again 5 min after measuring the kinetics. 10 μ L of reaction mixtures were applied to carbon-coated collodium film on 200 or 400 mesh copper grid, negatively stained with 2 % (w/v) uranyl acetate and viewed on a Philips CM 10 transmission electron microscope operating at 100 KV (SERCOMI, Bordeaux, France).

The neuroprotective effects against A β_{25-35} peptide.

Chemicals: A β_{25-35} peptide and 3-(4,5-dimethyl-2-thiazolyl)-2,5-diphenyl-2H-tetrazolium bromide (MTT) were purchased from Bachem (Bubendorf, Switzerland) and Sigma Chemical Co. (St. Louis, MO), respectively. All other reagents were of the highest grade of purity commercially available.

A β_{25-35} peptide preparation for neurotoxicity assay: A β_{25-35} peptide was dissolved in hexafluoro isopropanol (HFIP) to 1 mg/mL, sonicated and incubated at room temperature for 24 h to produce unaggregated A β peptide. The HFIP was dried under vacuum in a Speed Vac and the resulting peptide film was dissolved in DMSO to 1 mM. The unaggregated A β_{25-35} stock solution was then

aliquoted and stored at -20 °C until use. For neurotoxicity assay, the A β ₂₅₋₃₅ stock solution was diluted directly into cell culture media.

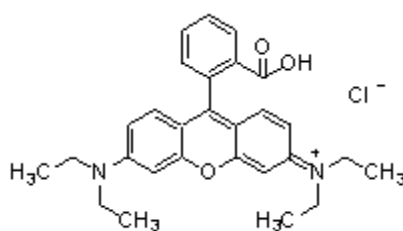
Cell culture and neurotoxicity assay: Human neuronal-like SH-SY5Y cells were routinely grown at 37 °C in a humidified incubator with 5 % CO₂ in Dulbecco's modified Eagle's medium supplemented with 10 % fetal bovine serum, 2 mM glutamine, 50 U/mL penicillin and 50 μ g/mL streptomycin. To evaluate the protective effects of compounds against A β ₂₅₋₃₅ peptide induced neurotoxicity, the SH-SY5Y cells were seeded in 96-well plates at 3 \times 10⁴ cells/well, incubated for 24 h and subsequently treated with 10 μ M of unaggregated A β ₂₅₋₃₅ peptide for 3 h at 37 °C in 5 % CO₂, in presence or absence of various concentrations of compounds (1-30 μ M). The neuronal viability in terms of mitochondrial metabolic function was evaluated by the reduction of MTT to formazan as previously described.⁽⁴⁷⁾ The cellular reduction of MTT represents an indicator of the initial events underlying the mechanism of A β ₂₅₋₃₅ peptide neurotoxicity. Briefly, after removal of the treatment, SH-SY5Y cells were washed with phosphate buffered saline (PBS) and incubated with MTT (5 mg/mL) in PBS for 2 h at 37 °C in 5 % CO₂. After further washing, the formazan crystals were dissolved with isopropanol. The amount of formazan was measured (570 nm, ref. 690 nm) with a spectrophotometer (TECAN[®], Spectra model Classic, Salizburg, Austria). The neuronal viability was expressed as a percentage of control cells and calculated by the formula:
(absorbance of treated neurons/absorbance of untreated neurons) \times 100.

Inhibition of BACE-1 activity

Purified Baculovirus-expressed BACE-1 (β -secretase) and rhodamine derivative substrate were purchased from Panvera (Madison, WI, U.S). Sodium acetate and DMSO were from Sigma Aldrich (Milan, Italy). Purified water from Milli-RX system (Millipore, Milford, MA, USA) was used to prepare buffers and standard solutions. Spectrofluorometric analyses were carried out on a Fluoroskan Ascent multiwell spectrofluorometer (excitation: 544 nm; emission: 590 nm) by using black microwell (96 wells) Cliniplate plates (Thermo LabSystems, Helsinki, Finland). Stock solutions of the tested compounds were prepared in DMSO and diluted with 50 mM sodium acetate buffer pH=4.5. Specifically, 20 μ L of BACE-1 enzyme (25 nM) were incubated with 20 μ L of test compound for 60 minutes. To start the reaction, 20 μ L of substrate (0.25 μ M) were added to the well. The mixture was incubated at 37 °C for 60 minutes. To stop the reaction, 20 μ L of BACE-1 stop solution (sodium acetate 2.5 M) were added to each well. Then the spectrofluorometric assay was performed by reading the fluorescence signal at 590 nm. Assays were done with a blank

containing all components except BACE-1 in order to account for non enzymatic reaction.. The reaction rates were compared and the percent inhibition due to the presence of test compounds was calculated. Each concentration was analyzed in triplicate. The percent inhibition of the enzyme activity due to the presence of increasing test compound concentration was calculated by the following expression: $100 - (v_i/v_o \times 100)$, where v_i is the initial rate calculated in the presence of inhibitor and v_o is the enzyme activity. To demonstrate inhibition of BACE-1 activity, a peptido mimetic inhibitor (inhibitor IV, Calbiochem, Darmstadt, Germany) was used as reference inhibitor ($IC_{50}=13.61$ nM).

Substrate: Rhodamine-Glu-Val-Asn-Leu-Asp-Ala-Glu-Phe-Lys-quencher



Rhodamine

References

- 1) Brookmeyer R, Gray S, Kawas C. Projections of Alzheimer's disease in the United States and the public health impact of delaying disease onset. *Am J Public Health* **88**, (9), 1337–42.
- 2) "Understanding stages and symptoms of Alzheimer's disease". National Institute on Aging. 2007-10-26.
- (3) Bartus, R. T. On neurodegenerative diseases, models, and treatment strategies: lessons learned and lessons forgotten a generation following the cholinergic hypothesis. *Exp. Neurol.* **2000**, *163*, 495-529.
- (4) Hardy, J.; Selkoe, D. J. The amyloid hypothesis of Alzheimer's disease: progress and problems on the road to therapeutics. *Science* **2002**, *297*, 353-356.
- (5)(a) Perry, G.; Cash, A. D.; Smith, M. A. Alzheimer disease and oxidative stress. *J. Biomed. Biotechnol.* **2002**, *2*, 120-123. (b) Zhu, X.; Raina, A. K.; Perry, G.; Smith, M. A. Alzheimer's disease: the two-hit hypothesis. *Lancet Neurol.* **2004**, *3*, 219-226.
- (6) Tolnay, M.; Probst, A. REVIEW: tau protein pathology in Alzheimer's disease and related disorders. *Neuropathol. Appl. Neurobiol.* **1999**, *25*, 171-187.
- (7) Fred M. Hershenson and Walter H. Moos. Drug Development for Senile Cognitive Decline. *J. Med. Chem.* **1986**, *29*, 1125-30.
- (8) P J Harrison. Pathogenesis of Alzheimer's disease- beyond the cholinergic hypothesis: discussion paper. *Journal of the Royal Society of Medicine*, **1986**, *79*, 347-352.
- (9) Varghese John, James P. Beck, Michael J. Bienkowski, Sukanto Sinha, and Robert L. Heinrikson. Human β -Secretase (BACE) and BACE Inhibitors. *Journal of Medicinal Chemistry*, **2003**, *46*, 4625-30.
- (10) Ghosh, A. K.; Bilcer, G.; Harwood, C.; Kawahama, R.; Shin, D.; Hussain, K. A.; Hong, L.; Loy, J. A.; Nguyen, C.; Koelsch, G.; Ermolieff, J.; Tang, J. Structure-Based Design: Potent Inhibitors of Human Brain Memapsin 2 (β -secretase). *J. Med. Chem.* **2001**, *44*, 2865-2868.
- (11) Qiao, L.; Etcheberrigaray, R. Patent WO 02/96897, 2002.
- (12) Bhisetti, G. R.; Saunders, J. O.; Murcko, M. A.; Lepre, C. A.; Britt, S. D.; Come, J. H.; Deninger, D. D.; Wang, T. Patent WO 02/88101, 2002.
- (13) Cummings, J. L.; Doody, R.; Clark, C. Disease-modifying therapies for Alzheimer disease: challenges to early intervention. *Neurology* **2007**, *69*, 1622–1634.
- (14) Cecilia B., Emanuele P., Christian P., Gregor F., and Dorian L., Three Dimensional Structure of a Complex of Galanthamine (Nivalin[®]) with Acetylcholinesterase from *Torpedo Californica*: Implications for the Design of New Anti-Alzheimer Drugs. *PROTEINS: Structure, Function, and Genetics.* **2001**, *42*, 182-191.

- (15) Giancarlo V. De Ferrari, Mauricio A. Canales, Irina Shin, Lev M. Weiner, Israel Silman, and Nibaldo C. Inestrosa. A Structural Motif of Acetylcholinesterase That Promotes Amyloid β -Peptide Fibril Formation *Biochemistry*, **2001**, *40*, 10447-10457.
- (16) Inestrosa, N. C.; Alvarez, A.; Pe´rez, C. A.; Moreno, R. D.; Vicente, M.; Linker, C.; Casanueva, O. I.; Soto, C.; Garrido, J. Acetylcholinesterase accelerates assembly of amyloid- β -peptides into Alzheimer’s fibrils: possible role of the peripheral site of the enzyme. *Neuron* **1996**, *16*, 881-891.
- (17) Qiong Xie, Hao Wang, Zheng Xia, Meiyang Lu, Weiwei Zhang, Xinghai Wang, Wei Fu, Yun Tang, Wei Sheng, Wei Li, Wei Zhou, Xu Zhu, Zhuibai Qiu, and Hongzhan Chen Bis(-)-normeptazins as Novel Nanomolar Cholinesterase Inhibitors with High Inhibitory Potency on Amyloid- β Aggregation. *J. Med. Chem.* 2008, *51*, 2027–2036.
- (18) Richard Morphy, and Zoran Rankovic. Designed Multiple Ligands. An Emerging Drug Discovery Paradigm *Journal of Medicinal Chemistry*, **2005**, *48*, 6523-43.
- (19) Paul A. Wender, Vishal A. Verma, Thomas J. Paxton, and Thomas H. Pillow. Function-Oriented Synthesis, Step Economy, and Drug Design. ACCOUNTS OF CHEMICAL RESEARCH **2008**, *41*, 140-49.
- (20) Andrea Cappelli, Andrea Gallelli, Monica Manini, Maurizio Anzini, Laura Mennuni, Francesco Makovec, M. Cristina Menziani, Stefano Alcaro, Francesco Ortuso, and Salvatore Vomero Further Studies on the Interaction of the 5-Hydroxytryptamine₃ (5-HT₃) Receptor with Arylpiperazine Ligands. Development of a New 5-HT₃ Receptor Ligand Showing Potent Acetylcholinesterase Inhibitory Properties *J. Med. Chem.* **2005**, *48*, 3564-3575.
- (21) Yuan-Ping Pang, Polly Quiram, Tanya Jelacic, Feng Hong, and Stephen BrimiJoin Highly Potent, Selective, and Low Cost Bis-tetrahydroaminacrine Inhibitors of Acetylcholinesterase THE JOURNAL OF BIOLOGICAL CHEMISTRY. **1996**, *271*, 23646–23649.
- (22) Varghese John, James P. Beck, Michael J. Bienkowski, Sukanto Sinha, and Robert L. Heinrikson Human β -Secretase (BACE) and BACE Inhibitors *Journal of Medicinal Chemistry*, **2003**, *46*, 4625-4630.
- (23) Roman Manetsch, Antoni Krasiski, Zoran Radi, Jessica Raushel, Palmer Taylor, K. Barry Sharpless, and Hartmuth C. Kolb In Situ Click Chemistry: Enzyme Inhibitors Made to Their Own Specifications. *J. Am. Chem. Soc.*, **2004**, *126* (40), 12809-12818.
- (24) Weiming Luo, Qian-sheng Yu, Santosh S. Kulkarni, Damon A. Parrish, Harold W. Holloway, David Tweedie, Avigdor Shafferman, Debomoy K. Lahiri, Arnold Brossi, and Nigel H. Greig Inhibition of Human Acetyl- and Butyrylcholinesterase by Novel Carbamates of (-)- and (+)-Tetrahydrofurobenzofuran and Methanobenzodioxepine. *J. Med. Chem.*, **2006**, *49* (7), 2174-2185.
- (25) Antoni Krasiski, Zoran Radi, Roman Manetsch, Jessica Raushel, Palmer Taylor, K. Barry Sharpless, and Hartmuth C. Kolb. In Situ Selection of Lead Compounds by Click Chemistry: Target-Guided Optimization of Acetylcholinesterase Inhibitors. *J. Am. Chem. Soc.*, **2005**, *127* (18), 6686-6692.
- (26) Pelayo Camps, Xavier Formosa, Carles Galdeano, Tania Gomez, Diego Munoz-Torrero, Michele Scarpellini, Elisabet Viayna, Albert Badia, M. Victoria Clos, Antoni Camins, Merce

Palla#s, Manuela Bartolini, Francesca Mancini, Vincenza Andrisano, Joan Estelrich, Mo#nica Lizondo, Axel Bidon-Chanal, and F. Javier Luque Novel Donepezil-Based Inhibitors of Acetyl- and Butyrylcholinesterase and Acetylcholinesterase-Induced #-Amyloid Aggregation *J. Med. Chem.*, **2008**, *51* (12), 3588-3598.

(27) Paul W. Elsinghorst, Camino M. Gonzalez Tanarro, and Michael Gtschow Novel Heterobivalent Tacrine Derivatives as Cholinesterase Inhibitors with Notable Selectivity Toward Butyrylcholinesterase *J. Med. Chem.*, **2006**, *49* (25), 7540-7544.

(28) Novel Tacrine–Melatonin Hybrids as Dual-Acting Drugs for Alzheimer Disease, with Improved Acetylcholinesterase Inhibitory and Antioxidant Properties Mara Isabel Rodrguez-Franco, Mara Isabel Fernndez-Bachiller, Concepcin Prez, Blanca Herrndez-Ledesma, and Begoa Bartolom. *J. Med. Chem.*, 2006, *49* (2), 459-462.

(29) Petra Kapkov, Eberhard Heller, Matthias Unger, Gerd Folkers, and Ulrike Holzgrabe Random Chemistry as a New Tool for the Generation of Small Compound Libraries: Development of a New Acetylcholinesterase Inhibitor *J. Med. Chem.*, **2005**, *48* (23), 7496-7499.

(30) Michael S. Wolfe. Secretase Targets for Alzheimer's Disease: Identification and Therapeutic Potential. *J. Med. Chem.*, **2001**, *44* (13), 2039-2060.

(31) Lei Fang, Dorothea Appenroth, Michael Decker, Michael Kiehntopf, Carolin Roegler, Thomas Deufel, Christian Fleck, Sixun Peng, Yihua Zhang, and Jochen Lehmann Synthesis and Biological Evaluation of NO-Donor-Tacrine Hybrids as Hepatoprotective Anti-Alzheimer Drug Candidates. *J. Med. Chem.*, **2008**, *51* (4), 713-716.

(32) Dror Noy, Inna Solomonov, Ory Sinkevich, Talmon Arad, Kristian KJaer, and Irit Sagi Zinc-Amyloid β Interactions on a Millisecond Time-Scale Stabilize Non-fibrillar Alzheimer-Related Species. *J. Am. Chem. Soc.*, **2008**, *130* (4), 1376-1383.

(33) Ellman, G. L.; Courtney, K. D.; Andres, V.; Featherstone, R. M. A new rapid colorimetric determination of acetylcholinesterase activity. *Biochem. Pharmacol.* **1961**, *7*, 88–95.

(34) Klegeris, A.; Walker, D. G.; McGeer, P. L. Activation of macrophages by Alzheimer beta amyloid peptide. *Biochem. Biophys. Res. Commun.* **1994**, *199*, 984–991.

(35) Pike, C. J.; Walencewicz-Wasserman, A. J.; Kosmoski, J.; Cribbs, D. H.; Glabe, C. G.; Cotman, C. W. Structure-activity analyses of beta-amyloid peptides: contributions of the beta 25-35 region to aggregation and neurotoxicity. *J. Neurochem.* **1995**, *64*, 253–265.

(36) Ono, K.; Hasegawa, K.; Naiki, H.; Yamada, M. Curcumin has potent anti-amyloidogenic effects for Alzheimer's beta-amyloid fibrils in vitro. *J. Neurosci. Res.* **2004**, *75*, 742–750.

(37) Tarozzi, A.; Morroni, F.; Hrelia, S.; Angeloni, C.; Marchesi, A.; Cantelli-Forti, G.; Hrelia, P. Neuroprotective effects of anthocyanins and their in vivo metabolites in SH-SY5Y cells. *Neurosci. Lett.* **2007**, *424*, 36–40.

(38) Shearman, M. S.; Hawtin, S. R.; Taylor, V. J. The intracellular component of cellular 3-(4,5-dimethylthiazol-2-yl)-2,5-diphenyltetrazolium bromide (MTT) reduction is specifically inhibited by betaamyloid peptides. *J. Neurochem.* **1995**, *65*, 218–227.

- (39) Darvesh, S.; Hopkins, D. A.; Geula, C. Neurobiology of butyrylcholinesterase. *Nat. Rev. Neurosci.* **2003**, *4*, 131–138
- (40) Farlow, M.; Anand, R.; Messina, J., Jr.; Hartman, R.; Veach, J. A 52-week study of the efficacy of rivastigmin in patients with mild to moderately severe Alzheimer's disease. *Eur. Neurol.* **2000**, *44*, 236–241.
- (41) Bartolini, M.; Bertucci, C.; Bolognesi, M. L.; Cavalli, A.; Melchiorre, C.; Andrisano, V. Insight into the kinetic of amyloid beta (1-42) peptide self-aggregation: elucidation of inhibitors' mechanism of action. *ChemBioChem* **2007**, *8*, 2152–2161.
- (42) Pike, C. J.; Walencewicz-Wasserman, A. J.; Kosmoski, J.; Cribbs, D. H.; Glabe, C. G.; Cotman, C. W. Structure-activity analyses of beta-amyloid peptides: contributions of the beta 25-35 region to aggregation and neurotoxicity. *J. Neurochem.* **1995**, *64*, 253–265.
- (43) Johansson, A. S.; Bergquist, J.; Volbracht, C.; Pa'ivio", A.; Leist, M.; Lannfelt, L.; Westlind-Danielsson, A. Attenuated amyloid-beta aggregation and neurotoxicity owing to methionine oxidation. *Neuro- Report* **2007**, *18*, 559–563.
- (44) Clementi, M. E.; Marini, S.; Coletta, M.; Orsini, F.; Giardina, B.; Misiti, F. Abeta(31-35) and Abeta(25-35) fragments of amyloid betaprotein induce cellular death through apoptotic signals: role of the redox state of methionine-35. *FEBS Lett.* **2005**, *579*, 2913–2918.
- (45) Rivie`re, C.; Richard, T.; Quentin, L.; Krisa, S.; Me´rillon, J.-M.; Monti, J.-P. Inhibitory activity of stilbenes on Alzheimer's β -amyloid fibrils in vitro. *Bioorg. Med. Chem.* **2007**, *15*, 1160–1167.
- (46) Klegeris, A.; Walker, D. G.; McGeer, P. L. Activation of macrophages by Alzheimer beta amyloid peptide. *Biochem. Biophys. Res. Commun.* **1994**, *199*, 984–991.
- (47) Shearman, M. S.; Hawtin, S. R.; Tailor, V. J. The intracellular component of cellular 3-(4,5-dimethylthiazol-2-yl)-2,5-diphenyltetrazolium bromide (MTT) reduction is specifically inhibited by betaamyloid peptides. *J. Neurochem.* **1995**, *65*, 218–227.
- (48) Richard Morphy and Zoran Rankovic. Designed multiple ligands. An emerging drug discovery paradigm. *J. Med. Chem.* **2005**, *48*, 6523-6543.
- (49) Richard Morphy, Corinne kay and Zoran Rankovic. From Magic Bullets to designed multiple ligands. *DDT* **2004**, *9*, 641-651.
- (50) (L. Bartorelli, C. Giraldi, M. Saccardo, S. Cammarata, G. Bottini, A. M. Fasanaro, A. Trequattrini. Effects of switching from an AChE inhibitor to a dual AChE-BuChE inhibitor in patients with Alzheimer's disease. *Curr. Med. Res. Opin.* **2005**, *21*, 1809-18.)
- (51) L. Piazzzi, A. Rampa, A. Bisi, S. Gobbi, F. Belluti, A. Cavalli, M. Bartolini, V. Andrisano, P. Valenti, M. Recanatini ω -3-(4-[[Benzyl(Methyl)Amino]Methyl]Phenyl)-6,7-Dimethoxy-2H-2-Chromenone (AP2238) Inhibits Both Acetylcholinesterase And Acetylcholinesterase-Induced β -Amyloid Aggregation: A Dual Function Lead For Alzheimer's Disease Therapy - *J. Med. Chem.* **46**, 2279-2282 (2003).
- (52) Belluti, F.; Rampa, A.; Piazzzi, L.; Bisi, A.; Gobbi, S.; Bartolini, M.; Andrisano, V.; Cavalli, A.;

Recanatini, M.; Valenti, P. Cholinesterase Inhibitors: Xanthostigmine Derivatives Blocking the Acetylcholinesterase-Induced β -Amyloid Aggregation. *J. Med. Chem.* **2005**, *48*, 4444-4456.

(53) Lorna Piazzzi, Andrea Cavalli, Francesco Colizzi, Federica Belluti, Manuela Bartolini, Francesca Mancini, Maurizio Recanatini, Vincenza Andrisano, Angela Rampa. Multi-target-directed coumarin derivatives: hAChE and BACE1 inhibitors as potential anti-Alzheimer compounds. *Bioorg. Med. Chem. Letters*, **2008**, *1*, 423-426.

(54) Stefano Rizzo, Andrea Cavalli, Luisa Ceccarini, Manuela Bartolini, Federica Belluti, Alessandra Bisi, Vincenza Andrisano, Maurizio Recanatini, Angela Rampa. Structure-Activity Relationships and Binding Mode in the Human Acetylcholinesterase Active Site of Pseudo-Irreversible Inhibitors Related to Xanthostigmine. *ChemMedChem*, **2009**, Feb. 16 on line.

(55) Howlett, D. R.; Perry, A. E.; Godfrey, F.; Swatton, J. E.; Jennings, K. H.; Spitzfaden, C.; Wadsworth, H.; Wood, S. J.; Markwell, R. E. Inhibition of fibril formation in *b*-amyloid peptide by a novel series of benzofurans. *Biochem. J.* **1999**, *340*, 283-289.

(56) A. Rampa, L. Piazzzi, F. Belluti, S. Gobbi, A. Bisi, M. Bartolini, V. Andrisano, V. Cavrini, A. Cavalli, M. Recanatini, P. Valenti - Acetylcholinesterase Inhibitors: SAR and kinetic studies on ω -[N-Methyl-N-(3-alkylcarbamoyloxyphenyl)-methyl]-aminoalkoxyaryl Derivatives - *J. Med. Chem.* **2001**, *44*, 3810-3820.

(57) Piazzzi, L.; Belluti, F.; Bisi, A.; Gobbi, S.; Rizzo, S.; Bartolini, M.; Andrisano, V.; Recanatini, M.; Rampa, A. Cholinesterase inhibitors: SAR and enzyme inhibitory activity of 3-[ω -(benzylmethylamino)alkoxy]xanthen-9-ones. *Bioorg. Med. Chem.* **2007**, *15*, 575-585.

(58) A. Rampa, A. Bisi, P. Valenti, M. Recanatini, A. Cavalli, V. Andrisano, V. Cavrini, L. Fin, A. Buriani, P. Giusti. Acetylcholinesterase Inhibitors: Synthesis and Structure-Activity Relationships of ω -[N-Methyl-N-(3-alkylcarbamoyloxyphenyl)-methyl]-aminoalkoxyheteroaryl Derivatives. *J. Med. Chem.* **1998**, *41*, 3976-3986

(59) P. Valenti, A. Rampa, A. Bisi, V. Andrisano, V. Cavrini, L. Fin, A. Buriani, P. Giusti. Acetylcholinesterase Inhibition by Tacrine Analogues. *Bioorg. Med. Chem. Lett.* **1997**, *7*, 2599-2602.

(60) A. Rampa, A. Bisi, F. Belluti, S. Gobbi, P. Valenti, V. Andrisano, V. Cavrini, A. Cavalli, M. Recanatini. Acetylcholinesterase inhibitors for potential use in Alzheimer's disease: molecular modeling, synthesis and kinetic evaluation of 11*H*-Indeno-[1,2-*b*]-quinolin-10-ylamine derivatives. *Bioorg. Med. Chem.* **2000**, *8*, 497-506.

(61) M. Recanatini, A. Cavalli, F. Belluti, L. Piazzzi, A. Rampa, A. Bisi, S. Gobbi, P. Valenti, V. Andrisano, M. Bartolini, V. Cavrini. SAR of 9-amino-1,2,3,4-tetrahydroacridine-based acetylcholinesterase inhibitors: synthesis, enzyme inhibitory activity, QSAR, and structure-based CoMFA of Tacrine analogues. *J. Med. Chem.* **2000**, *43*, 2007-2018.

(62) Stefano Rizzo, Celine Riviere, Lorna Piazzzi, Alessandra Bisi, Silvia Gobbi, Manuela Bartolini, Vincenza Andrisano, Fabiana Morroni, Andrea Tarozzi, Jean-Pierre Monti, Angela Rampa. Benzofuran-Based Hybrid Compounds for the Inhibition of Cholinesterase Activity, β Amyloid Aggregation, and $A\beta$ Neurotoxicity. *J. Med. Chem.* **2008**, *51*, 2883-2886.

Acknowledgments

Thanks to my parents for their grant toward every kind of support I've been in need of through the years.

Thanks to Dr. Angela Rampa for sharing with me her experience and knowledge on the Alzheimer's topic, making possible the realization of this thesis. An extra thanks for helping me out whenever I was in trouble.

Thanks to my tutor Professor Alessandra Bisi for supervising the whole project.

Thanks to Dr. Federica Belluti, Dr. Silvia Gobbi and Dr. Lorna Piazzini for stimulating discussions and priceless advices.

Thanks to Professor Jean Pierre Monti, Professor Vincenza Andrisano, Dr. Manuela Bartolini, Dr. Francesca Mancini, Dr. Andrea Tarozzi for testing the biological activity of the compounds shown in this thesis.

Thanks to PhD student Luisa Ceccarini for providing docking simulation of compound 49c in hAChE gorge.